# APPROPRIATE ANALYSES FOR AN ABSORBER PLATE IN FLAT-PLATE SOLAR COLLECTOR

**Thesis submitted by**

**Jayanarayan Mahakud**

**Doctor of Philosophy (Engineering)**

**Department of Mechanical Engineering**

**Faculty Council of Engineering and Technology**

**Jadavpur Univesity Kolkata, India**

**2025**

# INDEX NO. – 231/18/E

| | | |
|---|---|---|
| **1.** | **Title of the thesis:** | Appropriate Analyses for an Absorber Plate in Flat-Plate Solar Collector |
| **2.** | **Name, Designation and Institution of the Supervisor:** | Dr. Balaram Kundu<br>Professor<br>Department of Mechanical Engineering,<br>Jadavpur University,<br>Kolkata-700032, India. |
| **3.** | **List of Publications:** | ***International Journal*** |

**1. Mahakud J., & Kundu B. (2024)**. Two-Dimensional Analysis of Absorber Plates in Solar Collectors with a Nonlinear Plate Temperature at the Tube Section. ***Energies (MDPI)***, *17*(23), 5979. https://doi.org/10.3390/en17235979

**2.**

**3.**

**4. List of patents:** NIL

**5. List of Presentation in National / International Conference / Workshops / Symposiums:**

**1. Mahakud J., & Kundu B. (2020)**. Trapezoidal Approach to Establish One-Dimensional Analysis of an Absorber Plate for Two-Dimensional Heat Flow. In *Advances in Mechanical Engineering: Select Proceedings of ICRIDME 2018* (pp. 1361-1372). Singapore: Springer Singapore. International Conference on Recent Innovations and Developments in Mechanical Engineering, NIT Meghalaya **(ICRIDME 2018 ),** November 8 – 10, 2018, Shillong, India.

**2. Mahakud J., & Kundu B. (2019)**. Simple Analytical Method for Performance of an Absorber Plate in Flat-Plate Solar Collectors for Two-Dimensional Heat Flow. In *Advances in Fluid and Thermal Engineering: Select Proceedings of FLAME 2018* (pp. 1-12). Springer Singapore. 1st International Conference on Future Learning Aspects of Mechanical Engineering **(FLAME - 2018)**, October 3 - 5 , 2018, Amity School of Engineering & Technology, Amity University Uttar Pradesh, Noida, India.

**3. Mahakud J., & Kundu B. (2016)**. A New Approach for Thermal Analysis of Absorber Plates in a Solar Collector, National Conference on Advances in Thermal Engineering **(NCATE 2016)**, 23rd-24th September 2016, Jadavpur University, Kolkata, West Bengal, India.

# Statement of Originality

I, Jayanarayan Mahakud registered on 16th April 2018 do hereby declare that this thesis entitled "**Appropriate Analyses for an Absorber Plate in Flat-Plate Solar Collector**" contains literature survey and original research work done by the undersigned candidate as part of Doctoral studies. All information in this thesis have obtained and presented in accordance with existing academic rules and ethical conduct. I declare that, as required by these rules and conduct, I have fully cited and referred all materials and results that are not original to this work.

I also declare that I have checked this as per the "Policy on Anti Plagiarism, Jadavpur University, 2019", and the level of similarity as checked by iThenticate software is 5 **%.**

Jayanarayan Mahakud

Signature of the candidate:

Date: 31.12.2025

Certified by Supervisor:

31-12-2025

(Signature with date, seal)

Professor
Dept. of Mechanical Engineering
Jadavpur University, Kolkata-32

# Certificate from the Supervisor

This is to certify that the thesis entitled **"Appropriate Analyses for an Absorber Plate in Flat-Plate Solar Collector"** submitted by **Shri Jayanarayan Mahakud** who got his name registered on 16th April 2018 for the award of Ph. D. (Engg.) degree of Jadavpur University is absolutely based upon his own work under the supervision of **Dr. Balaram Kundu,** Professor, Mechanical Engineering Department, Jadavpur University and that neither his thesis nor any part of the thesis has been submitted for any degree / diploma or other academic award anywhere before.

31-12-2025

(Dr. Balaram Kundu)

Professor

Department of Mechanical Engineering

Jadavpur University

Kolkata-700032. India

Professor
Dept. of Mechanical Engineering
Jadavpur University, Kolkata-32

**(Signature of Supervisor and date with office with seal)**

# Acknowledgement

A PhD is a journey of curiosity, patience, and perseverance where every setback is a step toward new knowledge. The pursuit of this PhD journey has been filled with obstacles, challenges and learning opportunities, and I am deeply grateful to those who have supported me along the way

First and foremost, I would like to express my deepest gratitude to the Almighty God for granting me patience, courage, and wisdom to complete this project.

I extend my deepest gratitude to my supervisor, Dr.Balaram Kundu , Professor, Department of Mechanical Engineering, Jadavpur University, whose guidance, patience, and unwavering support have been instrumental in shaping this research. I feel extremely fortunate to have worked under the guidance of Prof. Balaram Kundu. His passion for research, unwavering enthusiasm, and dynamic approach have left a profound impact on me. I am truly grateful for his insightful advice, holistic perspective on research, and constant motivation. This is my humble opportunity to express my highest regards to Prof. Kundu for his unconditional support and for shaping a new dimension in my career. I firmly believe that his influence on my life cannot be adequately expressed in mere words.

I am equally thankful to my research advisory committee members Prof. Sudipta De, Prof. Prokash Chandra Roy, Prof. Sudip Simlandi for their valuable insights and constructive feedback.

My appreciation goes to my colleagues and friends for their encouragement and enriching discussions that kept me motivated

throughout this journey. I want to thank Dr. Mrutyunjay Rout, Dr. Sudhir Ch. Murmu, Dr. Syedmujibur Rahman, Mr. Sujit Saha and all the technical staff of Heat Power Lab for their continuous help and support from very initial period of this journey. I will always cherish my working days at Heat Power Laboratory. I would also like to thank especially Dr. Pramod AtmaramWankhade my QIP colleague for his motivations and support during these tough days.

I would also like to appreciate the Hon'ble Vice Chancellor and the Registrar, BPUT, Odisha, Rourkela, for their support and granting me the study leave under AICTE's QIP scheme. I owe a special thanks to my departmental Head/s and colleagues especiallyMrs. Anukampa Chau Pattnaik, Mr. Saumes Harichandan, Mr Krushna Chandra Patra, Dr Asisha Ranjan Pradhan and Mr. Mukesh Kumar Panigrahi for their absolute support and co-operation.

I would like to express the deepest sadness for my father Shri Bhaskar Chandra Mahakud and mother Smt. Sumitra Mahakud to whom I lost during this period.

Lastly, I acknowledge, a special thanks to my family, whose love, sacrifices, and constant belief in me provided the strength to persevere. This moment of joy is dedicated to my beloved mother, Smt. Sumitra Mahakud, my loving wife, Biswabhara Behera, my cherished daughter, Bandana Chandradhara Mahakud, and my dear elder sister Smt. Asima Mahakud...!!!

Jayanarayan Mahakud

**(Signature)**

*Dedicated*

*to my*

*parents*

# Abstract

The global energy crisis and environmental concerns have accelerated the shift toward renewable energy sources. As fossil fuels deplete and climate change worsens, cleaner alternatives have become essential. Renewable energy not only addresses ecological challenges but also supports economic growth and energy independence. Among these, solar power stands out as a sustainable option due to its abundance and cleanliness. Solar thermal systems utilize solar collectors to capture sunlight and convert it into thermal energy, using fluids like water or air for heating and power generation. Key components of a flat-plate collector include the absorber plate, fluid-carrying tubes, transparent cover, insulation, and casing, all designed for high efficiency in various applications.

Each category of solar collectors is designed for specific energy needs, chosen based on economic viability and climate. Enhancing the efficiency of these collectors is a key research area. The prominent Hottel-Whillier-Bliss (H-W-B) model, developed from earlier works in 1942, 1953, and 1959, is one-dimensional and follows a lumped formulation. While research has evaluated various parameters affecting collector performance, a comprehensive theoretical analysis is still needed. This PhD study aims to fill that gap by conducting a two-dimensional thermal analysis of flat-plate collectors to improve thermal performance through analytical and numerical modeling. It will examine heat transfer dynamics, fluid flow behavior, and efficiency improvements, focusing on their overall impact on system performance.

A study develops an approximate analytical method to calculate the two-dimensional temperature circulation in an absorber plate and validates it against finite-difference method results. The findings show excellent agreement, with deviations of less than 5%, confirming the model's reliability for practical use.

A study provides a closed-form solution for 2D heat transfer in absorber plates, accounting for nonlinear temperature variations at the plate-tube interface. The energy equation is solved analytically using the separation of variables method and validated with the finite difference method. Results show a strong correlation between both approaches, confirming the model's accuracy. This framework offers a reliable method for thermal evaluation of solar collector absorber plates.

A modified one-dimensional method using the trapezoidal rule is proposed for approximating two-dimensional analysis, with validation against the finite difference method showing good agreement. The classical one-dimensional model is inadequate for absorber plates, whereas the modified model aligns closely with the two-dimensional approach, offering a more straightforward, more efficient solution. This study enhances the accuracy of thermal analysis for absorber plates, aiding in the design and optimization of flat-plate solar collectors.

Analytical studies of solar flat-plate collectors typically use the classical Fourier heat conduction model, which assumes an infinite thermal wave propagation speed and a linear relationship between heat flux and the temperature gradient. This assumption conflicts with Einstein's relativity, even though it adheres to the second law of thermodynamics. To address this, the Cattaneo-Vernotte model

introduces a finite thermal wave speed by incorporating a relaxation term, transforming the heat conduction equation from parabolic to hyperbolic. Previous research simplified this model by neglecting the time relaxation term. However, analyses that do include this term show that it reduces temperature circulation on the absorber plate.

In solar flat-plate collectors, the working fluid is crucial for heat transport. Nanofluids outperform conventional fluids like water, enhancing absorber plate performance and overall efficiency. A comprehensive thermodynamic analysis, including energy and exergy evaluations, identifies various losses, improving the efficiency of thermal systems. This research examines the energy and exergy of absorber plates in solar flat-plate collectors using nano-hybrid fluids containing CuO, MgO, and $TiO_2$ nanoparticles, providing insights into more efficient absorber plate models and improved thermal performance in solar thermal systems.

# TITLE OF THE THESIS

# Appropriate Analyses for an Absorber Plate in Flat-Plate Solar Collector

# Contents

# List of figures

# List of Tables

# Nomenclature and Abbreviations

| | |
|---|---|
| $A$ | dimensionless variable defined in Eq. (3.5b), (5.2b) |
| $A_1$ | dimensionless constant |
| $a$ | Arbitrary constant |
| $A_c$ | Absorber plate area, $m^2$ |
| $B_1$ | dimensionless constant |
| $b$ | Arbitrary constant |
| $Bi$ | Biot number, $hW/k$ |
| $Bi_1$, $Bi_2$ | Biot number, $h_1W/k$ , $h_2W/k$ |
| $C$ | Thermal propagation speed, $m/s$ |
| $C_1$, $C_2$, $C_3$, $C_4$ | Arbitrary constant |
| $C_m$, $C_n$ | Constant used for series solution |
| $C_p$ | specific heat ( J $kg^{-1}$ $K^{-1}$) |
| | |
| $D$ | Differential operator |
| $D_1$, $D_o$ $D_2$ | root, defined in Eq. (6.31) |
| $d_o$ | Outer diameter of the tube |
| $d_i$ | Inner diameter of the tube |
| $E_1$ | Arbitrary constant |
| $E_2$ | Arbitrary constant |

| | |
|---|---|
| Er | deviation of temperature, $\left(\theta_{analytical} - \theta_{numerical}\right)/\theta_{analytical}$ |
| $Fo$ | Fourier number |
| $F^{I}$ | collector efficiency factor |
| $F^{II}$ | capacitance |
| $F_R$ | collector heat removal factor |
| $h_f$ | Convective heat transfer coefficient in side the tube, $W/m^2K$ |
| $I_T$ | absorbed solar flux intensity (W $m^{-2}$) |
| $k$ | thermal conductivity of an absorber plate material (W $m^{-1}K^{-1}$) |
| $L$ | half-pitch distance between flow tubes as shown in Fig. 3.1 (m) |
| $\dot{m}$ | Mass flow rate in the tube [kg/s] |
| $m$ | Parameter in Eqs. 7.13 |
| $M$ | dimensionless thermo-geometric parameter of absorber plate, see Eq. (3.3) |
| $N$ | dimensionless absorbed solar flux, see Eq. (3.3) |
| $P$ | Parameter , see Eq. (6.6) |
| $Q_{useful}$ | useful energy gain |
| $S$ | Absorbed solar flux, $(\alpha\chi)I_T$ |
| $t$ | thickness of the absorber plate, $m$ |
| $T$ | local absorber plate temperature , $^oC$ |
| $T_{in}$ | Inlet temperature, $^oC$ |
| $T_\infty$ | ambient temperature $^oC$ |

| | |
|---|---|
| $T_{fi}$ | temperature of fluid at inlet |
| $T_{fo}$ | temperature of fluid at outlet |
| $T_o$ | Environment or dead state for calculating exergy |
| $U_L$ | overall heat loss coefficient (W $m^{-2}$ $K^{-1}$) |
| $U(X)$ | Variable dependents on space |
| $Ve$ | Vernotte number, $\tau C/L$ |
| $V(Fo)$ | Variable for time function |
| $W$ | length of the symmetric heat transfer module $m$ |
| $x$ | x-coordinate for absorber plate, $m$ |
| $X$ | dimensionless Coordinate, x/L |
| $y$ | y-coordinate for absorber plate, $m$ |
| $Y$ | dimensionless y-coordinate, y/W |
| **Greek letters** | |
| $\alpha$ | Absorptivity of the absorber plate |
| $\tau$ | thermal relaxation time |
| $\beta$ | temperature variable along y-direction, see Eq. (3.6) |
| $\gamma$ | temperature variable along x-direction, defined in Eq. (3.6) |
| $\delta$ | aspect ratio, defined in Eq. (3.3) |
| $\kappa$ | Thermal diffusivity, $k/\rho c_p$ |
| $\theta$ | dimensionless temperature $=(T-T_\infty)/(T_{in}-T_\infty)$ |
| $\phi(Y)$ | temperature variable along y-direction, see Eq. (4.6) |
| $\lambda$ | Eigen constant |
| $\eta$ | Collector efficiency |

| | |
|---|---|
| $t$ | Time, $s$ |
| $\zeta$ | Transmisivity of the absorber plate |
| $\psi(X)$ | A spatial function in Eq. (6.11) |
| $\lambda_m$, $\lambda_n$ | Eigen constants |
| $\rho$ | Density of the plate material, $kg/m^3$ |
| $\phi(X, Fo)$ | Variable for space and time function |
| **Subscripts** | |
| *in* | inlet condition |
| *f* | fluid |
| *out* | Outlet condition |
| **Abbreviations** | |
| FPSC | Flat plate solar collector |
| FPC | Flat plate collector |
| FHC | Fourier heat conduction |
| NFHC | Non- Fourier heat conduction |

# Abstract

The global energy crisis and environmental concerns have accelerated the shift toward renewable energy sources. As fossil fuels deplete and climate change worsens, cleaner alternatives have become essential. Renewable energy not only addresses ecological challenges but also supports economic growth and energy independence. Among these, solar power stands out as a sustainable option due to its abundance and cleanliness. Solar thermal systems utilize solar collectors to capture sunlight and convert it into thermal energy, using fluids like water or air for heating and power generation. Key components of a flat-plate collector include the absorber plate, fluid-carrying tubes, transparent cover, insulation, and casing, all designed for high efficiency in various applications.

Each category of solar collectors is designed for specific energy needs, chosen based on economic viability and climate. Enhancing the efficiency of these collectors is a key research area. The prominent Hottel-Whillier-Bliss (H-W-B) model, developed from earlier works in 1942, 1953, and 1959, is one-dimensional and follows a lumped formulation. While research has evaluated various parameters affecting collector performance, a comprehensive theoretical analysis is still needed. This PhD study aims to fill that gap by conducting a two-dimensional thermal analysis of flat-plate collectors to improve thermal performance through analytical and numerical modeling. It will examine heat transfer dynamics, fluid flow behavior, and efficiency improvements, focusing on their overall impact on system performance.

A study develops an approximate analytical method to calculate the two-dimensional temperature circulation in an absorber plate and validates it against finite-difference method results. The findings show excellent agreement, with deviations of less than 5%, confirming the model's reliability for practical use.

A study provides a closed-form solution for 2D heat transfer in absorber plates, accounting for nonlinear temperature variations at the plate-tube interface. The energy equation is solved analytically using the separation of variables method and validated with the finite difference method. Results show a strong correlation between both approaches, confirming the model's accuracy. This framework offers a reliable method for thermal evaluation of solar collector absorber plates.

A modified one-dimensional method using the trapezoidal rule is proposed for approximating two-dimensional analysis, with validation against the finite difference method showing good agreement. The classical one-dimensional model is inadequate for absorber plates, whereas the modified model aligns closely with the two-dimensional approach, offering a more straightforward, more efficient solution. This study enhances the accuracy of thermal analysis for absorber plates, aiding in the design and optimization of flat-plate solar collectors.

Analytical studies of solar flat-plate collectors typically use the classical Fourier heat conduction model, which assumes an infinite thermal wave propagation speed and a linear relationship between heat flux and the temperature gradient. This assumption conflicts with Einstein's relativity, even though it adheres to the second law of thermodynamics. To address this, the Cattaneo-Vernotte model

introduces a finite thermal wave speed by incorporating a relaxation term, transforming the heat conduction equation from parabolic to hyperbolic. Previous research simplified this model by neglecting the time relaxation term. However, analyses that do include this term show that it reduces temperature circulation on the absorber plate.

In solar flat-plate collectors, the working fluid is crucial for heat transport. Nanofluids outperform conventional fluids like water, enhancing absorber plate performance and overall efficiency. A comprehensive thermodynamic analysis, including energy and exergy evaluations, identifies various losses, improving the efficiency of thermal systems. This research examines the energy and exergy of absorber plates in solar flat-plate collectors using nano-hybrid fluids containing CuO, MgO, and $TiO_2$ nanoparticles, providing insights into more efficient absorber plate models and improved thermal performance in solar thermal systems.

# TITLE OF THE THESIS

# Appropriate Analyses for an Absorber Plate in Flat-Plate Solar Collector

# Contents

# List of figures

# List of Tables

# Nomenclature and Abbreviations

| | |
|---|---|
| $A$ | dimensionless variable defined in Eq. (3.5b), (5.2b) |
| $A_1$ | dimensionless constant |
| $a$ | Arbitrary constant |
| $A_c$ | Absorber plate area, $m^2$ |
| $B_1$ | dimensionless constant |
| $b$ | Arbitrary constant |
| $Bi$ | Biot number, $hW/k$ |
| $Bi_1$, $Bi_2$ | Biot number, $h_1W/k$ , $h_2W/k$ |
| $C$ | Thermal propagation speed, $m/s$ |
| $C_1$, $C_2$, $C_3$, $C_4$ | Arbitrary constant |
| $C_m$, $C_n$ | Constant used for series solution |
| $C_p$ | specific heat ( J $kg^{-1}$ $K^{-1}$) |
| | |
| $D$ | Differential operator |
| $D_1$, $D_o$ $D_2$ | root, defined in Eq. (6.31) |
| $d_o$ | Outer diameter of the tube |
| $d_i$ | Inner diameter of the tube |
| $E_1$ | Arbitrary constant |
| $E_2$ | Arbitrary constant |

| | |
|---|---|
| Er | deviation of temperature, $\left(\theta_{analytical} - \theta_{numerical}\right)/\theta_{analytical}$ |
| $Fo$ | Fourier number |
| $F^{I}$ | collector efficiency factor |
| $F^{II}$ | capacitance |
| $F_R$ | collector heat removal factor |
| $h_f$ | Convective heat transfer coefficient in side the tube, $W/m^2K$ |
| $I_T$ | absorbed solar flux intensity (W $m^{-2}$) |
| $k$ | thermal conductivity of an absorber plate material (W $m^{-1}K^{-1}$) |
| $L$ | half-pitch distance between flow tubes as shown in Fig. 3.1 (m) |
| $\dot{m}$ | Mass flow rate in the tube [kg/s] |
| $m$ | Parameter in Eqs. 7.13 |
| $M$ | dimensionless thermo-geometric parameter of absorber plate, see Eq. (3.3) |
| $N$ | dimensionless absorbed solar flux, see Eq. (3.3) |
| $P$ | Parameter , see Eq. (6.6) |
| $Q_{useful}$ | useful energy gain |
| $S$ | Absorbed solar flux, $(\alpha\chi)I_T$ |
| $t$ | thickness of the absorber plate, $m$ |
| $T$ | local absorber plate temperature , $^oC$ |
| $T_{in}$ | Inlet temperature, $^oC$ |
| $T_\infty$ | ambient temperature $^oC$ |

| | |
|---|---|
| $T_{fi}$ | temperature of fluid at inlet |
| $T_{fo}$ | temperature of fluid at outlet |
| $T_o$ | Environment or dead state for calculating exergy |
| $U_L$ | overall heat loss coefficient (W $m^{-2}$ $K^{-1}$) |
| $U(X)$ | Variable dependents on space |
| $Ve$ | Vernotte number, $\tau C/L$ |
| $V(Fo)$ | Variable for time function |
| $W$ | length of the symmetric heat transfer module $m$ |
| $x$ | x-coordinate for absorber plate, $m$ |
| $X$ | dimensionless Coordinate, x/L |
| $y$ | y-coordinate for absorber plate, $m$ |
| $Y$ | dimensionless y-coordinate, y/W |
| **Greek letters** | |
| $\alpha$ | Absorptivity of the absorber plate |
| $\tau$ | thermal relaxation time |
| $\beta$ | temperature variable along y-direction, see Eq. (3.6) |
| $\gamma$ | temperature variable along x-direction, defined in Eq. (3.6) |
| $\delta$ | aspect ratio, defined in Eq. (3.3) |
| $\kappa$ | Thermal diffusivity, $k/\rho c_p$ |
| $\theta$ | dimensionless temperature $=(T-T_\infty)/(T_{in}-T_\infty)$ |
| $\phi(Y)$ | temperature variable along y-direction, see Eq. (4.6) |
| $\lambda$ | Eigen constant |
| $\eta$ | Collector efficiency |

| | |
|---|---|
| $t$ | Time, $s$ |
| $\zeta$ | Transmisivity of the absorber plate |
| $\psi(X)$ | A spatial function in Eq. (6.11) |
| $\lambda_m$, $\lambda_n$ | Eigen constants |
| $\rho$ | Density of the plate material, $kg/m^3$ |
| $\phi(X, Fo)$ | Variable for space and time function |
| **Subscripts** | |
| *in* | inlet condition |
| *f* | fluid |
| *out* | Outlet condition |
| **Abbreviations** | |
| FPSC | Flat plate solar collector |
| FPC | Flat plate collector |
| FHC | Fourier heat conduction |
| NFHC | Non- Fourier heat conduction |

# Chapter1

# Introduction

## 1.1Background

Energy is a crucial foundation of contemporary civilization, propelling organizations, transportation, and everyday existence. It manifests in multiple forms, involving mechanical, thermal, electrical, and chemical energy, each playing a critical role in economic growth and technological progress [1]. With rapid industrialization and urbanization, global energy demand has surged, making energy production and consumption key areas of study. Fossil fuels—coal, crude oil, and natural gas—have historically prevailed in the energy portfolio, comprising over 80% of worldwide use [2]. However, their continued reliance raises concerns over resource depletion, energy security, and environmental sustainability. The combustion of fossil fuels contributes approximately 75% of global carbon dioxide emissions, accelerating weather alteration and its related risks, including increasing sea levels, severe meteorological phenomena, and loss of biodiversity [3]. Furthermore, air pollution from fossil fuel use has been linked to severe public health issues, while geopolitical tensions over energy resources expose the vulnerabilities of fossil fuel dependency. These pressing challenges underscore the urgent need for a changeover to cleaner, enhanced renewable power solutions to guarantee sustainability economic stability and environmental resilience.

## 1.2 Renewable Energy

The evolution to renewable energy offers a viable solution to mitigate environmental degradation while augmenting energy sources security. The International Renewable Energy Agency (IRENA) emphasises that sustainable are becoming increasingly cost-competitive, making them a pragmatic selection for long-term energy planning. Supportive policies, subsidies, and research initiatives are accelerating clean energy adoption, fostering an energy future that is more sustainable and robust [4]. According to the Global Renewable Energy Status Report (REN21), renewable sources now contribute approximately 29% of global power generation, driven by environmental concerns, economic benefits, and technological advancements [5]. The Intergovernmental Panel on Climate Change (IPCC) underscores that transitioning to renewable energy is crucial for limiting global warming to 1.5°C, reinforcing the urgency of integrating clean energy solutions. Beyond environmental advantages, renewables also stimulate economic expansion by cultivating new sectors and generating employment, and advancing infrastructure expansion [6].

Renewable energy encompasses a varied spectrum of sustainable sources, comprising solar, wind, hydroelectric, biomass, and geothermal power. Among these, Solar energy is among the greatest plentiful and extensively employed energy sources, serving a pivotal function in the worldwide the energy revolution (IRENA, 2023). In 2022, solar power constituted 3.6% of global electricity production and over 31% of installed renewable energy capacity, with a 22% growth from 2021. It is projected to supply approximately 25% of the world's electricity by 2050 [7]. As of December 2024, fossil fuels contributed 47.6% of total net

electricity generation, followed by renewables at 34.5% and nuclear at 17.5%. Renewable electricity generation continues to rise, with a 2.8% annual increase, while solar power saw the highest growth at 26.4% year-on-year, reaching 4.8% of total OECD electricity generation (IEA, 2024). Beyond environmental benefits, renewable energy enhances social development through the enhancement of energy accessibility in isolated areas and off-grid communities [8].Technologies like solar household systems and mini-grids can deliver dependable electricity to neglected regions, enhancing living conditions and promoting economic possibilities, particularly in low-income areas [9].

## 1.3 Solar Energy

Solar energy, originating from the Sun's emitted light and thermal radiation, is among the most prevalent and sustainable sources of energy available. Unlike fossil fuels, it is a renewable resource that reduces carbon emissions, mitigates global warming, and offers an eco-friendly alternative for energy production. The Sun serves as Earth's primary energy powerhouse, emitting an immense $4.7\times10^{2} GW$ of energy into space, a small fraction of which sustains life and meets global energy needs. Solar power is harnessed primarily through photovoltaic (PV) panels, that convert solar energy into electrical power, and solar energy systems, which transform sunlight into usable thermal energy for domestic heating and industrial applications. India, ranking fifth globally in solar PV adoption, had an installed capacity of approximately 70.10 GW as of mid-2023, reflecting the growing reliance on solar energy. Despite its numerous advantages, solar energy faces challenges such as intermittency, energy transmission limitations, and efficiency constraints, necessitating continued advancements in technology and infrastructure

for widespread adoption. Solar energy plays a crucial role in electricity generation, water heating, space heating, and cooling uses. As global efforts intensify toward more efficient and environmentally friendly energy solutions, solar power remains a key pillar during the shift towards a more sustainable future [10-12].

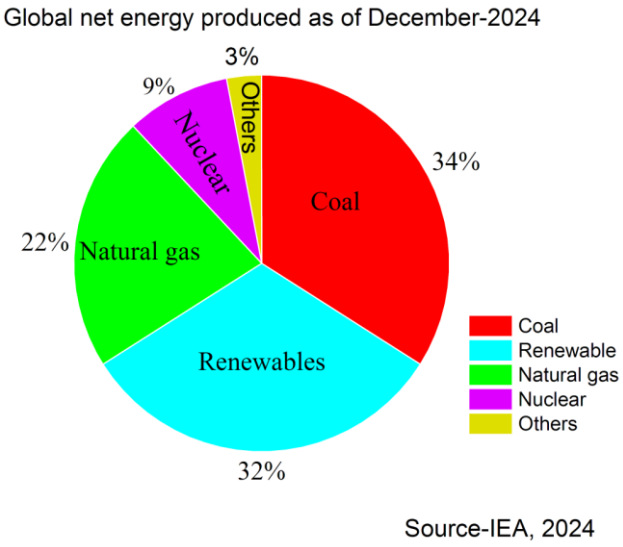


**Fig. 1.1** Global net energy data

## 1.4 Solar collector

Solar collectors are vital elements of solar thermal systems, engineered to effectively gather and convert solar radiation into useful thermal energy. These collectors absorb sunlight and transfer the captured heat to a working fluid, which can subsequently be utilized for diverse applications like water heating, space heating, and engineering progressions. Solar collectors can be categorised into two primary types according to their concentration capacities:

i. **Concentrating collectors**: Concentrated solar collectors utilise mirrors or lenses to concentrate sunlight onto a confined area, significantly increasing the temperature of a working fluid for various applications. Their ability to achieve high temperatures makes them highly efficient and ideal for industrial processes and large-scale electricity generation in solar power plants. Due to the Sun's changing position throughout the day, these collectors require tracking mechanisms to continuously focus sunlight onto the absorber plate, ensuring optimal energy capture. Examples of concentrating collectors include Parabolic Trough Collectors, Parabolic Dish Collectors, Fresnel Reflectors, and Heliostat Systems. Exhibiting a significantly more focus proportion than non-concentrating collectors, these devices can attain temperatures surpassing 100°C, making them appropriate for elevated-temperature thermal applications.

ii. **Non-Concentrating Collectors**: These collectors absorb sunlight directly through a large surface zone deprived of the use of focusing mechanisms. Commonly referred to as flat plate solar collectors, they are widely utilised in applications requiring low operating temperatures, such as those with 50°C to 100°C. Non-concentrating collectors are optimal for home and commercial thermal requirements, including water heating, space heating, and various domestic applications. By effectively using solar energy, they aid in sustainable energy solutions, decreasing reliance on fossil fuels and mitigating carbon emissions. Non-concentrating collectors including Flat Plate Solar Collectors and Evacuated Tube Collectors.

Further, solar collectors can also be categorized based on their applications and operating temperature ranges:

i. **0 to 40°C** – Primarily used for pool heating and heat pump applications, these systems typically employ unglazed collectors, such as pool absorbers, which efficiently capture solar energy for low-temperature heating.

ii. **40 to 90°C** – Suitable for domestic hot water production, low-temperature industrial processes (e.g., drying and desiccation), solar cooling, and water desalination. Flat-plate collectors or evacuated tube collectors are commonly used in this temperature range due to their effective heat retention and versatility.

iii. **70 to 150°C** – Ideal for medium-temperature applications, including process heat, solar cooling, and steam generation. High-efficiency flat-plate collectors with anti-reflective coatings and superior insulation, as well as evacuated tube collectors, are preferred for their enhanced thermal performance.

iv. **90 to 250°C** – Designed for high-temperature industrial applications, such as advanced process heating, these systems utilize concentration and monitoring of collectors, such as Fresnel and parabolic trough collectors, to achieve optimal efficiency by focusing sunlight onto a smaller surface area.

## 1.5 Flat-plate solar collector

Among the numerous types of solar collectors, Flat Plate Solar Collectors (FPCs) are among the predominantly utilised solar thermal energy systems for heating applications due to their simplicity, cost-effectiveness, and ability to capture both direct and prolix solar radiation.

These collectors function by capturing solar energy, transforming it into thermal energy, and transmitting the heat to a fluid of operation. Their design features a large absorbing surface to maximize solar interception, ensuring efficient heat capture. Since flat plate collectors are typically fixed in position, proper orientation is essential to optimize their performance and energy output.

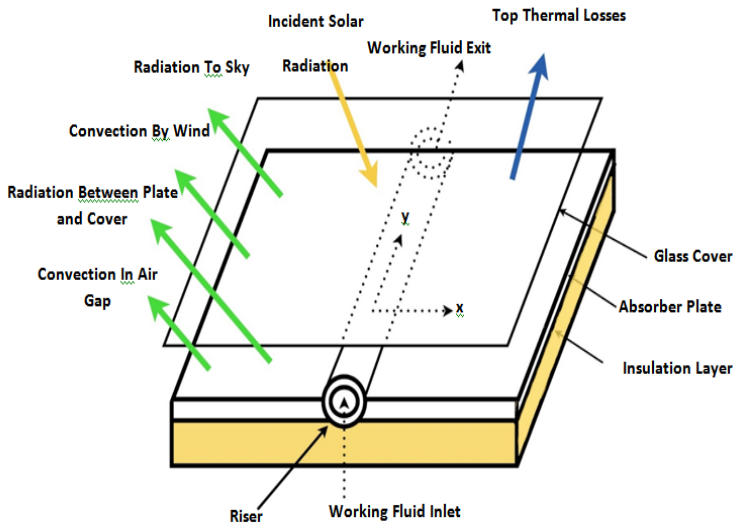


**Fig. 1.2** Diagrammatic representation of a flat plate solar collector panel.

The main components of an FPC include:

**i. Absorber Plate**

The absorber plate is the primary component accountable for capturing solar radiation and transforming it into thermal energy. It is generally composed of substances with excellent thermal conductivity, like copper or aluminum, and is plated with a selective surface to maximize absorption while minimizing radiation losses.

**ii. Fluid carrying Tubes or Channels**

Heat transfer tubes, often made of copper or aluminum, are connected to the absorber plate to transport the working fluid. The solar heat flux collected by the absorber plate is transferred to the fluid-carrying tube, resulting in a surge in the fluid's temperature to give an useful energy. The fluid can be conventional such as water, oil, glycol etc. or nanofluid-based such as $Al_2O_3$, MgO. CuO, and $TiO_2$ etc.

**iii. Transparent Cover (Glazing)**

A transparent cover, usually made of glass or a polymer-based material, allows sunlight to reach the absorber plate while preventing convective and radiative heat loss.

**iv. Insulation**

Thermal insulation minimizes heat loss from the back and sides of the collector. Common materials include polyurethane foam, mineral wool, and fiberglass, which are used to maintain high thermal retention The use of aerogels as insulation material has also been investigated due to their exceptional thermal resistance and potential to improve the efficacy of flat plates collectors.

**v. Casing or Enclosure**

The entire collector is enclosed within a durable, weather-resistant casing that provides structural support and protection from environmental conditions. The selection of materials and design affects the thermal efficiency and durability of the system

Flat plate solar collectors operate based on fundamental principles of solar radiation absorption and heat transfer. The general working mechanism is outlined as follows:

- **Solar Radiation Absorption:**
  Incoming solar radiation passes via the glass cover and is assimilated by the black-coated absorber plate.
- **Heat Transfer to Working Fluid:**
  The absorbed thermal energy is conveyed to the working fluid circulating through the embedded tubes or channels, raising its temperature.
- **Minimization of Heat Loss:**
  The transparent cover and insulation materials help reduce convection and radiation losses, ensuring more effective heat retention.
- **Circulation and Utilization:**
  The heated working fluid is then transported to a heat exchanger or storage tank, where It can be employed for residential water heating, space heating, or industrial uses

## 1.6 Types of flat plate solar collector

Flat plate collectors can be positioned based on the orientation of the fluid-carrying tube

- **Category I**
  Here the tubes are bonded with below the plate. At the intersection of the plate and tube, the temperature over the plate and inside the tube may vary due to presence of bond conductance. Graphically it can be shown as

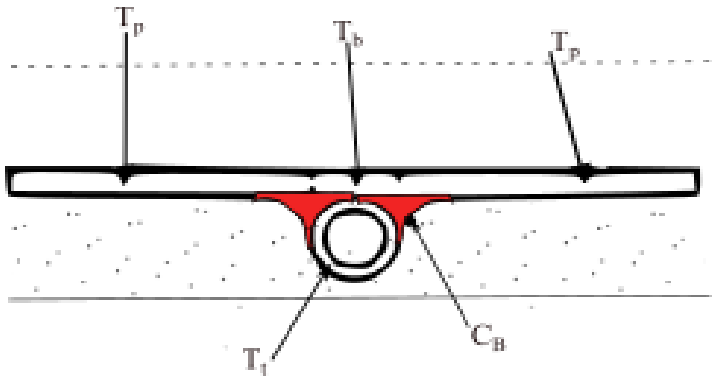


**Fig. 1.3 (a)** Category I type FPSC

**Category II**

Here the tubes are bonded with in line to the plate. At the intersection of the plate and tube, the temperature over the plate and inside the tube are equal as there is no bond conductance. Graphically it can be shown as

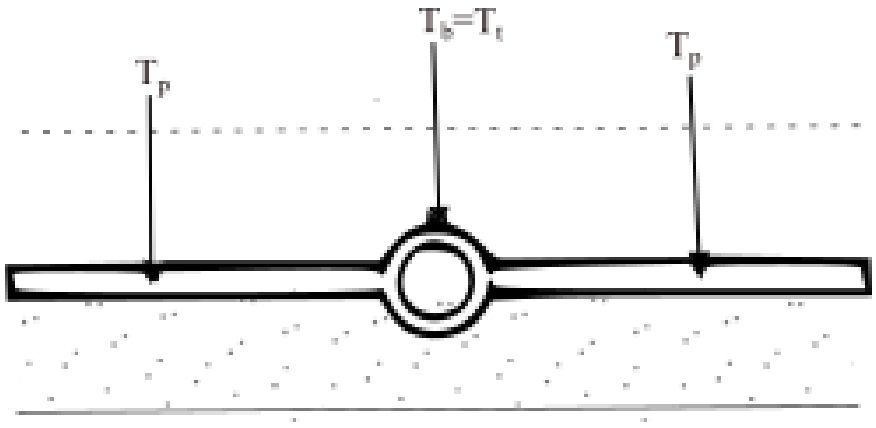


**Fig. 1.3 (b)** Category II type FPSC

- **Category III**

  Here the tubes are bonded with above the plate. At the intersection of the plate and tube, the temperature over the plate and inside the tube may vary due to presence of bond conductance. Graphically it can be shown as

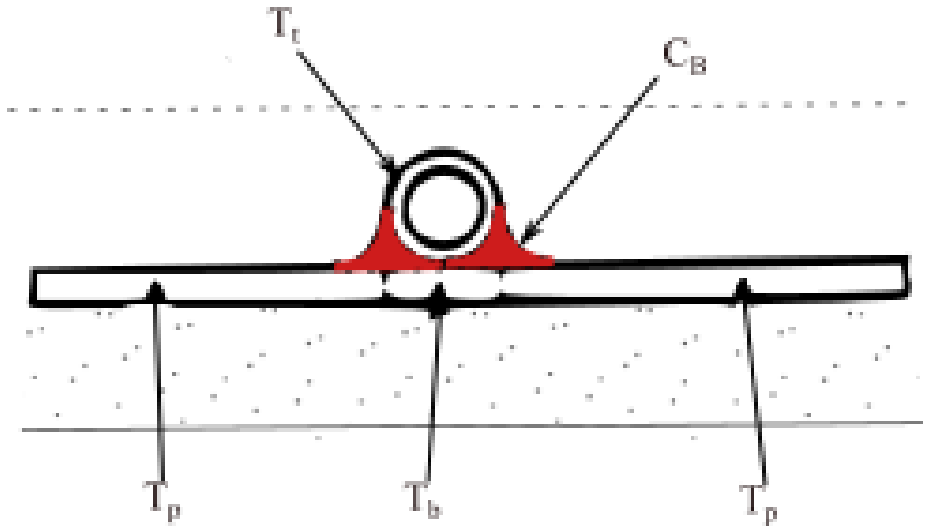


**Fig. 1.3 (c)** Category III type FPSC

Each category of solar collectors is designed to meet specific energy demands, and the choice is made based on economic viability and climatic circumstances, ensuring the efficient and sustainable utilization of solar thermal energy across various sectors [13-15]. However, improving the efficiency of these collectors remains a critical research area. The widely used theoretical model of the flat-plate collector is predicated on the first work of Hottel and Woertz in 1942 [17], further developed by Whillier [18] and Bliss [19], and is commonly known as the Hottel-Whillier-Bliss (H-W-B) model. This model is essentially one-dimensional and follows a lumped formulation. Extensive theoretical and

empirical research has been conducted to assess the influence of various factors on solar collector performance. However, despite these investigations, a complete theoretical investigation is missing in this area. The objective of this study is to address this gap by providing a more rigorous analytical approach. Over period of time, numerous modifications have been introduced for FPSCs performance, namely; Duffie and Beckman with considering fixed thickness, thermal conductivity and overall loss coefficient [15,27], effects of axial conduction in absorber plate [20], non-linear model for absorber plate [21-25], with step-change in absorber plate local thickness [26], different shapes of absorber plates [28-32], measurement of bond conductance [33,34] with considering variable thermal conductivity & overall loss coefficient [35,36], Many authors with different aspects [37-41] have put their contribution for the improvement of performance of FPSCs. A two-dimensional study is expected to provide a precise assessment of flat-plate solar collectors instated of one-dimensional. With this some authors considered two dimensional modeling of absorber plate [42-51]. The 2D analyses have been done analytically and numerically with considering different boundary conditions. Due to complexity of 2D heat conduction 1D modification is proposed by the author of [52, 53]. Analytical studies of flat plate collectors are generally conducted under steady state condition however, the unsteady-state operating conditions will be appropriate due to change in solar flux, wind velocity etc.. With considering the transient effect many have contributed [54-74] their efforts towards the analysis of FPSCs. During analysis many have used the classical Fourier heat conduction model. Fourier's law posits that heat flux has a linear correlation with the temperature gradient, and assumes an infinite thermal wave propagation speed. This paradox contradicts

Einstein's theory of relativity while still following the thermodynamics' second law of. To resolve this ambiguity, a hyperbolic heat conduction equation derived from a relaxation model is introduced, ensuring a limited thermal propagation velocity. This methodology is frequently termed non-Fourier heat conduction and called as the Cattaneo-Vernotte model [75-83]. Considering this few work have been devoted towards the study of Fourier and non-Fourier heat conduction in the flat-plate solar collector's absorber plates [84-88]. The non-Fourier approach has also been employed by several researchers [89-91] to analyze heat transfer in fins.

The performance evaluation of any thermal system is assessed using the principles of both the first and second laws of thermodynamics simultaneously. The first law, based on energy conservation, ensures that the total energy input is accounted for in various forms, such as useful work and heat losses. Meanwhile, the second law provides insight into the quality of energy conversion by assessing entropy generation and irreversibilities within the system. A comprehensive thermodynamic analysis, incorporating energy and exergy evaluations, helps in identifying the direction of various loss thus the potential for improvement in efficiency and the performance of thermal systems can be optimized. Exciting studies using the energy and exergy principles on solar collectors were also undertaken to maximize the characteristics and operating circumstances of these systems [92–100]. Furthermore, the working fluid is essential in the heat transfer assessment of the absorber plate in a flat-plate solar collector, as it is responsible for carrying heat away from the absorber plate. Compared to conventional fluids like water, nanofluids enhance the execution of the absorber plate, improving the overall efficiency of the flat-plate solar collector. Utilizing various

nanofluids can enhance both energy output and efficiency in flat plate solar collectors [101-157].

## 1.7 Organization of the thesis

This thesis is arranged into eight chapters, each covering a distinct aspect of the study. A brief summary of each chapter is provided as follows:

***Chapter 1*** gives brief Introduction provides an overview of flat-plate solar collectors, highlighting their fundamental working principles, design, and significance in harnessing solar energy. It discusses their role in various thermal applications. Additionally, this chapter outlines the merits of flat-plate solar collectors compared to other solar thermal technologies, focusing on their simplicity, durability, and ability to operate under different climatic conditions. The chapter sets the foundation for the study by explaining the importance of refining the thermal performance of these collectors through advanced heat transfer techniques and innovative working fluids.

***Chapter 2*** presents a comprehensive literature survey on the advancements in flat-plate solar collector technology over the past two decades. It explores various research studies focused on enhancing the performance of these collectors through innovative design modifications, improved heat transfer techniques, and the application of sophisticated working fluids. The chapter reviews key contributions from researchers, highlighting developments in absorber plate materials, coatings, and flow channel configurations. Additionally, it examines the role of nanofluids and hybrid nanofluids in improving thermal efficiency. By analyzing past and recent works, this chapter provides a strong foundation for

identifying research gaps and justifying the need for further investigation in this field.

***Chapter 3,*** the thermal analysis of absorber plates in flat-plate solar collectors has traditionally been conducted using one-dimensional heat conduction models. However, due to the inherent shape and thin structure of absorber plates, a two-dimensional temperature circulation naturally occurs. While temperature variation in the thickness direction is often negligible, a comprehensive two-dimensional heat flow analysis remains essential. In this chapter an analysis of the two-dimensional temperature distribution in the absorber plate of a flat-plate solar collector using an approximate analytical approach. Determining the temperature field under two-dimensional heat flow and actual boundary constraints is challenging with exact analytical methods. As an alternative, numerical techniques such as the finite difference method (FDM) offer a viable solution; however, they come with increased computational complexity. To overcome this challenge, an approximate analytical model has been developed to provide a simplified yet effective means of evaluating the temperature distribution. The accuracy of this approach has been validated through a comparative analysis with numerical results, showing strong agreement between the two methods. The deviations between the analytical and numerical results do not exceed 5%, demonstrating the reliability of the proposed model. This approach serves as an efficient alternative to computationally intensive numerical techniques, making it a valuable tool for thermal analysis in solar energy applications.

***Chapter 4*** presents a closed-form solution to the energy equation, establishing a two-dimensional heat flow model for the absorber plate while accounting for nonlinear temperature variance at the plate-tube section. The energy equation is solved by means of the method of

variable separation, and for validation, the same equation is numerically solved using the finite difference method (FDM). The results demonstrate a close agreement between the analytical and numerical solutions, confirming the accurateness of the projected model. Ultimately, this study develops a reliable analytical model for practical thermal examination of absorber plates in solar collectors, ensuring precise and efficient implementation.

***Chapter 5*** introduces a modified one-dimensional method based on the trapezoidal rule to approximate two-dimensional heat conduction on the absorber plate of flat plate solar collector. The results indicate that the modified 1-D model closely aligns with the 2-D model, demonstrating its improved accuracy over the conventional 1-D classical model. Consequently, the classical 1-D approach is insufficient for accurately predicting absorber plate performance. The proposed modified 1-D model offers a simplified yet effective method for understanding and calculating temperature distributions, making it a valued tool for thermal analysis in solar collector applications.

***Chapter 6*** analytically investigates both Fourier and non-Fourier heat conduction in the absorber plate of a flat-plate solar collector. To account for non-Fourier behavior, the single-phase-lag model incorporating the loss coefficient is applied to the energy equation. The analytical results are validated through computational simulations using the finite difference method (FDM).Additionally, the study explores the impact of key the influence of parameters—including the Vernotte number, dimensionless time, and thermo-geometric parameter—on the heating behaviour of the absorber plate. The proposed model is further compared with the published results of Kundu and Lee, who did not consider the phase lag associated with the loss coefficient. The observed differences in

temperature distribution highlight the significance of phase lag effects in accurately predicting the transient thermal response of the absorber plate.

***Chapter 7*** investigates the thermodynamic performance of a flat-plate solar collector (FPSC) utilizing ternary nanofluid as a heat transfer medium. The study evaluates the effects of mono, hybrid, and ternary nanofluids (THNF) on system efficiency groundedon energy and exergy study.Specifically, the analysis considers CuO–MgO–$TiO_2$ ternary nanofluids, MgO–$TiO_2$ binary nanofluid, and mono nanofluids including MgO/water, $TiO_2$/water, and CuO/water. Their performance is studied with that of nanoparticle volume contentvarying from 0.1% to 0.5% by energy and exergy analysis. The findings highlight the superior efficiency of nanofluids in improving the thermal characteristics of flat-plate solar collectors, demonstrating their possible for improving solar energy operation.

***Chapter 8*** presents the key findings and common observations derived from the research. The conclusions are summarized in concise points, highlighting the significant outcomes of the study. This section offers an extensive summary of the research contributions and insights gained, reinforcing the effectiveness of the proposed methods and models in enhancing the thermal performance of flat-plate solar collectors.

This chapter also outlines the future scope of the research, highlighting potential areas for further exploration and development. This section discusses possible enhancements to the proposed models, advanced computational techniques, and the integration of innovative materials or hybrid nanofluids to enhance the efficiency of flat-plate solar collectors.

# Chapter 2

# Literature Review

## 2.1 Introduction

Flat plate solar collectors (FPSC) are a vital factor of solar thermal systems, with ongoing research focused on enhancing their efficiency and thermal performance. Despite significant advancements, improving their efficiency remains a critical challenge. Extensive studies have explored heat transfer mechanisms, fluid dynamics, and material optimization to improve their overall effectiveness. Two-dimensional (2D) analysis provides a more detailed understanding of temperature distribution and heat losses compared to conventional one-dimensional models, making it a valuable tool for performance evaluation. This chapter presents a comprehensive review of existing research on FPSCs, covering mathematical modeling, experimental studies, and numerical simulations, with a specific focus on 2D analytical approaches, Fourier and non-Fourier heat transfer models, and energy-exergy analysis. The review highlights key advancements, identifies research gaps, and establishes the foundation for the present study.

## 2.2 One-dimensional steady state

The widely used theoretical model of the flat-plate collector originates from the foundational work of Hottel and Woertz (1942) [17], later refined by Whillier (1953) and Bliss (1959). This model, commonly known as the Hottel-Whillier-Bliss (H-W-B) model [18, 19], is primarily

one-dimensional and relies on a lumped formulation. While efficiency factors are introduced to account for the problem's multi-dimensional nature, they assume infinite thermal conductance within the system. Consequently, the model cannot properly anticipate the temperature of the collector plate or the fluid. Furthermore, it does not consider the variation in thermal losses along the length of the collector, from the inlet to the outlet. Since estimating the overall heat-loss coefficient requires knowledge of the plate temperature distribution, the model instead assumes an average plate temperature, which may not always be precise. Additionally, the internal resistances of the plate and tube are neglected.

Starting in the 1970s, interest in solar energy applications for space heating and cooling grew significantly. Given that the economic viability of solar energy systems serves a crucial role in their practical implementation, a more detailed and rigorous analysis of collector models became essential. The HWB model's analysis disregards axial conduction in both the fluid and the receiver. To address this limitation, Phillips [20] developed a closed-form solution that explicitly incorporates the belongings of axial conduction within the receiver. His findings reveal that ignoring axial conduction can consequence in errors of up to 30% in calculating the collector heat removal factor, though the typical deviation for most collectors is less than 12%. This study highlights the importance of accounting for axial conduction in the thermal performance of solar collectors to improve the accuracy of performance predictions.

Cooper and Dunkle [21] developed a non-linear model for flat-plate solar collectors, addressing the complexities of heat transfer and efficiency prediction. The study incorporated non-linear effects such as radiation losses and temperature-dependent properties to enhance the

accuracy of performance estimations. Results demonstrated that the non-linear approach provides a more precise representation of collector behavior compared to traditional linear models.

In another work Chiou [22] investigated the influence of non-uniform fluid flow dispersion on the thermal characteristics of solar collectors, highlighting its impact on heat transfer efficiency. The study analyzed how variations in flow distribution lead to temperature imbalances, reducing overall collector performance. Findings suggested that optimizing flow uniformity improves heat absorption and minimizes thermal losses, thereby enhancing efficiency.

Francken [23] explored the effectiveness of flat plate solar collectors, focusing on key factors that influence their thermal performance. The study examined various design parameters, including absorber plate material, collector orientation, and heat loss factors, to assess their impact on efficiency. Findings indicated that optimizing these variables significantly enhances the collector's overall effectiveness in capturing solar energy. This technical note provides valuable insights for improving flat plate collector designs and optimizing their use in solar thermal applications.

O'Brien-Bernini [24] developed a performance model for non-metallic flat plate solar collectors, exploring their thermal efficiency and feasibility as an alternative to conventional metallic collectors. The study analyzed the impact of material properties, absorber design, and insulation on overall performance, demonstrating that non-metallic materials can offer cost-effective and durable solutions for solar thermal applications. The proposed model provided insights into optimizing

collector design for improved energy absorption and heat retention, contribute to the progression of sustainable solar energy knowledges.

Samdarshi and Mullick [25] analyzed the primary thermal loss coefficient of flat plate solar collectors featuring single and double glazing, focusing on its impact on overall collector efficiency. The study examined how glazing configurations influence heat retention and thermal losses, with particular attention to the differences between single and double glazing. Results showed that double glazing substantially lowers thermal loss, enhancing the thermal recital of the collector. This work gives valuedvisions into optimizing glazing choices for improving the energy efficiency of flat plate solar collectors.

Hollands and Stedman [26] examined an absorber plate fin with a step-varried in local thickness to optimize and enhance the thermal behaviour of solar collectors. The work focused on how variations in the thickness of the absorber plate fin affect heat transfer efficiency and fluid flow distribution. Results demonstrated that strategically varying the thickness improves heat absorption and reduces thermal losses, leading to better overall collector performance. This research offers valuable design insights for optimizing absorber plate geometry in solar thermal systems.

Matrawy and Farkas [27] conducted a proportional study on the behaviour of three diverse types of solar collectors for water heating, evaluating their efficiency under varying operating conditions. The research analyzed flat plate, evacuated tube, and concentrating collectors, highlighting their thermal performance, heat retention capabilities, and suitability for different applications. Results indicated that while each

collector type has distinct advantages, selection depends on factors such as climate, cost, and efficiency requirements.

Keeping in view for the shape of flat plate collector Kundu [28,32] conducted a performance investigation and to optimize the absorber plates with dissimilar geometries for flat-plate solar collectors, presenting a proportional study to evaluate their thermal efficiency. The research examined various absorber plate designs, including their material properties and geometric configurations, to determine the optimal structure for enhanced heat absorption and reduced thermal losses. Findings indicated that specific geometries significantly improve collector performance, offering guidance for designing more efficient solar thermal systems.

Kaushika and Sumathy [29] reviewed solar transparent insulation materials (TIMs) and their role in enhancing the efficiency of solar energy systems. The work explored various TIM types, their optical and thermal properties, and their applications in passive and active solar technologies. The review highlighted how TIMs reduce heat loss while allowing maximum solar radiation transmission, improving the performance of solar collectors and building-integrated solar systems. This research provides a comprehensive understanding of TIMs' potential in increasing energy efficiency and sustainability in solar thermal applications.

Kalogirou [30] provided a complete evaluation of solar thermal collectors and their applications, covering various collector designs, counting flat plate, evacuated tube, and concentrating collectors. The study discussed their working principles, efficiency factors, and

suitability for various thermal used like space heating, water heating, and industrial processes. The research emphasized advancements in solar thermal technology and the potential for integrating these systems into sustainable energy solutions. This work serves as a fundamental reference for optimizing solar collector performance and expanding their applications in renewable energy systems.

Kundu [31] used a step-finned flat-plate collector to examine how the temperature of the collector fluid at the intake affected the efficiency of a solar-assisted absorption system. The study examined how variations in the inlet temperature affect the thermal efficiency and heat transfer features of the system. Outcomes indicated that higher inlet temperatures progress the thermal effectiveness of the collector, resulting better heat absorption and system efficiency. This study delivers valuable perceptions into optimizing the operating conditions of solar-assisted absorption systems for enhanced energy utilization.

Kundu [32] investigated the thermal performance and optimal geometric configuration of absorber plate fins with a recto-trapezoidal cross-section in flat-plate solar collectors. The analysis emphasized the influence of fin geometry on heat transfer enhancement and associated flow behavior. The findings demonstrated that the recto-trapezoidal fin profile provides superior thermal efficiency compared to conventional shapes, primarily due to improved heat absorption and a reduction in conductive thermal resistance within the fin. The study highlights the importance of geometric optimization in absorber plate design and provides a useful foundation for improving the overall performance of solar thermal collector systems.

Badran et al. [33] examined the bond conductance in solar collector absorber plates, a critical factor influencing thermal performance and heat transfer efficiency. The study examined different bonding techniques between the absorber plate and the heat transport medium, analyzing their impact on overall collector efficiency. Experimental findings demonstrated that optimizing bond conductance significantly enhances heat transfer, reducing thermal resistance and improving energy absorption. This research provides valuable insights into material selection and fabrication methods for improving the effectiveness of solar thermal collectors.

Villar et.al. [34] performed numerical 3-D heat flux simulations on flat plate solar collectors to analyze their thermal performance. The study focused on modelling heat transfer processes, including the effects of fluid flow and thermal losses, using three-dimensional simulations. Results provided detailed insights into the distribution of heat flux across the collector surface, helping to identify design improvements for more efficient energy capture.

Kundu [35] developed an analytic technique for assessing the thermal behaviour and the improvement of an absorber plate fin with capricious thermal conductivity and overall loss coefficient. The study analyzed how changes in thermal properties and loss parameters impact the efficiency of flat-plate solar collectors. The outcomes indicated that accounting for variable thermal conductivity significantly improves the accuracy of performance predictions, while optimizing the overall loss coefficient enhances heat retention and efficiency. This research provides a deeper understanding of absorber plate fin design for more efficient solar thermal systems.

Kundu et al.[36] performed a statistical investigation on the operational design parameters of a solar-powered vapour absorption cooling system using an absorber plate with various profiles. The research focused on how various absorber plate geometries affect system performance, particularly in terms of heat absorption and efficiency under different operating conditions. The study highlighted that optimizing the absorber plate profile can pointedly improve the thermal performance and overall efficiency of solar-powered cooling systems. This work provides valuable insights for refining the design of solar absorption cooling systems for better energy utilization.

Alvarezet.al [37] presented an investigational analysis with numerical simulation using Finite Element Method (FEM) for a newly premeditated flat-plate solar collector featuring a ridged channel and an increased surface area in direct contact with the heat transfer fluid. The collector's thermal and hydrodynamic performance validated against investigative outcomes for a conventional fin-and-tube solar collector.

Roberts and Forbes [38] developed an analytical model to assess the immediate performance of glazed flat plate solar water heaters, emphasizing the role of absorber plate properties in thermal performance. The findings highlight that increasing absorptance enhances energy absorption, while lower emittance minimizes radiative heat losses, leading to improved overall performance. However, the study cautions against reducing emittance at the expense of absorptance, as it may negatively affect efficiency.

Subiantoro and Tiow [39] developed analytical models to compute and optimize the performance of single and double glazing flat

plate solar collectors, considering normal and small air gap spacing. The study analyzed the effect of glazing configurations on heat transfer, thermal losses, and overall collector efficiency. Findings indicated that double glazing with optimized air gap spacing reduces heat loss while maintaining high solar transmittance, enhancing collector performance.

Eismann and Prasser [40] addressed the inaccuracies in traditional analytical models of flat plate solar collectors caused by neglecting edge effects. They introduce a correction factor that accounts for heat losses at the absorber's edges, enhancing the precision of performance predictions. This advancement is particularly significant for optimizing collector designs, especially in systems with high-temperature gradients or compact configurations.

Bhowmik and Amin [41] examined the effectiveness enhancement of flat plate solar collectors by integrating reflectors to increase solar radiation absorption. Their study demonstrated that adding reflectors significantly improves thermal performance by directing additional sunlight onto the collector surface, thereby increasing heat gain and overall efficiency. Experimental results showed a notable rise in collector efficiency, making this approach a cost-effective and practical solution for optimizing solar energy utilization. This research provides a strong foundation for further studies on solar collector modifications to enhance energy capture and sustainability in solar thermal applications.

In all the analyses discussed above, a one-dimensional heat conduction equation has been used. However, since the absorber plate of the collector exhibits a two-dimensional temperature distribution, a more accurate performance evaluation requires a two-dimensional analysis.

Consequently, extensive research has been conducted on two-dimensional heat conduction equations under various boundary conditions. A selection of studies on two-dimensional analysis of flat-plate solar collectors is listed below.

## 2.3 Two-dimensional steady state

Grossman et.al. [42] conducted an in-depth heat transfer study of a flat-plate solar collector, focusing on its two-dimensional geometry, which maximizes the contact area among the fluid and the sun-exposed collecting surface. Their analysis provided temperature and heat flow circulations across both dimensions of the collector, while also investigating the expansion of the thermal boundary layer. The study calculated overall efficiencies under conditions of uniform solar heat influx and flexible heat losses from the absorber plate.

Rao's study [43] presents a comprehensive two-dimensional theoretical model of a flat-plate solar collector, focusing on heat transfer dynamics, temperature distribution, using analytically and by perturbation method. The system, enabling accurate performance evaluation under varying operating conditions without assuming an average plate temperature. Unlike traditional lumped models, which may overestimate efficiency in certain flow regimes, this approach provides a more precise assessment of collector performance.

Rahman et.al. [44] presented a two-dimensional mathematical model for analyzing the thermal behaviour of an evacuated tubular solar collector. The collector features a thin flat plate spanning its diameter as the absorbing surface. The study develops a detailed performance model

by applying energy balance equations separately to the collector plate and tube. A zero-capacitance assumption is found to be adequate when using hourly meteorological data, allowing for a steady-state analysis of the system. By incorporating conduction, convection, and radiation effects, the model provides insights into temperature distribution, heat flux variations, and efficiency under different operating conditions.

Lund's study [45] presents a comprehensive thermal analysis of parallel-flow flat-plate solar collector absorbers, focusing on heat transfer mechanisms, temperature distributions, and overall thermal efficiency. The research develops a mathematical model that accounts for solar radiation absorption, conductive and convective heat transfer, and fluid flow dynamics to predict absorber performance.

Wijeysundera and Thevendran [46] presented a two-dimensional heat transfer examination of the thermal-trap collector, focusing on its thermal performance and efficiency. The study develops a mathematical model to examine temperature distributions, heat flux variations, and overall heat transfer mechanisms within the collector.

Hobson and Norton [47] presented a detailed analysis of heat transfer and fluid flow in direct thermosyphonic solar water heaters, emphasizing the impact of small buoyancy-driven flow rates. A two-dimensional formulation of the collector energy equations was employed to accurately simulate heat transfer and thermal capacitance effects. Incorporating a non-isothermal friction factor correlation for riser pipe energy losses resulted in predicted flow rates that matched experimental values within 2%. For the investigated laminar flow rates and storage configuration, axial conduction in the store walls was found to dominate

thermocline relaxation. An indoor microcomputer-controlled test facility simulated real operating conditions, with predicted system responses aligning well with experimental observations, achieving a heat delivery accuracy within 2.8%.

Kazeminejad's [48] study presents a numerical investigation of a two-dimensional parallel-flow flat-plate solar collector, focusing on thermal characteristics and heat transfer characteristics. A computational scheme is established to simulate temperature distributions, heat flux variations, and efficiency under various operating conditions. The study also compares one- and two-dimensional analyses to optimize collector design. Results indicate that while the performance curves and isotherms align closely, one-dimensional analysis slightly deviates from two-dimensional results, mainly at low mass flow rates. This highlights the importance of two-dimensional modeling for more accurate performance predictions in solar collector design.

Varol and Oztop [49] conducted relative numerical research on natural convection heat transfer in inclined wavy and flat-plate solar collectors to evaluate their thermal performance. By means of computational fluid dynamics (CFD) simulations, the study analyzes heat transfer and fluid flow characteristics under isothermal boundary conditions for the absorber and cover.

Li and Chen [50] applied entransy theory to optimize heat transfer in flat-plate solar collectors, providing a novel perspective on thermal performance enhancement. The study focuses on using entransy dissipation analysis to evaluate and improve heat transfer efficiency within the collector. By optimizing energy transport processes, the

research identifies key factors influencing collector performance, including absorber plate design, fluid flow characteristics, and heat loss mechanisms.

Mortazavinejad and Mozafarifard [51] conducted a numerical examination of two-dimensional heat transfer in the absorber plate of a flat-plate solar collector by means of the dual-reciprocity technique grounded on the boundary element approach. Their study focused on accurately modeling heat transfer mechanisms within the collector to enhance its thermal performance.

The two-dimensional analysis can be modified to one-dimensional one by applying trapezoidal rule. With this concept Kundu and Lee [52], Kundu et al. [53] presented an in-depth analysis of wet fins, optimizing their design using modified one-dimensional (1-D) and two-dimensional (2-D) approaches and the results shows that a 2D heat conduction models have been extensively studied for to deliver a further precise calculation of temperature circulation and thermal performance using modified 1D by using trapezoidal method.

Further the authors [54, 55] performed a transient multidimensional second law analysis and numerical analysis respectively for solar collectors subjected to time-varying insolation with diffuse components. Results highlighted how dynamic variations in insolation affect the thermal performance, contributing to the optimization of solar collector designs for enhanced energy efficiency and sustainability.

Previous research has predominantly focused on evaluating the behaviour of solar collectors under steady-state situations. However, in

practical applications, variations in insolation, ambient temperature, and wind conditions significantly influence their operation, requiring a transient analysis to understand these dynamic effects. Numerous studies in the literature have examined transient assessments of absorber plate fins, offering valuable insights into how changing environmental parameters affect the thermal efficiency of flat-plate solar collectors. Below is a compilation of studies on transient analyses of flat-plate solar collectors.

## 2.4 one-dimensional unsteady state

To address some of the limitations of HWB model, Duffie and Beckman [56] refined the lumped analysis by incorporating the resistances between the tube and the fluid. They first derived an expression for the average fluid temperature and then calculated the average plate temperature by accounting for the thermal resistance between the two. The study examined the thermal response of the collectors under varying conditions, providing a detailed understanding of how transient effects influence efficiency and energy capture.

Grossman et.al. [57] conducted a heat transfer examination of a flat-plate solar energy collector, focusing on the key thermal processes that govern energy absorption and heat loss. The study examined the effects of various factors, such as collector design, material properties, and environmental conditions, on the overall efficiency of the system. Results provided valuable insights into optimizing heat transfer mechanisms, leading to upgraded behaviour and energy utilization in solar thermal applications.

De Ron [58] established a dynamic model to simulate the effectiveness of a flat-plate solar collector, focusing on the transient thermal behavior and its impact on system efficiency. The study incorporated factors like fluid flow, heat loss, and solar radiation variations to accurately predict collector performance over time. Experimental verification of the model showed strong agreement with real-world data, validating its applicability for designing and optimizing solar thermal systems.

Mather [59] explored the transient response of solar collectors, focusing on how fluctuations in solar radiation and temperature affect their performance over time. The study analyzed the time-dependent thermal behavior of collectors, emphasizing the impact of start-up conditions and dynamic thermal responses on efficiency. Results indicated that understanding transient effects is crucial for optimizing collector performance, particularly under varying environmental conditions.

Tiwari and Srivastava [60] presented a simple transient analysis of plate temperature in flat-plate solar collectors, focusing on the time-dependent temperature variations and their effect on collector performance. The study established an logical model to envisage the transient thermal characteristics of the collector's absorber plate under different operating conditions. Results showed how factors like solar radiation and fluid flow influence plate temperature and overall efficiency.

Saito et.al. [61] examined the transient response of flat-plate solar collectors under periodic solar intensity variations, focusing on how fluctuating solar radiation impacts the thermal behaviour of the collector

over time. The study analyzed the dynamic temperature changes and heat transfer efficiency, providing insights into the collector's ability to adapt to varying solar intensity. Results highlighted that accounting for periodic intensity variations is vital for optimizing the enterprise and operation of solar thermal systems.

Kamminga [62] explored the knowledges of a solar collector test method utilizing Fourier transfer functions, aiming to improve the accuracy and efficiency of performance evaluations. The study focused on applying Fourier analysis to model the thermal behavior and transient response of solar collectors under varying conditions. By using transfer functions, the research provided a more precise way to assess thermal dynamics and efficiency. Results demonstrated that this method enhances the reliability of solar collector testing, offering value dperceptions for improving the enterprise and performance of solar thermal systems.

Yadavet.al. [63] conducted a transient examination of parallel flat-plate water collectors, focusing on the dynamic thermal performance under varying environmental conditions. The study examined how fluctuations in solar radiation, water flow, and temperature affect the performance of parallel configurations of flat-plate collectors. The outcomes presented that optimizing these factors can significantly enhance collector performance and energy efficiency.

Zhao [64] conducted a transient simulation of flat-plate solar collectors, focusing on the time-dependent thermal characteristics under varying environmental conditions. The study utilized dynamic modeling techniques to model the thermal response of the collector to changes in solar radiation, ambient temperature, and fluid flow. Results indicated the

significant impact of transient effects on collector efficiency and highlighted the importance of incorporating these variations in design and performance predictions.

Zeroual et.al.[65] compared two dynamic test approaches for evaluating the efficiency of solar flat-plate collectors. The study assessed the effectiveness and accuracy of each testing approach in capturing transient thermal responses and efficiency under varying conditions. Results demonstrated that both methods provided valuable insights, with specific advantages in different testing scenarios.

Amer et.al. [66,67] established a transient method for testing flat-plate solar collectors, aiming to improve the accuracy and reliability of performance evaluations under dynamic conditions. The study introduced a testing approach that accounts for time-dependent changes in temperature and solar radiation, providing more detailed insights into the collector's thermal behavior. Results highlighted the method's effectiveness in capturing transient energy variations, offering a better understanding of solar collector performance over time

El-Adawi [68] familiarized a new methodformodelling flat-plate solar collectors using the Fourier transform technique, aiming to improve the accuracy of thermal performance predictions. The study utilized Fourier transforms to analyze heat transfer processes in the collector, allowing for a more efficient evaluation of transient thermal behavior and system efficiency under varying solar radiation conditions.

Dhariwal and Mirdha [69] developed analytical equations to model the response of flat-plate collectors under numerous transient situations, focusing on the impact of time-varying solar radiation and

environmental factors on collector performance. The study provided a set of equations to forecast the thermal response of the collector over time, helping to understand how dynamic conditions influence efficiency.

The author of [70, 71] developed a comprehensive numerical model for flat-plate solar thermal system, aiming to accurately simulate the thermal performance under varying operational conditions. The study incorporated complex aspects such as heat transfer, fluid dynamics, and temperature variations to predict the collector's behavior.

Zima and Dziewa [72] modeled the operation of liquid flat-plate solar collectors in transient states, focusing on the time-dependent thermal behavior under varying environmental conditions. The study developed a model to simulate the dynamic response of the collector, considering aspects like fluctuating solar radiation, fluid temperature, and heat transfer processes. Results showed the impact of transient effects on system performance, helping to optimize collector design and operation for improved efficiency.

Zima and Dziewa [73] established a mathematical model for heat transfer in liquid flat-plate solar collector tubes, focusing on the complex thermal interactions between the absorber plate, fluid, and surrounding environment. The study incorporated key parameters like fluid flow dynamics, temperature gradients, and heat loss mechanisms to forecast the collector's behaviour under various operating circumstances.

Rodríguez et. [74] investigated the transient behavior of flat-plate thermal solar collector performance beneath working circumstances, presenting a detailed model explanation and investigational validation. The study established a comprehensive model to simulate the collector's

thermal performance over time, accounting for dynamic aspects like solar radiation variations and fluid temperature changes.

In the above analysis, traditional heat conduction models based on Fourier's law assume instant thermal wave propagation, resulting in a parabolic heat equation. This assumption contradicts Einstein's theory of relativity, especially at extremely short time scales or near absolute zero. To address this issue, a finite thermal wave propagation speed has been proposed, introducing a delay in heat flux response. This approach, known as non-Fourier heat conduction, was developed by Cattaneo and Vernotte. By incorporating relaxation time, it transforms the governing equation into a hyperbolic form, overcoming the limitations of classical models. A selection of studies on non-Fourier analysis is listed below.

Peshkov [75] introduced the concept of second sound in helium II, a quantum hydrodynamic phenomenon where heat propagates as a wave rather than by diffusion. This groundbreaking study provided experimental evidence for the existence of temperature waves in super fluid helium, challenging classical heat conduction theories. Peshkov's work laid the foundation for further research into non-Fourier heat transfer, influencing the study of anomalous thermal transport in various materials, including high-temperature superconductors and microscale heat transfer applications.

Cattaneo [76] introduced a modified form of the heat equation that removes the paradox of immediate heat circulation, which was a limitation of the classical Fourier heat conduction theory. By incorporating a time delay in the heat transfer process, this formulation, now known as the Cattaneo equation, accounts for finite speed of heat

propagation, addressing the unrealistic assumption of infinite heat speed in traditional models. Cattaneo's work laid the foundation for non-Fourier heat conduction theories, contributing significantly to the study of transient heat transfer and influencing subsequent developments in thermal transport, particularly in systems involving high-speed or complex materials.

Vernotte [77] addressed the paradoxes inherent in the continuous theory of heat conduction by analyzing the limitations of the classical heat equation. He highlighted the issues arising from the assumption of infinite propagation speed for heat, which led to non-physical results, such as the instantaneous transmission of thermal energy. Vernotte proposed a modification to the classical theory, incorporating a finite propagation speed for heat, similar to Cattaneo's later work, to resolve these paradoxes. His contributions laid the groundwork for the development of non-Fourier heat conduction models, providing a more realistic framework for analyzing heat transfer in various physical systems.

Tzou [78, 79] carried out an investigational study on the lagging performance in heat propagation, focusing on how delayed thermal responses affect the performance of heat transfer systems, including solar collectors. The research provided experimental support for the concept of heat propagation lag, analyzing how this phenomenon influences efficiency and thermal dynamics. Results showed that the lag in heat transfer can significantly affect system performance, especially under varying environmental conditions.

Antak [80] explored the key features of analytical resolutions for hyperbolic heat conduction, focusing on the mathematical modeling of heat transfer in materials under transient conditions. The study examined how hyperbolic equations, which account for finite speed of heat propagation, provide more accurate predictions compared to classical Fourier-based models, especially in scenarios involving rapid temperature changes. Results highlighted the importance of using hyperbolic heat conduction models for systems where thermal waves and transient effects play a significant role.

Lin [81] investigated the non-Fourier effects on fin effectiveness underneath periodic thermal circumstances. The study developed a model that incorporates the impact of non-Fourier heat conduction, accounting for thermal lag and memory-dependent effects in fins subjected to periodic heating and cooling cycles. The research provided a thorough analysis of temperature circulation and heat flux variations, demonstrating how non-Fourier effects can influence the thermal efficiency of fins in real-world applications.

Moosaie [82] investigated non-Fourier heat conduction in a finite medium subjected to arbitrary non-periodic surface disturbances, focusing on the thermal response of materials when subjected to irregular and transient heat sources. The study explored heat transfer dynamics beyond the classical Fourier law, accounting for finite speed of heat propagation and the resulting thermal effects.

Ahmadikia and Rismanian [83] provided an analytical solution to non-Fourier heat conduction problems in a finite medium with recurring boundary circumstances. By applying this non-Fourier approach, the

researchers were able to model transient heat conduction more accurately, especially in systems where rapid or irregular temperature changes occur.

Kundu and Lee [84] conducted a Fourier and non-Fourier heat conduction analysis in the absorber plates of a flat-plate solar collector, focusing on how both classical and non-classical heat transfer models affect the thermal characteristics of solar collectors. The study explored the implications of using non-Fourier models, which account for the finite speed of heat circulation, in contrast to traditional Fourier-based methods. The findings showed that non-Fourier effects can significantly influence the efficiency and heat distribution in solar collectors, especially under rapid transient conditions.

Rodríguez et.al.[85] presented exact and analytic-numerical solutions of lagging models of heat transfer in a semi-infinite medium, focusing on the delayed thermal response that occurs when heat propagation is not instantaneous. The study explored how these lagging effects impact heat transfer dynamics, especially in systems subject to transient thermal conditions. By developing both exact and hybrid analytic-numerical solutions, the researchers provided a more comprehensive understanding of heat conduction in materials with finite thermal wave speeds.

Kundu and Lee [86] presented a non-Fourier analysis to study heat transmission in fins with internal heat generation. Their research developed a model that accounts for both non-Fourier heat conduction effects and the impact of internal heat sources, offering a more accurate representation of thermal behavior in such systems. The study explored the transient temperature distribution and heat flow in fins, providing

valuable insights into the optimization of fin designs for applications with internal heat generation. The findings contribute to the understanding of non-Fourier heat transfer and improve the thermal behaviour prediction in heat dissipation systems.

Bhowmik et.al. [87] conducted an inverse modelling study of a solar collector, incorporating both Fourier and non-Fourier heat conduction to enhance the accuracy of thermal characteristics predictions. The research focused on using inverse methods to estimate key parameters in solar collectors, such as heat transfer coefficients, by considering both classical and non-classical heat conduction effects. The study showed that accounting for non-Fourier heat conduction, which involves finite heat propagation speed, can significantly improve the modeling of transient thermal responses.

Panda et al. [88] conducted an inverse heat transfer analysis to identify key design parameters influencing the effectiveness of a flat-plate solar collector. The research utilized numerical techniques to estimate thermal properties and boundary conditions by minimizing discrepancies between experimental and simulated temperature distributions. The analysis focused on optimizing absorber plate characteristics, heat loss mechanisms, and fluid flow dynamics to enhance overall efficiency. The results provided a systematic approach for improving solar collector design, offering valuable insights for developing more effective and energy-efficient solar thermal systems.

Wankhade et.al.[89] established a non-Fourier heat conduction model to accurately predict the transient thermal response in wet fins. Their study accounted for phase change effects and thermal lag, which

are critical in applications involving condensation and evaporation. By employing an advanced heat conduction framework, the research improved the understanding of heat transfer dynamics in wet fins, leading to more precise thermal performance predictions and potential design optimizations for enhanced efficiency in heat exchanger systems

Mozafarifardet al.[90] carried outa numerical research on anomalous heat conduction in the absorber plate of a solar collector using the time-fractional single-phase-lag (TF-SPL) model. This approach accounts for non-Fourier heat conduction effects, capturing thermal lag and memory-dependent behavior in the heat transfer process. The study examined the effect of fractional-order parameters on temperature distribution and heat flux, providing deeper insights into transient thermal responses. The findings demonstrated the significance of non-Fourier conduction in solar collector absorbers and highlighted the potential for optimizing thermal performance through advanced heat transfer modeling.

Gamaounet al.[91] carried out a numerical work on non-Fourier heat transfer in a moving longitudinal radiative-convective dovetail fin, highlighting the impact of thermal lag effects on heat dissipation. Using advanced heat conduction models, the research analyzed the interplay between conduction, convection, and radiation in a dynamic setting. The study provided insights into optimizing fin geometries for enhanced thermal performance in high-speed applications, contributing to the broader understanding of non-Fourier heat transfer in advanced thermal management systems.

The energy proficiency of solar collectors is traditionally assessed using the first law of thermodynamics, which measures their ability to renovate solar energy into usable thermal energy. However, a more comprehensive evaluation incorporates exergy investigation grounded on the second law of thermodynamics, providing deeper insights into system performance and irreversibilities. Exergy analysis aids in optimizing design parameters and selecting the most effective working fluid properties, including nanoparticle concentration, size, and shape, to enhance efficiency. Extensive research has explored the thermodynamic presentation of flat-plate solar collectors using both energy and exergy analyses. Below is a compilation of works focusing on the exergy analysis of flat-plate solar collectors.

Bejan [92] analyzed the exergy removal from solar collectors under time-varying circumstances, emphasizing the influence of transient solar radiation on system efficiency. The study developed a theoretical framework to evaluate the exergy flow and losses, providing insights into optimizing collector performance. This work serves as a foundational reference for improving thermodynamic efficiency in solar thermal applications.

Fujiwara [93] conducted an exergy analysis to evaluate the efficiency of solar collectors, focusing on the thermodynamic efficiency of energy conversion. The study examined exergy losses in various collector designs and proposed methods to enhance their efficiency. By applying the exergy approach, the research provided a deeper understanding of irreversibilities in solar energy utilization, contributing to the development of more effective solar thermal systems.

Gribik and Osterle [94] investigated the second law efficiency of solar energy conversion, emphasizing the role of exergy in evaluating system performance. The study analyzed the fundamental limits of solar energy utilization and identified key factors affecting efficiency losses.

Chelghoum and Bejan [95] performed a second-law examination of solar collectors incorporating energy storage, focusing on exergy efficiency and entropy generation. The study evaluated how storage capability influences system performance and identified key thermodynamic losses.

Suzuki et.al. [96] applied the exergy concept to determine the optimal operating conditions of solar heat collectors. The study analyzed exergy efficiency and losses under varying conditions, providing insights into maximizing useful energy output.

Suzuki [97] formulated a important relation for exergy equilibrium in solar collectors, providing a theoretical framework to assess energy conversion efficiency. The study examined exergy flow, losses, and entropy generation to enhance system performance evaluation.

Farahat et.al. [98] carried out a work to optimize the exergy on flat plate solar collectors to regulate optimum performance and design parameters analytically. They performed detailed energy and exergy analyses, considering variables like absorber plate area, collector sizes, pipe dia., volume flow rate, fluid temperatures at the inlet and outlet, and overall heat loss coefficient.

Jafarkazemi and Ahmadifard [99] presented a comprehensive theoretical model for the energy and exergy scrutiny of flat plate solar collectors. After validating the model with experimental data, they examineed how design factors like the fluid flow rate, temperature at inlet, working fluid

type, and back insulation thickness, affect collector performance. Their findings indicate that setting the water temperature at the inlet about 40°C above atmospheric temperature and using a lower flow rate enhances overall effectiveness.

Ge et al. [100] conduct an exergy analysis of flat plate solar collectors analytically. The study examines energy efficiency, exergy destruction, and thermodynamic optimization**,** providing insights into performance improvements for solar thermal systems.

The working fluid is a key factor in the thermal performance of flat-plate solar collectors (FPSCs), directly affecting heat transfer capacity and thermal conductivity. Conventional fluids such as water, glycols, and oils have relatively low thermal conductivity, which limits their efficiency. Recent research has explored next-generation working fluids, including mono and hybrid nanofluids, which offer superior thermal and exergy efficiency. This section presents a computational analysis of these advanced fluids and their role in enhancing FPSC performance. Below is a compilation of studies focusing on the exergy analysis of flat-plate solar collectors using various nanofluids.

## 2.5 Analysis using nanofluids

The authors [101,102] experimentally examined impact of nanoparticle concentration on size, and material on thermal conductivity, revealing significant improvements compared to conventional fluids.

Duangthongsuk and Wongwises [103] experimentally measured the temperature-dependent thermal conductivity and viscosity of $TiO_2$-water nanofluids. Their study analyzed how temperature variations

influence the thermo-physical properties of nanofluids, showing enhanced thermal conductivity but increased viscosity at higher concentrations.

Yousefi et al. [104] carried out a investigational study on the consequence of $Al_2O_3$-$H_2O$ nanofluid on the efficiency of flat-plate solar collectors. The research analyzed the influence of nanoparticle absorption and surfactant addition on thermal performance, demonstrating a notable increase in collector efficiency.

Rahman and Aziz [105] investigated heat transfer behaviour of water-based nanofluids ($TiO_2$-$H_2O$, $Al_2O_3$-$H_2O$, and Cu-$H_2O$) over a extending cylinder. Results showed that nanofluids significantly enhance heat transfer rates associated to conventional fluids, with variations depending on nanoparticle properties.

Faizal et. al. [106] conducted a complete energy, economic, and ecological examination for flat-plate solar collectors by means of metal oxide nanofluids of CuO, $SiO_2$, $TiO_2$, and $Al_2O_3$.With numerical techniques and published data the study evaluated thermal efficiency improvements, economic feasibility, and environmental impact. Findings indicated that metal oxide nanofluids enhance heat transfer performance, resulting in higher energy savings and lower carbon emissions.

Alim et al. [107] used multiple metal oxide nanofluids, like $Al_2O_3$, CuO, $SiO_2$, and $TiO_2$, distributed in water for volume portions and mass flow rates in the range of 1–4% and 1–4 L/min, respectively, to analyze the entropy production and pressure drop for a standard flat plate solar collector. The analytical data indicate that, relative to water as an absorbing fluid, the CuO nanofluid may potentially improve the heat transfer coefficient by 22.15% and reduce entropy formation by 4.34%. Additionally, there is a slight 1.58% drop in pumping power

Said et al. [108] performed an experiment on the thermos-physical characteristics of $Al_2O_3$-water nanofluid and its influence on the efficiency of a flat-plate solar collector.The research examined variations in thermal conductivity, viscosity, and heat transfer characteristics, demonstrating improved collector efficiency with nanofluid usage. The study highlighted the potential of $Al_2O_3$ nanofluids in enhancing solar thermal system performance while considering the trade-offs associated with viscosity and pressure drop.

Mahian et al. [109] inspected the efficacy of a mini-channel solar collector using diverse nanofluids. The work assessed heat transfer enhancement, head loss, and overall thermal efficiency under various operating circumstances. The findings exhibited that nanofluids significantly improved the collector's performance by increasing thermal conductivity and convective heat transfer. However, the study also highlighted the need to balance efficiency gains with potential pressure drop challenges.

Madhesh et al. [110] conducted an experimentation on the convective heat transfer and rheological behaviour of Cu-$TiO_2$ hybrid nanofluids. The study analyzed the impact of hybrid nanoparticles on thermal conductivity, viscosity, and overall heat transfer performance. Results demonstrated that Cu-$TiO_2$ nanofluids enhance convective heat transfer more effectively than single-component nanofluids, though increased viscosity may impact flow characteristics.

Verma and Tiwari [111], Gupta et al.[112]provided a complete assessment of nanofluid use in solar collectors, summarizing advancements in thermal performance enhancement. The study analyzed

various nanofluids, their thermo-physical properties, and their impact on heat transfer efficiency. It also discussed challenges such as stability, pressure drop, and economic feasibility.

Shojaeizadeh et al. [113] examined the exergy performance and optimization of a flat-plate solar collector using $Al_2O_3$-water nanofluid. The work analyzed the infulence of nanoparticle concentration, temperature at the inlet, and mass flow rate on system performance. Results demonstrated that nanofluid-enhanced collectors achieved higher exergy efficiency associated to conventional fluids.

Faizal et al. [114] carried out an environmental economic energy analysis of a flat-plate solar collector using $SiO_2$ nanofluid. The research assessed the impact of nanofluid on thermal efficiency, cost-effectiveness, and environmental benefits.

Said et.al. [115] analyzed the exergy efficiency of a flat-plate solar collector using graphene-based nanofluid. The study examined the impact of graphene nanoparticles on heat transfer performance, entropy generation, and overall system efficiency. Results indicated that graphene-based nanofluids significantly enhanced exergy performanceas equated to conventional fluids.

Esfe et al. [116] examined the thermal conductivity of Cu/$TiO_2$-water/EG hybrid nanofluid through investigational analysis and predictive modelling by means of artificial neural networks. The work studied the impact of nanoparticle content and base fluid composition on thermal performance. Their outcomes exhibited that the hybrid nanofluid exhibited superior thermal conductivity associated to single-component nanofluids. The research provided empirical correlations and ANN-based

models for accurately predicting thermal behavior, contributing to the enhancement of nanofluids in heat transfer uses.

Esfe et al. [117] experimentally determined the thermal conductivity and dynamic viscosity of Ag-MgO/water hybrid nanofluid. The work examined the impacts of nanoparticle content and temperature on thermo-physical aspects.

Verma et.al [118] examined the performance improvement of a flat-plate solar collector by MgO/water nanofluid. The work analyzed the impact of nanoparticle concentration on thermal efficiency, heat transfer rate, and overall system effectiveness. Results indicated that MgO nanofluid significantly enhanced the collector's performance by enhancing thermal conductivity and convective heat transfer

Said et.al. [119] conducted an energy and exergy analysis of a flat-plate solar collector using aluminum oxide-based nanofluids of different particle sizes. The study examined the impact of nanoparticle size on heat transfer characteristics, entropy generation, and system efficiency.

Authors of [120,121] projected a novel method to enhance the thermal conductivity of $CuO/H_2O$-based nanofluids. Results demonstrated a significant improvement in thermal conductivity, making CuO nanofluids more effective for thermal management applications.

Verma et.al.[122] conducted an investigational assessment of a flat-plate solar collector using nanofluids to enhance thermal performance. Results indicated that nanofluids significantly improved the

collector's thermal conductivity and overall effectiveness associated to conventional fluids.

Dasaien and Elumalai [123] investigated the performance improvement of a thermo-syphon flat-plate solar water heater using CuO nanofluid.

Said and Saidur [124] provided ainclusive review of the thermo-physical beahviour of metal oxide nanofluids, emphasizing their potential uses in heat and mass transfer engineering. The study discussed key parameters like specific heat, viscosity, thermal conductivity, and density, highlighting their dependence on nanoparticle concentration, temperature, and base fluid properties. The findings underscored the advantages of metal oxide nanofluids in enhancing heat transfer efficiency, creating a prime factor for various thermal management equipments, including solar energy systems.

In another work authors of [125], conducted a theoretic study to appraise the effectiveness of a flat-plate solar collector utilizing CuO-water, nanofluid using energy and exergy analysis of a flat-plate solar collector.

. Kiliç et al. [126] examined the influence of using $TiO_2$-water based nanofluid on the thermal characteristics of a flat-plate solar collector. The study analyzed energy efficiency, heat transfer enhancement, and general system effectiveness when linked to conventional water-based fluids. The outcomes presented that the usage of $TiO_2$ nanofluid enhanced thermal efficiency because of its enhanced thermo-physical characteristics, including higher thermal conductivity.

Ziyadanogullari et al. [127] explored the thermal efficiency improvement of flat-plate solar collectors using three dissimilar

nanofluids. The outcomes demonstrated a visible development in thermal efficiency due to the superior thermo-physical properties of the nanofluids, such as increased thermal conductivity and heat absorption.

Verma et al. [128] examined the performance of hybrid nanofluids in flat plate solar collectors, highlighting their potential as advanced working fluids. The study compared hybrid nanofluids with conventional nanofluids and base fluids, emphasizing improvements in various thermal factors. The outcomes exhibited that hybrid nanofluids prominently heightened the collector's thermal efficiency due to the synergistic effect of multiple nanoparticles.

Farajzadeh et al. [129] conducted experimentation and numerical study on the impact of $Al_2O_3/TiO_2$-$H_2O$ based nanofluids on the thermal performance of a flat plate solar collector. Their research aimed to assess how the combination of aluminum oxide ($Al_2O_3$) and titanium dioxide ($TiO_2$) nanoparticles in water could improve heat transfer efficiency associated to conventional fluids.

Dehaj and Mohiabadi [130] conducted experimentation study on the effectiveness of a heat pipe solar collector (HPSC)by means of magnesium oxide (MgO) nanofluids as the base fluid. Results indicated that MgO nanofluids significantly improved heat transfer characteristics associated to conventional fluids.

Mousavi et al. [131] conducted an in-depth experimental study on the thermos-physical and rheogram of a dual hybrid nanofluid containing MgO and $TiO_2$ nanoparticles dispersed in water. The research focused on analyzing the impact of temperature and volume concentration of nanoparticle on thermal conductivity, viscosity, and stability. The results

indicated that increasing nanoparticle concentration significantly enhanced thermal conductivity**,** while also increasing viscosity, which could influence flow performance. This study underscores the potential of $MgO/TiO_2$ hybrid nanofluids for efficient heat transfer applications, particularly in solar energy and cooling systems.

Mousavi et al. [132] carried out an experimentation on the thermo-physical and rheological properties of a ternary hybrid nanofluid composed of CuO, MgO, and $TiO_2$ nanoparticles distributed in water. The study analyzed the effects of temperature variations and nanoparticle volume concentration on the thermal conductivity, viscosity, and overall stability of the nanofluid. The results showed that increasing the

nanoparticles concentration enhanced thermal conductivity but also led to higher viscosity, which could impact flow characteristics. These findings highlight the potential of ternary hybrid nanofluids in advanced heat transfer applications**,** particularly in energy and cooling systems.

Okonkwo et al. [133] done a proportional examination on the thermal performance of alumina/iron mono and hybrid nanofluids using both experimental and theoretical methods. Their research aimed to evaluate the accuracy of predictive models in estimating thermo-physical properties such as thermal conductivity and viscosity.

Tong et al.[134] conducted an energy and exergy analysis of a flat-plate solar collector using water, $Al_2O_3$ nanofluid, and CuO nanofluid as working fluids. The results demonstrated that nanofluids enhanced

both the efficiencies as equated to water, with CuO nanofluid exhibiting the highest performance improvement.

Choudhary et al. [135] investigated experimental the stability of MgO nanofluid and its influence on the thermal properties of a flat-plate solar collector. Their study focused on the dispersion characteristics and long-term stability of MgO nanoparticles in the working fluid, ensuring optimal heat transfer properties.

Okonkwo et al. [136] conducted a thermodynamic assessment and optimization of a flat-plate solar collector utilizing alumina and iron-based mono and hybrid nanofluids**.** Their study examined the energy and exergy performance of these nanofluids, identifying optimal concentrations for maximum efficiency.

Tong et al. [137] performed a comparative efficiency sensitivity analysis of a flat-plate solar collector using various nanofluids**.**

Sundar et al.[138] investigated the thermo-physical aspects, heat transfer performance, and ecological impactof a flat-plate solar collector utilizing nanodiamond-based nanofluids**.**

Liu et al. [139] conducted an energy analysis of solar collectors utilizing carbon and metallic oxide-based nanomaterials as main fluids. Their study demonstrated that these nanomaterials significantly enhance heat transfer efficiency**.**

Sarsam et al. [140] investigated the thermal efficiency of a flat-plate solar collectorby means of aqueous based colloidal dispersions of graphene nanoparticles with varying specific surface areas. Their findings indicate that graphene nanoplatelets enhance thermal conductivity and heat absorption**.**

Eltaweelet al.[141] carried out a comparative study of flat-plate and evacuated tube solar collectors using nanofluidsas a factor of energy and exergy performance**.** Their study highlights that evacuated tube collector's exhibit higher thermal efficiency and exergy gain compared to flat-plate collectors.

Akram et al. [142] conducted experimentation on the efficiency of a flat-plate solar collector using carbon and metal oxide-based nanofluids**.** Their findings indicate that nanofluids significantly enhance thermal conductivity and heat transfer efficiency**,** leading to improved energy absorption in the solar collector.

Mostafizur et al. [143] performed energy and exergy evaluation of a flat-plate solar collector utilizing different nanofluids through an analytical method**.**

Adun et al. [144] performed a multi-objective optimization and energy-exergy analysis of a parabolic trough solar collector (PTSC)integrated with a Kalina cycle, utilizing ternary nanofluids**.**

Nfawa et al. [145] examined the novel use of MgO nanoparticles as an additive to enhance the thermal conductivity of CuO/water nanofluid. Their work demonstrated that the addition of MgO significantly improved heat transfer properties, making the hybrid nanofluid a more efficient working medium for thermal energy systems.

Asadi et al. [146] carried out an investigation into the stability, characterization, and dynamic viscosity of CuO-$TiO_2$/water hybrid nanofluid. Their study aimed on evaluating the thermo-physical aspects of the hybrid nanofluid, particularly its long-term stability and viscosity behavior under varying conditions.

Said et al. [147] provided an inclusive assessment on the uses of nanofluids in low to medium temperature solar collectors**,** analyzing their energy, exergy, economic feasibility, and environmental effect**.**

Kumar et al. [148] conducted an energy, exergy, and cost-effective study of a liquid flat-plate solar collector utilizing green covalent functionalized graphene nanoplatelets (GNPs) as the primary working fluid. Their experimentation findings demonstrated that functionalized GNPs significantly enhance thermal conductivity and heat transfer performance**,** leading to improved energy and exergy efficiency of the solar collector.

Choudhary et al. [149] performed a time-based evaluation of the thermal performance of a flat-plate solar collector utilizing magnesium oxide (MgO) nanofluid**.** They demonstrating that the MgO nanofluid significantly enhances thermal conductivity and collector performance compared to conventional fluids.

Esfe et al. [150] carried an experimentation and sensitivity studyon anew group of ternary hybrid nanofluids (THNFs)**,** focusing on thermal conductivity enhancements.

Khan et al. [151] studied the thermal conductivity performance of a ternary hybrid nanomaterial, emphasizing its impact on entropy generation. The findings revealed that ternary hybrid nanofluids exhibit superior thermal performance

Ajeena et al. [152] conducted a complete examination of nanofluids and their uses in flat plate solar collectors, focusing on fundamental principles, thermo-physical properties, and stability challenges**.**

Desisa [153] conducted an experiment as well as numerical investigation into the heat transfer behaviour of a solar flat plate collector utilizing nanofluids. Findings highlighted progresses in heat transfer performance and collector efficiency when using nanofluids,

Kumar et al. [154] explored a novel approach of mixing MgO in CuO/water nanofluid to enhance thermal conductivity. Their experiment demonstrated a noteworthy enhancement in heat transfer performance.

Ajeena et al. [155] carried out experimentation on the energy and exergy valuation of a flat plate solar thermal collector using silicon carbide (SiC) nanofluid. Their findings highlight the potential of SiC nanofluid in enhancing thermal efficiency.

Senthilkumar [156] presents anovel approach to enhance the thermal conductivity of dihybrid nanofluids. The study investigates the synergistic influence of combining two different nanoparticles**,** evaluating their impact on heat transfer performance and potential applications in thermal management systems**.**

Khan et al. [157] conducted a numerical analysis on the effects of multiple slip conditions in a CuO/MgO/$TiO_2$-water ternary hybrid nanofluid**.** The study explores how thermal and exponential space-based heat sources influence heat transfer dynamics**,** emphasizing the synergistic role of multiple nanoparticles in improving thermal efficiency and flow characteristics**.**

## 2.6 Research Gaps

- Inadequate analytical analysis considering 2-D heat conduction.
- Very few works have been demonstrated considering 2-D heat conduction, with a constant or convected boundary condition. No work has been found with variation of temperature at the plate-tube junction.
- Non-Fourier analysis considering the relaxation time with loss coefficient has not yet considered.
- No work is found for Thermodynamic analysis considering ternary nanofluid .

## 2.7 Objective of the thesis

- Analytical model for the steady state energy transfer in absorber plate to heat the collector fluid.
- 2D analysis with nonlinear variation of temperature at the plate tube junction.
- Established 1-D analysis for 2-D heat conduction in absorber plates.
- Fourier and non-Fourier heat conduction analysis in transient states of flat-plate solar collector.
- A generalized analytical analysis of flat-plate solar collectors based on a revised non-Fourier model.
- Energy and Exergy analysis for performance of solar collector using ternary nanofluids.

This PhD research focuses on the 2D analysis of flat-plate collectors, aiming to enhance their thermal performance through

analytical and numerical modeling. The study explores heat transfer dynamics, fluid flow behavior, working fluid properties, and efficiency enhancements, focusing on their collective impact on overall system performance. Furthermore, This also includes, a comparison of Fourier and non-Fourier heat conduction models, and an energy and exergy analysis utilizing various mono and hybrid nanofluids to improve the thermal effectiveness of the absorber plate in flat plate solar collectors.

# Chapter3

# Simple Analytical Solution for Performance of an Absorber Plate in Flat-Plate Solar Collectors for Two-Dimensional Heat Flow

## 3.1 Introduction

Numerous researchers do thermal evaluation of an absorber plate in flat-plate solar collectors, focussing on one-dimensional heat conduction. Nonetheless, a two-dimensional temperature distribution invariably occurs in the absorber plate owing to its characteristic form. The absorber plate has a minimal thickness, and temperature change in the thickness direction is negligible, allowing heat conduction within the absorber to be approximated as two-dimensional. Due to typical shape of the symmetric sector of the plate for the thermal analysis, exactly closed form solution might not be possible however, it is believed that the two-dimensional analysis will enable a more accurate evaluation to be made of the collector. There is a continual requirement for the establishment of an analytical framework for two-dimensional heat transfer in absorber plates.

This chapter analyses the temperature profile in the absorber plate of a flat-plate solar collector, using two-dimensional steady-state heat transmission within the plate. In certain instances, determining the temperature field for two-dimensional heat flow over a plate under certain boundary conditions using a precise analytical technique may be impractical. An approximate analytical model has been suggested in this work to address this challenge. The precision of the current analytical

approach has been evaluated against a numerical method. The current work utilizes the finite difference method as a numerical tool. However, the numerical calculations increase the computational cost. The results exhibit a strong correlation, with the variation between them not above 5%. Consequently, the current approach may be crucial for analyzing the performance of an absorber plate in a straightforward manner to ascertain the two-dimensional temperature field.

## 3.2 Mathematical formulation

The flat-plate solar collector primarily comprises an absorber plate and fluid-carrying tubes, as seen in Fig. 3.1. The solar energy is collected by the plate and subsequently transferred by the collector fluid running through the tubes, resulting in a rise in the fluid's internal energy and temperature in the direction of flow. As the solar flu**x** is collected in the plate, both the plate and fluid temperatures are increased.

For the current study on the flat plate collector the subsequent assumptions are considered.

- Heat transfer for the absorber plate is two-dimensional heat conduction considering steady state.
- For simplicity, only flat plate collectors without transparent covers are taken into consideration.
- The solar insolation reaching the absorber plate is uniformly distributed over the plate and remains constant throughout.
- The thermal conductivity of the plate material remains constant.
- The surrounding temperature and the overall loss coefficient are constant
- At the plate and tube junction, the heat conducted through the plate is convected to the fluid flowing in the tube.

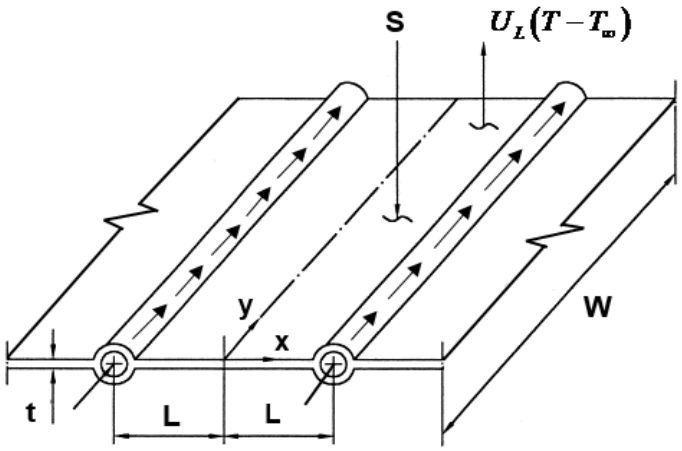


**Fig.3.1** Representation of a symmetric module of an absorber plate

For the thermal analysis of absorber plate, a symmetric heat transfer module of length *W* and width *L* repeats between two fluid carrying tubes as depicted in Fig. 3.1. As the temperature of the plate is higher than the ambient, there is heat loss occurred between the absorber plate and the surrounding by convection and radiation. These heat losses are incorporated with the calculation of overall heat loss coefficient.

The governing heat conduction equation under steady state and two-dimensional heat flow, the energy equation for an absorber plate can be written as

$$\frac{\partial}{\partial x}\left(k\frac{\partial T}{\partial x}\right)+\frac{\partial}{\partial y}\left(k\frac{\partial T}{\partial y}\right)+\frac{S}{t}-\frac{U_L\left(T-T_\infty\right)}{t}=0 \qquad (3.1)$$

The temperature of the absorber plate in the flat-plate collector must not be excessively elevated owing to direct solar energy absorption. The minimal temperature fluctuation allows for the assumption that the

thermo-physical parameters of an absorber plate remain constant. Consequently, Equation (3.1) may be expressed in non-dimensional form as follows:

$$\frac{\partial^2\theta}{\partial X^2}+\delta^2\frac{\partial^2\theta}{\partial Y^2}+N-M^2\theta=0 \tag{3.2}$$

where

$$\theta=\frac{T-T_\infty}{T_{in}-T_\infty};\quad X=\frac{x}{L};\quad Y=\frac{y}{W};\ \delta=\frac{L}{W};$$

$$M^2=\frac{U_L L^2}{kt};\quad N=\frac{SL^2}{kt\left(T_{in}-T_\infty\right)} \tag{3.2}$$

The closed form solution of Eq. (3.2), two boundary constraints in the x-direction and two boundary conditions in the y-direction are necessary. Along the x-direction, there is no net heat transfer at the midsection of the plate between two tubes due to line of symmetry and at the plate-tube junction an energy balance can be made between conduction through the plate and convecton into the fluid. In the y-direction, negligible heat exchange at the edge of the plate can be assumed. Mathematically, the boundary conditions taken in the present study are expressed as follows:

at $x=0\left(0\le y\le W\right),\ \partial T/\partial x=0$ (3.4a)

at $x=L\left(0\le y\le W\right),\ -kt\frac{\partial T}{\partial x}dy=\dot{m}\,c_p dT_f$ (3.4b)

at $y=0\left(0\le x\le L\right),\ \partial T/\partial y=0$ (3.4c)

at $y = W\left(0 \le x \le L\right),\ \partial T/\partial y = 0$ (3.4d)

In the non-dimensional form the boundary conditions can be written as

at $X = 0\left(0 \le Y \le 1\right),\ \partial\theta/\partial X = 0$ (3.5a)

at $X = 1\left(0 \le Y \le 1\right),\ \partial\theta/\partial X = -\dfrac{\dot{m}c_p L}{kt\left(T_{in} - T_\infty\right)}\dfrac{dT_f}{dy} = -A$ (3.5b)

at $Y = 0\left(0 \le X \le 1\right),\ \partial\theta/\partial Y = 0$ (3.5c)

at $Y = 1\left(0 \le X \le 1\right),\ \partial\theta/\partial Y = 0$ (3.5d)

For the approximate closed form solution of Eq. (3.2), the following variables are chosen:

$$\theta\left(X,Y\right) = \gamma\left(X\right) + \beta\left(Y\right) + e^{-MX} + e^{-\left(\frac{M}{\delta}\right)Y} \tag{3.6}$$

By integrating Equations (3.2) and (3.6), the subsequent conditions may be derived:

$$\frac{d^2\gamma\left(X\right)}{dX^2} - M^2\alpha\left(X\right) + N = 0 \tag{3.7}$$

and

$$\frac{d^2\beta\left(Y\right)}{dY^2} - \frac{M^2}{\delta^2}\beta\left(Y\right) = 0 \tag{3.8}$$

Eqs. (3.7) and (3.8) are solved separately along with the boundary conditions expressed in Eq, (3.5) and the following unknown variables are determined as

$$\gamma(X) = C_1 \cosh(MX) + C_2 \sinh(MX) + \frac{N}{M^2} \tag{3.9}$$

and

$$\beta(Y) = C_3 \cosh\left[\left(\frac{M}{\delta}\right)Y\right] + C_4 \sinh\left[\left(\frac{M}{\delta}\right)Y\right] \tag{3.10}$$

where

$$C_1 = \frac{M\left[e^{-M} - \cosh(M)\right] - A}{M \sinh(M)}; C_3 = \left[e^{-\frac{M}{\delta}} - \cosh\left(\frac{M}{\delta}\right)\right] \Big/ \sinh\left(\frac{M}{\delta}\right);$$

$$C_2 = C_4 = 1 \tag{3.11}$$

Combining Eqs. (3.6), (3.9), (3.10), and (3.11) the final expression for the non-dimensional temperature distribution of an absorber plate can be expressed as

$$\theta(X,Y) = \left[\frac{M\left[e^{-M} - \cosh(M)\right] - A}{M \sinh(M)}\right] \cosh(MX) + \sinh(MX)$$

$$+ \frac{N}{M^2} + e^{-MX} + \left[\frac{e^{-\frac{M}{\delta}} - \cosh\left(\frac{M}{\delta}\right)}{\sinh\left(\frac{M}{\delta}\right)}\right] \cosh\left[\left(\frac{M}{\delta}\right)Y\right] + \sinh\left[\left(\frac{M}{\delta}\right)Y\right] + e^{-\left(\frac{M}{\delta}\right)Y} \tag{3.12}$$

## 3.3 Results and Discussion

The primary concern of the current model is to check the accuracy level of the proposed approximate analytical model. This can be done with a numerical method. For obtaining the numerical data, the finite difference techniques utilized to solve Eq. (3.2) with the appropriate boundary constraints written in Eq. (3.5). The difference equations are formulated from the governing equations by discretized using Taylor series central difference method with the second order of accurateness. These difference equations are then solved by Gauss-Seidel iteration and results are taken with satisfying necessary and sufficient criteria of convergence [159].The grid independent test has also been made by selecting number of nodal points to satisfy less than 0.1% error with respect to results determined by taking higher lattice points [160].

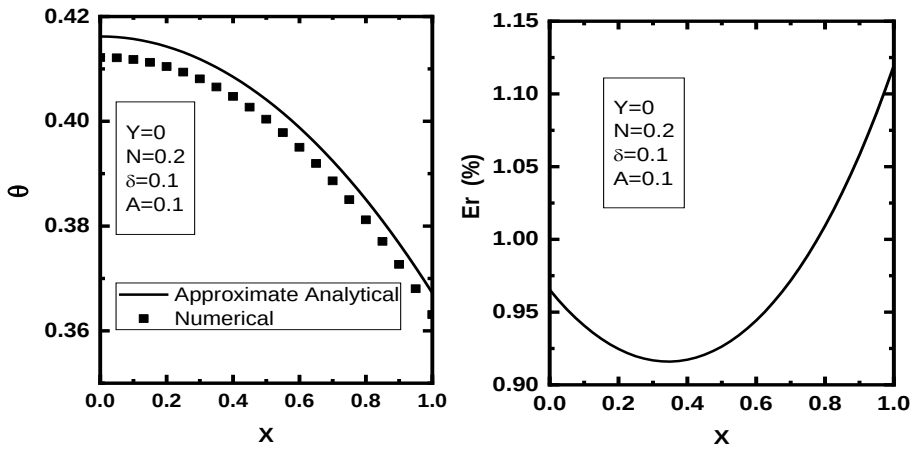


(a) Temperature distribution (b) Percentage of deviation

**Fig. 3.2** Comparison of temperature distribution in an absorber plate as a function of *X* predicted by approximate analytical and numerical methods for $M = 0.5$.

For comparisons of outcomes between the current approximate analytical and numerical values, Fig. 3.2 has been plotted. Fig. 3.2 depicts the temperature profile in an absorber plate in the x-direction for a set of design constant. Solar energy is absorbed by the absorber plate and transferred to the fluid-carrying tubes. Therefore, the temperature at the mid-section of the plate between two successive tubes is always a maximum and the temperature of that section rises in the direction of fluid flow in tubes as the absorbed energy is taken by the collector fluid. In the plate, heat transfer takes place towards the collector fluid. The temperature is plotted in Fig. 3.2(a) as function of $X$ for a thermo-geometrical parameter $M = 0.5$, a constant solar incident rate of $N = 0.2$, and collector fluid temperature gradient, and aspect ratio both taken as 0.1. There is an excellent agreement between the nature of curves for the proposed approximate analytical outcomes and the numerical values, which confirms the validity of the analytical method. Fig. 3.2(b) depicts the trend of the percentage of deviation between the analytical and numerical determinations as a function of $X$ for the same design variables taken in Fig. 3.2(a). The variation is contingent upon the geographical coordinates. A peculiar variation of the deviation of temperature has been found. There is a position where the deviation becomes a minimum. Overall, the deviation of temperature predictions reaches a maximum at the plate attached to the fluid carrying tube. However, the maximum deviation value is around 1% which indicates a negligible variation from the engineering accuracy point of view.

The same observation can be made by plotting Fig. 3.3 for $M = 0.4$ to understand the accuracy level of the proposed approximate analytical model depending upon the thermo-geometric parameter participated in the design analysis. For this observation, it has been mentioned that the

accuracy of the analytical model is also function of $M$. However, the trend of deviation is obtained same as shown in Fig. 3.2. Moreover, a little high difference is found in this figure and the maximum percentage relative deviation is below 4.6%. Therefore, it can be concluded that the accuracy level of proposed approximate model enhances with an increase in $M$ clearly obtained by comparing Figs. 3.2 and 3.3. On the other hand, as the thermo-geometric parameter $M$ increases the overall loss coefficient increases, as a consequence, the plate temperature decreases due to more heat loss from the plate to the surrounding. This effect can clearly be understood from the plotted Figs.3.2 and 3.3

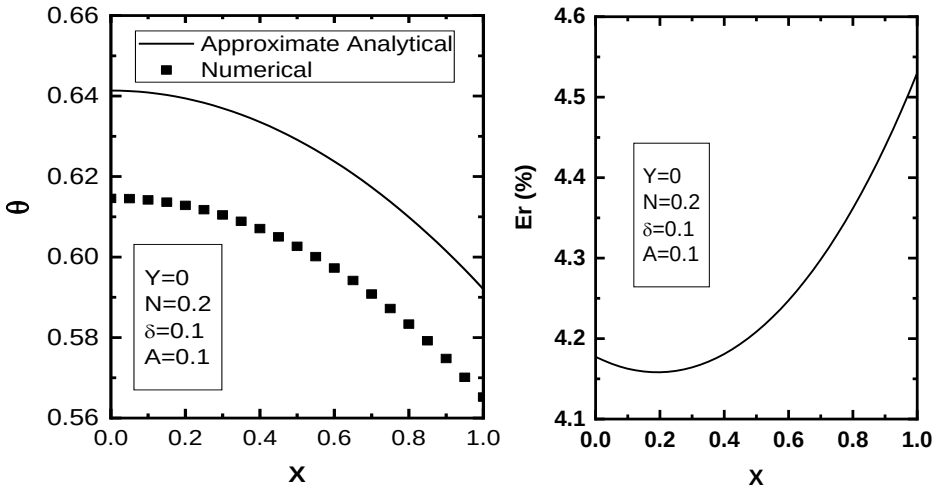


(a) Temperature distribution (b) Percentage of deviation

**Fig. 3.3** Comparison of temperature distribution in an absorber plate as a function of *X* predicted by approximate analytical and numerical methods for $M = 0.4$

Next an effort has been devoted to obtain the temperature in the absorber plate predicted by the present analytical and numerical methods to show the effect of the solar flux and the collector fluid temperature gradient by plotting Fig. 3.4. An increasing the parameter $N$ causes to

absorb solar flux more in the absorber plate and thus the plate temperature enhances. This effect can be verified by comparing the results shown in Figs. 3.2(a) and 3.4(a). The deviation of percentage of temperature $Er$ at $N = 0.3$ as a function $X$ has been displayed in Fig. 3.4(b). From this figure, it is clearly understood that the relative difference in temperature prediction is an incremented function with $N$.

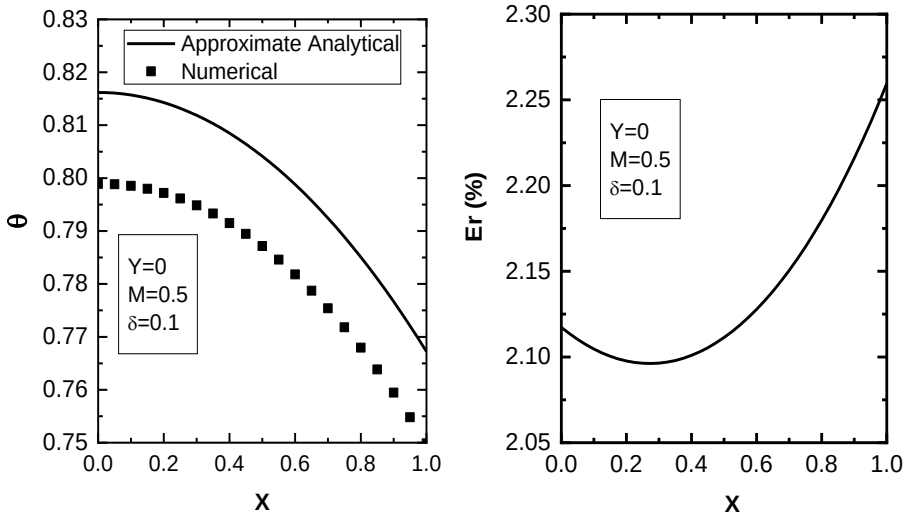


(a) Temperature vs. $X$ at $N$=0.3, $A$=0.1

(b) Deviation vs. $X$ at $N$=0.3, $A$=0.1

**Fig. 3.4** Accuracy analysis for approximate analytical model for higher value of solar incident $N = 0.3$ at $M = 0.5$

Fig. 3.5 shows the temperature profile in the absorber plate determined at a collector fluid temperature gradient parameter $A$=0.15. The influence of this gradient parameter on the absorber plate temperature can be envisaged by comparing the temperature shown in Figs. 3.4(a) and 3.5(a). A correct trend has been displayed as the temperature diminishes with $A$ due to more amount of energy carried out

by the collector fluid. The deviation results have also been plotted in Fig. 3.5(b). By comparing the data from Figs. 3.4(b) and 3.5(b), it is obvious that the relative deviation of temperature from approximate analytical and numerical methods amplifies with an upsurge in temperature gradient of collector fluid.

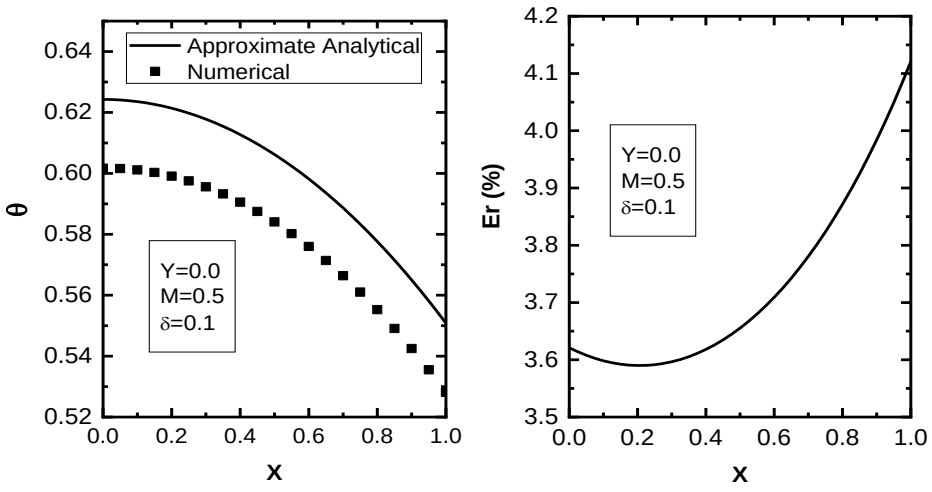


(a) Temperature vs. $X$ at $N$=0.3, $A$=0.1

(b) Deviation vs. $X$ at $N$=0.3, $A$=0.15

**Fig. 3.5** Accuracy analysis for approximate analytical model depending on collector fluid temperature gradient parameter.

Finally, the exact values of the dimensionless temperature at various locations in the absorber plate for different values of solar insolation and collector fluid temperature gradient are tabulated in Tables 3.1 and 3.2. The relative deviation of temperature of the approximate analytical analysis from the numerical value does not exceed 5% in a range of design input values taken in this study. Thus, from the results, it can be emphasized that the proposed analytical model has been correctly

established and has a high accuracy to predict temperature field of the absorber plate in a wide range of design aspects using its simple mathematical expressions.

**Table 3.1** Absorber plate temperature determined by the present approximate analytical and numerical methods for $N = 0.2$, $M = 0.5$, $\delta = 0.1$, and $A = 0.1$.

| Coordinates $X, Y$ | Temperature $(\theta_{analytical})$ | Temperature $(\theta_{numerical})$ | % of Er = $\left(\frac{\theta_{analytical} - \theta_{numerical}}{\theta_{analytical}}\right) \times 100$ |
|---|---|---|---|
| 0.0, 0.0 | 0.41619 | 0.41218 | 0.96538 |
| 0.1, 0.0 | 0.41571 | 0.41180 | 0.94072 |
| 0.2, 0.0 | 0.41427 | 0.41044 | 0.92463 |
| 0.3, 0.0 | 0.41187 | 0.40809 | 0.91679 |
| 0.4, 0.0 | 0.40849 | 0.40474 | 0.91728 |
| 0.5, 0.0 | 0.40414 | 0.40039 | 0.92632 |
| 0.6, 0.0 | 0.39879 | 0.39503 | 0.94426 |
| 0.7, 0.0 | 0.39244 | 0.38863 | 0.97166 |
| 0.8, 0.0 | 0.38508 | 0.38119 | 1.00927 |
| 0.9, 0.0 | 0.37667 | 0.37269 | 1.05809 |
| 1.0, 0.0 | 0.36721 | 0.3631 | 1.11943 |

**Table 3.2** Temperature determined by the present approximate analytical and numerical methods for $N = 0.3$, $M = 0.5$, $\delta = 0.1$, and $A = 0.15$.

| Coordinates $X, Y$ | Temperature $(\theta_{analytical})$ | Temperature $(\theta_{numerical})$ | % of Er= $\left(\frac{\theta_{analytical} - \theta_{numerical}}{\theta_{analytical}}\right) \times 100$ |
|---|---|---|---|
| 0.0, 0.0 | 0.62429 | 0.60168 | 3.62100 |
| 0.1, 0.0 | 0.62357 | 0.60113 | 3.59826 |
| 0.2, 0.0 | 0.62141 | 0.59910 | 3.59003 |
| 0.3, 0.0 | 0.6178 | 0.59558 | 3.59654 |
| 0.4, 0.0 | 0.61274 | 0.59057 | 3.61811 |
| 0.5, 0.0 | 0.6062 | 0.58405 | 3.65534 |
| 0.6, 0.0 | 0.59819 | 0.5760 | 3.70911 |
| 0.7, 0.0 | 0.58867 | 0.56641 | 3.78064 |
| 0.8, 0.0 | 0.57761 | 0.55525 | 3.87157 |
| 0.9, 0.0 | 0.56501 | 0.54250 | 3.98401 |
| 1.0, 0.0 | 0.55081 | 0.52812 | 4.12068 |

## 3.4 Summary

The primary aim of this study is to develop an analytical model for the thermal characterization of an absorber plate in flat-plate solar collectors, focusing on two-dimensional heat conduction within the plate. Alternatively, an approximate analytical analysis is developed in the present work to obtain the thermal design information easily. The precision of this model has been compared with the results produced by a numerical analysis grounded on the finite difference method. The percentage of relative deviation of temperature is a function of spatial coordinates as well as system design variables. From the results, it has been established that the maximum temperature deviation is within 5% and therefore, the model presented in this paper might be considered to analyze absorber plate under two-dimensional and steady state energy transfer since flat plate solar collector has many application in practical fields like, the heating needs of the food, beverage, textiles, paper and pulp industries. As the present analysis is very simple, no computational step is required to design the plate. Thus the present analysis may help to designers for determination of unknown thermal design information.

# Chapter 4

## Two-Dimensional Analysis of Absorber Plates in Solar Collectors with a Nonlinear Plate Temperature at the Tube Section

### 4.1 Introduction

In the previous chapter an approximate analytical model has been considered with convected boundary condition at the plate tube junction and insulated condition along the fluid flow direction. As fluid flow takes place in the tube, the temperature of fluid changes from inlet to outlet. In this chapter, a close form solution for two-dimensional heat conduction for absorber plate has analyzed by considering the change of temperature at the plate–tube junction.The energy equation for two dimensional heat conduction on absorber plate is solved with separation of variable method. For validation purposes, the identical problem is also solved numerically with the finite difference approach.The result obtained are compared and can be emphasized that the analytical and numerical outcomes are strongly consistent with one another.

Since the fluid temperature in the tube increases from inlet to exist, therefore at plate tube junction a variable temperature condition can be considered. Due to this variation the boundary condition for the energy equation becomes non-linear in nature.

### 4.2 Mathematical analysis

For the current analysis on the flat plate collector the subsequent assumptions are considered.

- Heat transfer for the absorber plate is two-dimensional heat conduction considering steady state.
- For simplicity, only flat plate collectors without transparent covers are taken into consideration.
- The solar insolation reaching the absorber plate is uniformly spread over the plate and remains constant throughout.
- The thermal conductivity of the plate material remains constant. The surrounding temperature and the overall loss coefficient are constant
- Due to minimal temperature fluctuations, the thermo-physical qualities may be regarded as constant, and the temporal variation of absorbed solar radiation can be disregarded.
- At the plate and tube junction the temperature transferred from the plate to the fluid varies non-linearly and it can be assumed as parabolic in nature.

A symmetric sector identified between two fluid carrying tubes has been taken as depicted in Fig. 4.1, for the thermal analysis on the plate in which $L$, $W$ and $t$ are the half centre distance, length of the fluid carrying tube, and thickness of the plate respectively.

The rate of mass flow through a single tube is $\dot{m}$. The solar insolation $S$, falls on the plate and some losses takes place from the upper side of the plate. As the collector plate is made up of thin material and the ratio between the volume of the plate to area of the plate always higher. Hence, neglecting the heat conduction in thickness direction, the flat-plate collector can be considered as two-dimensional heat conduction problem (in the x- direction along the plate width and in the y-direction along the tube length).

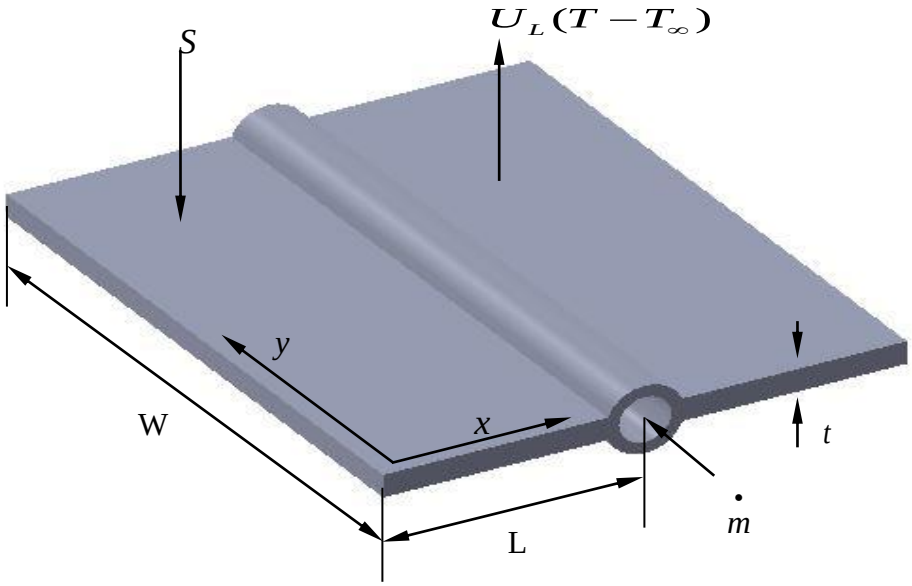


**Fig. 4.1** Schematic view of the symmetric heat transfer module of flat plate collector for thermal analysis.

### 4.2.1 Analytical methodology

The energy balance for a differential volume element in two-dimensional heat conduction within the absorber plate, assuming constant thermal conductivity, may be expressed as

$$\frac{\partial^2 T}{\partial x^2}+\frac{\partial^2 T}{\partial y^2}+\frac{S}{kt}-\frac{U_L\left(T-T_a\right)}{kt}=0 \tag{4.1}$$

The following dimension-less parameters are introduced

$$\theta=\frac{T-T_a}{T_{in}-T_a};\ X=\frac{x}{W}\ ;\ Y=\frac{y}{L}\ ;\ \delta=\frac{L}{W}\ ;\ M^2=\frac{U_L W^2}{kt}\ ;$$

$$N=\frac{SW^2}{kt(T_{in}-T_a)} \tag{4.2}$$

Consequently, Equation (4.1) may be expressed in a dimensionless format as follows.

$$\frac{\partial^2\theta}{\partial X^2}+\delta^2\frac{\partial^2\theta}{\partial Y^2}-M^2\theta+N=0 \tag{4.3}$$

As the plate temperature distribution is assumed to be two-dimensional, the fluid is flowing in the tube in $y$-direction and the plate width is in $x$-direction. Hence, the fluid in the tube is exposed to the surrounding and a mixed conductive-convective boundary condition can be considered at $y=0$ and $y=W$ .The peak plate temperature is located at the center of the absorber plate between the two tubes, as no net heat conduction occurs over this portion due to symmetry. In actual situation the plate temperature at the tube junction varies non-linearly. Hence the temperature at these sections can be written as function of $y$ and the coefficients can be found by regression analysis .Thus, the boundary conditions for the absorber plate in non-dimensional form can be written mathematically as follows:

$$\text{at } X=0;\ \frac{\partial\theta}{\partial X}=0 \tag{4.4a}$$

$$\text{at } X=1;\ \theta=A_1+B_1Y+C_1Y^2 \tag{4.4b}$$

$$\text{at } Y=0;\ \frac{\partial\theta}{\partial Y}=Bi_1\theta \tag{4.4c}$$

$$\text{at } Y=1;\ \frac{\partial\theta}{\partial Y}=-Bi_2\theta \tag{4.4d}$$

where

$$Bi_1 = \frac{h_1 W}{k};\ Bi_2 = \frac{h_2 W}{k};\ A_1 = \frac{a - T_\infty}{T_{in} - T_\infty}\ B_1 = \frac{bW}{T_{in} - T_\infty};\ C_1 = \frac{cW^2}{T_{in} - T_\infty} \quad (4.5)$$

Here $A_1, B_1, C_1$ are arbitrary constant whose actual values can be found by regression analysis.

Equation (4.3) may be resolved by the method of separation of variables [158]. The subsequent variables were selected for the solution process.

$$\theta(X,Y) = \phi(Y) + \psi(X,Y) \quad (4.6)$$

Combining Eqs. (4.3) and (4.6), the following conditions are obtained.

$$\delta^2 \frac{d^2\phi}{dY^2} - M^2\phi + N = 0 \quad (4.7)$$

And

$$\frac{\partial^2\psi}{\partial X^2} + \delta^2 \frac{\partial^2\psi}{\partial Y^2} - M^2\psi = 0 \quad (4.8)$$

The Eqs. (4.7) can be solved with the modified boundary conditions obtained from Eqs. (4.4a) - (4.4d)

and can be given as

$$\phi(Y) = E_1 \cosh\left(\frac{M}{\delta}Y\right) + E_2 \sinh\left(\frac{M}{\delta}Y\right) + \frac{N}{M^2} \quad (4.9)$$

where, the value of the constants are

$$E_1 = \frac{-\frac{\delta}{M^3}\left[NBi_1 \cosh\left(\frac{M}{\delta}\right) + \frac{\delta NBi_1 Bi_2}{M}\sinh\left(\frac{M}{\delta}\right) + NBi_2\right]}{\left[\frac{M^2 + \delta^2 Bi_1 Bi_2}{M^2}\sinh\frac{M}{\delta} + \frac{\delta\left(Bi_1 + Bi_2\right)}{M}\cosh\left(\frac{M}{\delta}\right)\right]} \quad (4.9a)$$

and

$$E_2 = \frac{\delta}{M} Bi_1 \left[ E_1 + \frac{N}{M^2} \right] \tag{4.9b}$$

The variable $\psi(X,Y)$ in Eqs. (4.8) is then separated by product rule in the subsequent expression.

$$\psi(X,Y) = \Gamma(X)\Omega(Y) \tag{4.10}$$

Combining Eqs. (4.8) and Eqs. (4.10) the subsequent conditions can be found with an Eigen condition as

$$\frac{d^2\Omega}{dY^2} + \frac{\lambda^2}{\delta^2}\Omega = 0 \tag{4.11}$$

and

$$\frac{d^2\Gamma}{dX^2} - \left(\lambda^2 + M^2\right)\Gamma = 0 \tag{4.12}$$

Solving Eqs.(4.11) with the modified boundary conditions obtained from (4.4c) and (4.4d) gives an Eigen condition as

$$\tan\left(\frac{\lambda_n}{\delta}\right) = \frac{\delta\left(Bi_1 + Bi_2\right)\lambda_n}{\left(\lambda_n^2 - \delta^2 Bi_1 Bi_2\right)} \text{ for } n = 1,2,3..... \tag{4.13}$$

The Eqs. (4.13) is a transcendental equation which can be solved by Newton-Rapson method to get the value of separation constant $(\lambda_n)$.

Eqs. (4.12) is solved with the modified boundary conditions obtained from (4.4a) and (4.4b) and by combining with Eqs. (4.10) gives

$$\psi(X,Y)=\sum_{n=1}^{\infty}C_n\cosh\left(\sqrt{\lambda_n^2+M^2}\,X\right)\left[\cos\left(\frac{\lambda_n}{\delta}Y\right)+\frac{\delta}{\lambda_n}Bi_1\sin\left(\frac{\lambda_n}{\delta}Y\right)\right] \quad (4.14)$$

Where $C_n$ is a constant and its value can be determined by orthogonality condition of Fourier series with the non homogeneous boundary condition (4.4b) as

$$C_n=\frac{1}{\cosh\left(\sqrt{\lambda_n^2+M^2}\right)}\times \frac{4\lambda_n^3\left(a_n-b_n+d_n\right)}{\left[2\lambda_n\left(\lambda_n^2+\delta^2Bi_1^2\right)+\delta\left(\lambda_n^2-\delta^2Bi_1^2\right)\sin 2\left(\frac{\lambda_n}{\delta}\right)+4\lambda_n\delta^2Bi_1\sin^2\left(\frac{\lambda_n}{\delta}\right)\right]} \quad (4.15)$$

Where, $a_n=\left\{\begin{array}{l}\left(A+B+C-\frac{N}{M^2}\right)\frac{\delta}{\lambda_n}\\ +\left(BBi_1+2CBi_1-2C\right)\left(\frac{\delta}{\lambda_n}\right)^3\\ -\left(\frac{D_1\delta\lambda_n^2+\delta^2D_2Bi_1M}{\lambda_n\left(\lambda_n^2+M^2\right)}\right)\cosh\left(\frac{M}{\delta}\right)\\ -\left(\frac{D_2\delta\lambda_n^2+\delta^2D_1Bi_1M}{\lambda_n\left(\lambda_n^2+M^2\right)}\right)\sinh\left(\frac{M}{\delta}\right)\end{array}\right\}\sin\left(\frac{\lambda_n}{\delta}\right)$ (4.16a)

$$b_n=\left\{\begin{array}{l}\left[\left(A+B+C-\frac{N}{M^2}\right)Bi_1+B-2C\right]\left(\frac{\delta}{\lambda_n}\right)^2\\ -2CBi_1\left(\frac{\delta}{\lambda_n}\right)^4\\ -\left(\frac{D_2\delta M-D_1\delta^2Bi_1}{\lambda_n^2+M^2}\right)\cosh\left(\frac{M}{\delta}\right)\\ -\left(\frac{D_1\delta M-D_2\delta^2Bi_1}{\lambda_n^2+M^2}\right)\sinh\left(\frac{M}{\delta}\right)\end{array}\right\}\cos\left(\frac{\lambda_n}{\delta}\right) \quad (4.16b)$$

$$d_n = \left\{ \begin{array}{l} \left[ B + \left( A - \dfrac{N}{M^2} \right) Bi_1 \right] \left( \dfrac{\delta}{\lambda_n} \right)^2 \\ -2CBi_1 \left( \dfrac{\delta}{\lambda_n} \right)^4 + \dfrac{D_2 M \delta - \delta^2 Bi_1 D_1}{\lambda_n^2 + M^2} \end{array} \right\} \tag{4.16c}$$

The final formula for the non-dimensional temperature distribution of the absorber plate may be derived by combining Eqs. (4.9), (4.9a), (4.9b), (4.14), and (4.15).

$$\theta(X,Y) = \left\{ \begin{array}{l} E_1 \cosh\left( \dfrac{M}{\delta} Y \right) + E_2 \sinh\left( \dfrac{M}{\delta} Y \right) + \dfrac{N}{M^2} \\ + \displaystyle\sum_{n=1}^{\infty} C_n \cosh\left( \sqrt{\lambda_n^2 + M^2}\, X \right) \left[ \cos\left( \dfrac{\lambda_n}{\delta} Y \right) + \dfrac{\delta}{\lambda_n} Bi_1 \sin\left( \dfrac{\lambda_n}{\delta} Y \right) \right] \end{array} \right\} \tag{4.17}$$

### 4.2.2 Parameter definition

The following formulae determine the mass flow rate, usable energy, fluid outlet temperature, heat removal factor, efficiency factor, and efficiency for the flat plate solar collector [15, 16].

The mass flow rate for the collector can be calculated as

$$\dot{m} = \frac{q_u}{c_p \left( T_{fo} - T_{fi} \right)} \tag{4.18}$$

The useful energy gain by the the absorber plate is

$$q_u = F_R A_c \left[ S - U_L \left( T_{fi} - T_\infty \right) \right] \tag{4.19}$$

The heat removal factor can be given as

$$F_R = \frac{\dot{m} c_p}{U_L A_c}\left(1-\exp\left\{-\frac{F^l U_L A_c}{\dot{m} c_p}\right\}\right) \qquad [4.20]$$

The

$$F^l = \frac{1}{LU_L\left[\frac{1}{U_L\left\{(L-d_o)\zeta + d_o\right\}} + \frac{1}{\pi d_i h_f}\right]} \qquad (4.21)$$

The fin efficiency

$$\zeta = \frac{\tanh\left[\dot{m}(L-d_o)/2\right]}{\left[\dot{m}(L-d_o)/2\right]} \qquad (4.22)$$

where

$$m = \sqrt{U_L/kt} \qquad (4.23)$$

The fluid outlet temperature can found

$$T_{fo} = T_{fi} + \frac{q_u}{\dot{m} c_p} = T_{fi} + \frac{F_R A_c\left[S - U_L\left(T_{fi} - T_\infty\right)\right]}{\dot{m} c_p} \qquad (4.24)$$

The efficiency of the collector

$$\eta = \frac{q_u}{(\alpha\tau) I_T A_c} \qquad (4.25)$$

### 4.2.3 Numerical methodology

Eq. (4.3) is solved numerically in consort with the boundary conditions mentioned in Eqs. (4.9a) – (4.9d) by the finite difference technique. The differential equations are discretized with Taylor's series central

difference scheme of second order accuracy [160]. The algebraic equations obtained from the governing equation and boundary conditions are solved by Gauss-Seidel iteration method. The final findings are achieved upon meeting the specified accuracy threshold of $10^{-6}$.

## 4.3 Results and discussion

The primary goal of this work is to provide an analytical expression for calculating thermal performance of an absorber plate for two-dimensional temperature distribution and variation of temperature at the plate tube junction. As an analytical tool, the Separation of variables method is employed. A numerical technique utilising finite differences is employed to ascertain the temperature, hence validating the current study. The input data for the simulations based on which all of the results were obtainedare tabulated in Table 4.1, and considering water as the circulating fluid.The aforementioned two-dimensional study, together with these geometric parameters and the physical behaviour of the flat plate collector, results were acquired by FORTRAN programming.

**Table 4.1**Input data for the calculation

| Para meter | $W$ | $L$ | $A_c$ | $C_p$ | $k$ | $U_L$ | $h_f$ | $S$ | $T_\infty$ | $d_o$ | $d_i$ | $T_{fi}$ |
|---|---|---|---|---|---|---|---|---|---|---|---|---|
| Value | 2 | 0.1 | 1 | 4178 | 350 | 8 | 205 | 718 | 35 | 0.01 | 0.015 | 40 |

Figure 4.2 represents the variation of non-dimensional temperature along the X-direction in an absorber plate according to

analytical results and numerical results. In Figure (a) the middle point surface (i.e. $Y$= 0.5) and in (b) unit step length surface (i.e. $Y$= 1) are shown. It is perceived from the figures that the analytical and numerical results are in good accordance, which validates the analytical methods of the present paper.

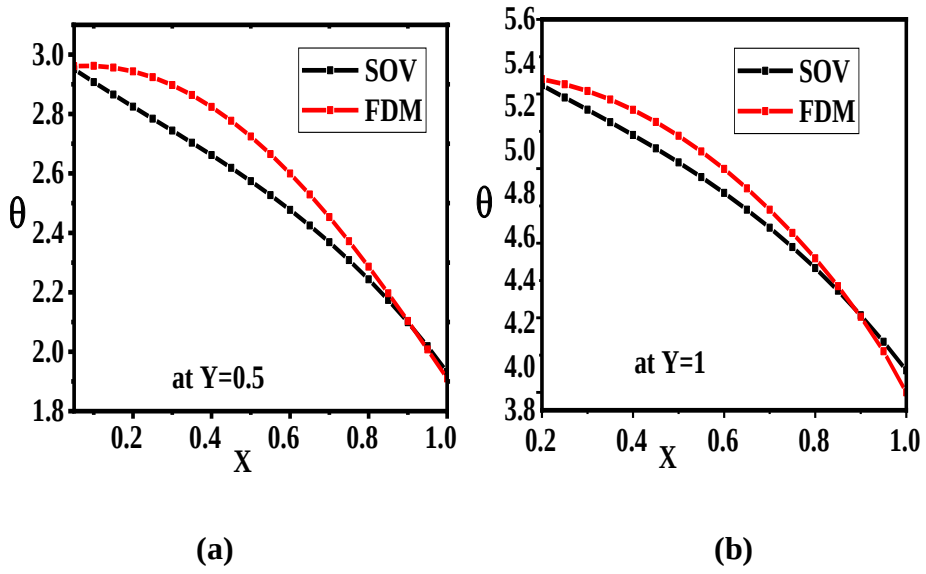


**Fig. 4.2** Non-Dimensional temperature distribution on the absorber plate along X –direction.

Figure 4.3 gives the non-dimensional temperature distribution along the Y-direction in an absorber plate at (a) $X$= 0.5 and (b) $X$ = 1 according to analytical results and numerical results. It is perceived from the figures that the analytical and numerical results are in good accordance, which validates the analytical methods of the present paper.

The isotherms are the most effective approach to illustrate the two-dimensional temperature distribution of the absorber plate. Fig. 4.4 depicts the isotherm patterns across the absorber plate. It's interesting to

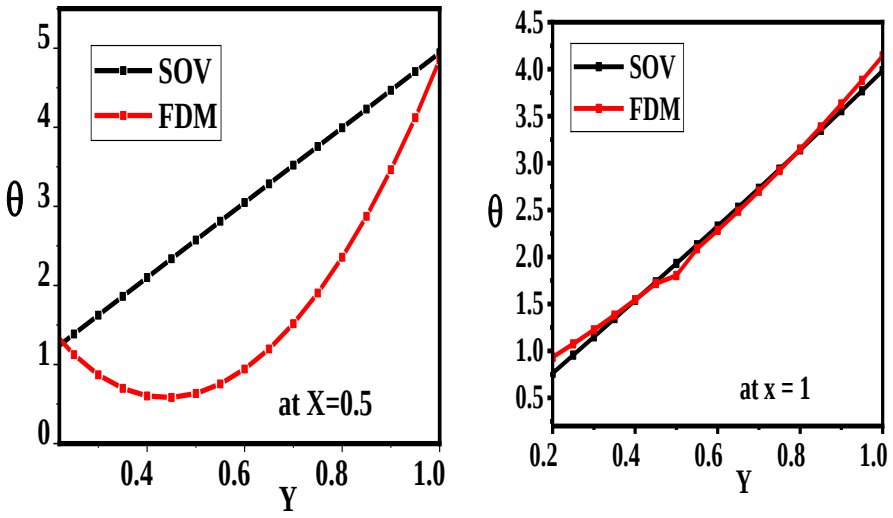


**Fig. 4.3** Non-Dimensional temperature distribution on the absorber plate along flow direction (*Y*).

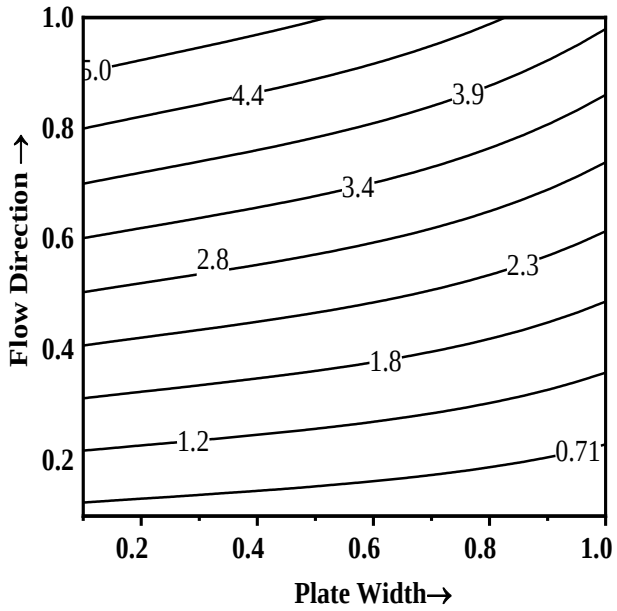


**Fig. 4.4** Contour plot for temperature distribution over the absorber plate.

note that as the isotherms eventually become normal to the tube, the heat flow exhibits a discernible two-dimensional impact.

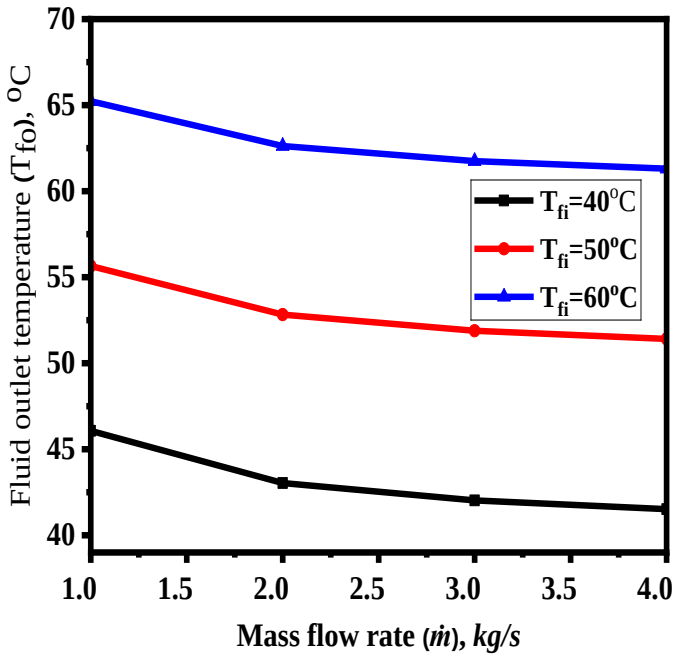


**Fig. 4.5** Impact of temperature variations in the fluid inlet on the fluid output temperature.

The effect of varying the inlet fluid temperature on the absorbing plate's outlet temperature is seen in Fig. 4.5 for various mass flow rates. It is evident that a surge in mass flow rate results in a drop in output temperature. Also, we can see, as temperature at the inlet increases, the outlet temperature also rises. Raising the entrance temperature reduces the rate at which heat is transmitted from the plate to the fluid, hence increasing the plate's exit temperature. In other words, rising the fluid inlet temperature reduces the fluid-absorbing plate temperature differential, which raises the absorber plate's outlet temperature.

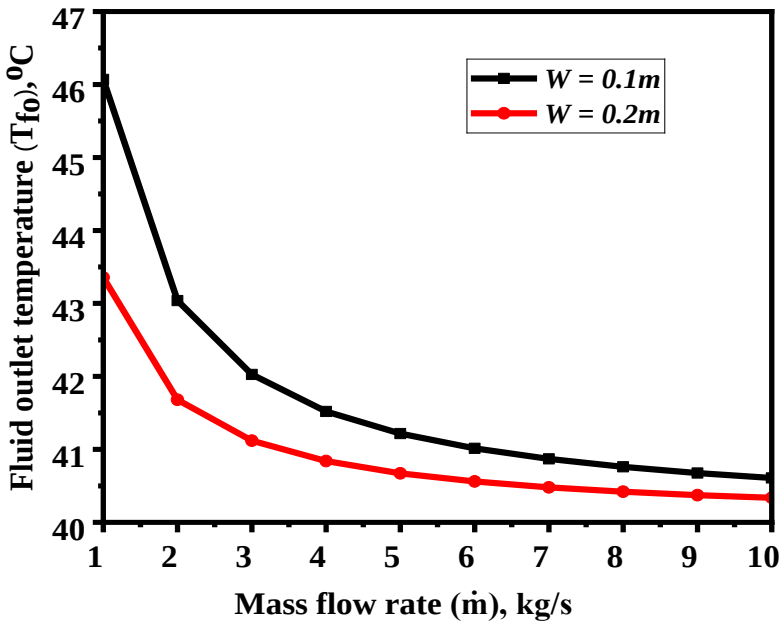


**Fig. 4.6** Effect of fluid outlet temperature on the spacing between fluid-carrying tubes.

Figure 4.6 highlights the link between the exit temperature and the distance between the tubes. It is addressed how the distance between the pipes affects the temperature at the exit. It can be detected that as distances rise, the fluid outlet temperature drops because of increase in loss coefficient. Furthermore, the outlet temperature drops as the mass flow rate rises because there is less heat transfer between the fluid inside the tube and the absorbing plate. The temperature has lowered as the fluid has insufficient time to transfer heat to the absorbent plate.

The effect of variations in the spacing between tubes that convey fluid on the efficiency of solar collectors is explained in Figure 4.7. Interestingly, efficiency falls off as the tube length grows. It is evident that the efficiency declines in an inverse relationship with the tubes' separation. The relationship between this and the Figure 4.6 output

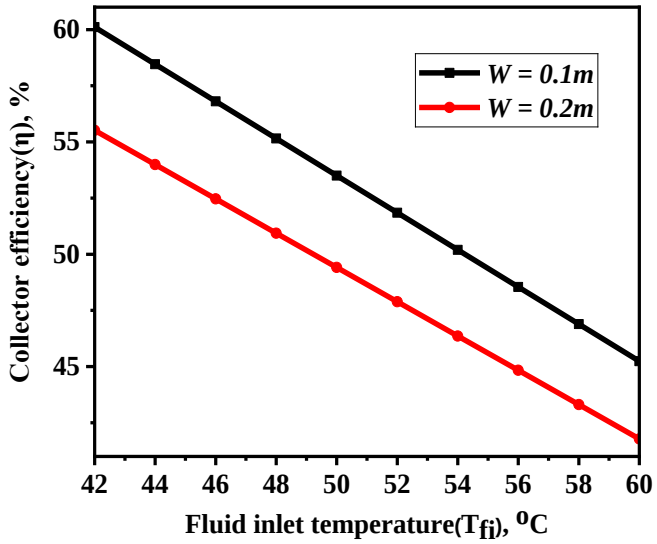


**Fig. 4.7** Effect of the distance between tubes transporting fluid on the collector efficiency.

temperature reduction is clear. The outlet temperature drops with increasing tube distance, which lowers the fluid's rate of heat transfer. As a result of decreased heat transfer, efficiency decreases.

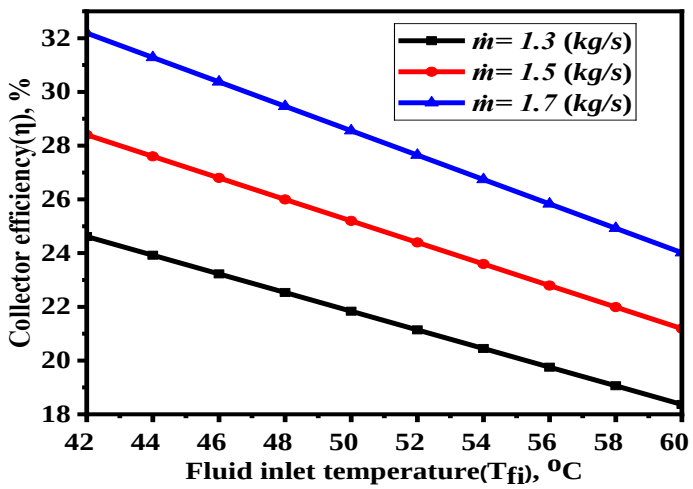


**Fig. 4.8** Effect of mass flow rate on efficiency.

Figure 4.8 depicts the variation of collector efficiency with fluid inlet temperature for different mass flow rate. It shows that the efficiency increases as mass flow rates increases, which could be explained by the fact that by increasing mass flow rate, the fluid's convective heat transfer coefficient rises, accelerating up the rate at which heat is transferred. Moreover, a rise in mass flow rate will lower the mean temperature of the plate and lessen heat loss to the environment. It also shows that as the fluid inlet temperature rises, collector efficiency falls for every flow rate. This decreasing trend holds true for all flow rates and suggests that the system's capacity to transform absorbed energy into usable heat output is diminished by higher input temperatures. This knowledge directs solar collector system optimization, allowing engineers to maximize efficiency and reduce energy loss.

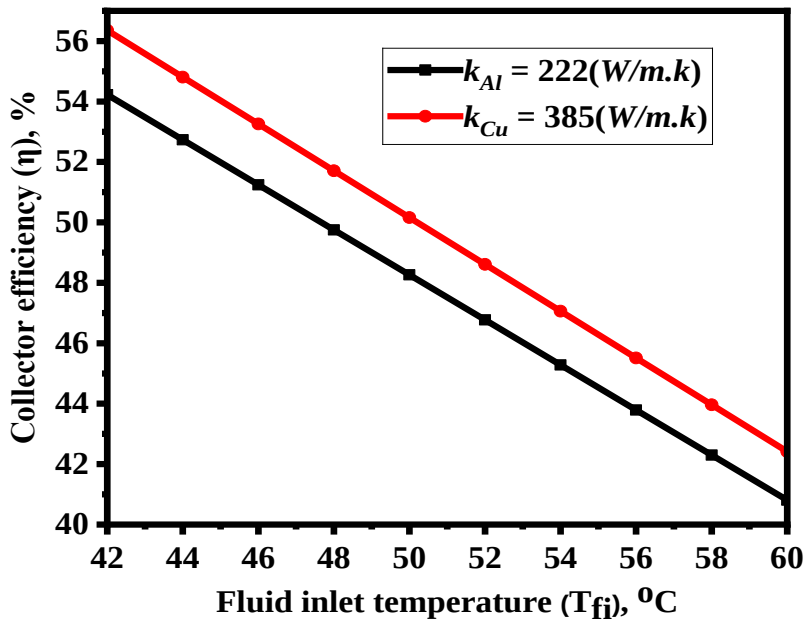


**Fig. 4.9** Impact of absorbing plate conductivity variations on collector efficiency

The effect of the absorbing plate's thermal conductivity on efficiency is investigated in Figure 4.9. According to the figure, efficiency increases by 2% as heat conductivity increases. Nevertheless, materials with lower thermal conductivity, such as aluminium rather than copper, can be used without losing performance, as this gain in conductivity does not significantly improve efficiency. There is a chance to drastically cut the collector's production expenses with this replacement. The linear nature of efficiency decline also suggests a controllable effect on performance as inlet temperatures vary, supports accurate modeling of system performance under various operating situations.

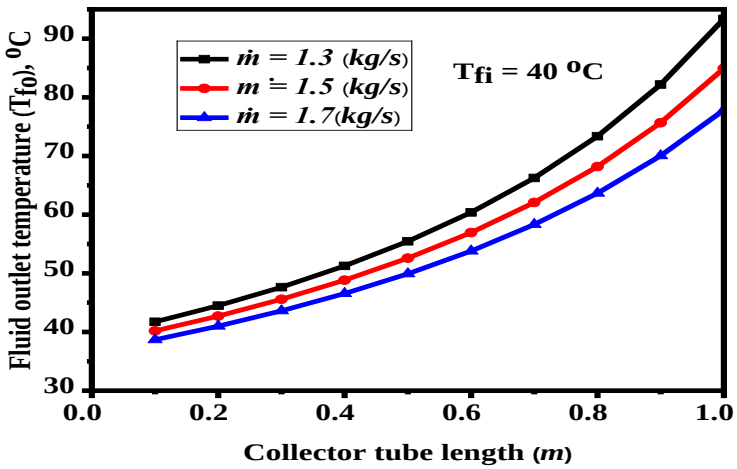


**Fig. 4.10** Temperature Distribution of Axial Fluid in the Absorber Tube

The results for the axial fluid temperature fluctuation are typical observations. Fig. 4.10 depicts fluid temperature distribution along the tube length for different mass flow rate at a given inlet temperature. The exit temperature rises with increasing tube length, indicating that the fluid acquires more thermal energy as it moves farther inside the collection. Lower mass flow rates result in `greater exit temperatures at any given

tube length. There is a nonlinear increase in output temperature with collecting tube length. This suggests that heat transfer efficiency may change as the fluid progresses along the tube. A lower flow rate could be better to optimize outlet temperature, particularly for applications that call for higher fluid temperatures. The temperature increase's nonlinearity indicates that it satisfies the problem's boundary condition.

## 4.4 Summary

In the present paper, the performance of two-dimensional liquid flat plate collector with the variation of temperature at the plate tube junction was investigated both analytically and numerically under steady state condition. The results of analytical method are in good agreement with numerical method. Predicted temperature distributions are in agreement at Biot no. 9. The marginal variations of efficiency on conductivity of the plate material suggests that collector plates could be made of less expensive materials, such aluminum, rather than copper. Even though the one-dimensional model performs well enough for engineering design purposes a two-dimensional model that is being described here is required for collector optimization research

# Chapter 5

## Trapezoidal Approach to Establish One-dimensional Analysis of an Absorber Plate for Two-dimensional Heat Flow

### 5.1 Introduction

1-D heat conduction has been assumed numerously for determining the thermal performance of an absorber plate. In case of 1-D model, thermal resistance for heat flow is lesser and thereby yields higher values of the performance parameters. As the absorber plate is made of a highly conducting material and very small in thickness, it is fact that the 2-D heat conduction will predict better results over 1-D heat conduction [43]. This chapter proposes a modified one-dimensional technique to facilitate a two-dimensional analysis utilising the trapezoidal rule. The results indicate that the improved 1-D model closely aligns with the 2-D model. Therefore, the 1-D classical model is unsuitable to predict the performance of an absorber plate. The modified 1-D model is continuously better than the 1-D classical model. The investigation of the proposed 1-D model is very simple for understanding and calculations.

### 5.2 Mathematical Formulation

For the thermal analysis the subsequent assumptions are made:

- Energy conduction in the absorber plate is two-dimensional and steady state.

- The solar insolation reaching the absorber plate is uniformly distributed over the plate and remains constant throughout.
- The thermal conductivity of the plate material remains constant.
- The surrounding temperature and the overall loss coefficient are constant

For the thermal analysis of absorber plate, the symmetric heat transfer module considered is remaining same as that in previous chapter 3. The governing energy equation and all the boundary conditions are remained same as described in chapter 3 except the boundary at Y=1,which is considered as convective one condition Instead of insulated. Therefore, the governing equation along with the boundary conditions in non-dimensional form can be expressed as

$$\frac{\partial^2\theta}{\partial X^2}+\delta^2\frac{\partial^2\theta}{\partial Y^2}-M^2\theta+N=0 \tag{5.1}$$

at $X=0\left(0\le Y\le 1\right),\ \partial\theta/\partial X=0$ (5.2a)

at $X=1\left(0\le Y\le 1\right),\ \partial\theta/\partial X=-\dfrac{\dot{m}c_pL}{kt\left(T_{in}-T_\infty\right)}\dfrac{dT_f}{dy}=-A$ (5.2b)

at $Y=0\left(0\le X\le 1\right),\ \partial\theta/\partial Y=0$ (5.2c)

at $Y=1\left(0\le X\le 1\right),\ \partial\theta/\partial Y=-Bi\theta$ (5.2d)

### 5.2.1 Numerical methodology

Eq. (5.2) is solved numerically along with the boundary conditions expressed in Eqs. (5.5a) – (5.5d) by the finite difference technique. The differential equations are discretized with Taylor's series central

difference method of second order precision as described in chapter 3. The algebraic equations obtained from the governing relations and boundary circumstances are resolved by Gauss-Seidel iteration method. The final findings are achieved upon meeting the specified accuracy threshold of $10^{-6}$.

### 5.2.2 Proposed modified 1-D model

Let a function $F(X,Y)$ be defined as $F(X,Y)=\partial\theta(X,Y)/\partial Y$ (5.3)

This function can be integrated in the fluid flow direction as

$$\int_0^1 F(X,Y)dY=\int_0^1 \frac{\partial\theta(X,Y)}{\partial Y}dY=\theta(X,1)-\theta(X,0) \tag{5.4}$$

From the trapezoidal rule, the integral form of $\theta(X,Y)$ in Eq. (5.4) yields

$$\int_0^1 F(X,Y)\,dY \approx \frac{1}{2}\left[F(X,1)+F(X,0)\right] \tag{5.5}$$

Combining Eqs. (5.4), (5.5) with (5.2c) and (5.2d)

$$\theta(X,1)-\theta(X,0)=\frac{1}{2}\left[\frac{\partial\theta(X,1)}{\partial Y}+\frac{\partial\theta(X,0)}{\partial Y}\right]$$

$$\Rightarrow \theta(X,0)=\left(\frac{2+Bi}{2}\right)\theta(X,1) \tag{5.6}$$

The average temperature in the flow direction

$$\bar{\theta}(X)=\int_0^1 \theta(X,Y)dY \tag{5.7}$$

Using the trapezoidal rule Eq. (5.7) can be expressed as

$$\bar{\theta}(X)\approx\frac{1}{2}\left[\theta(X,1)+\theta(X,0)\right] \tag{5.8}$$

Combining Eqs. (5.7) and (5.8) with (5.6) we have

$$\theta(X,1)=\frac{4\bar{\theta}(X)}{4+Bi} \tag{5.9}$$

The 2-D energy Eq. (5.1) can be recast in integral form as

$$\int_0^1 \frac{\partial}{\partial Y}\left(\frac{\partial \theta}{\partial Y}\right) dY = -\frac{1}{\delta^2}\int_0^1 \frac{\partial^2 \theta}{\partial X^2} dY + \frac{M^2}{\delta^2}\int_0^1 \theta dY - \frac{N}{\delta^2}\int_0^1 dY \tag{5.10}$$

Integrating and rearranging we have

$$\left(\frac{\partial \theta}{\partial Y}\right)_{Y=1} - \left(\frac{\partial \theta}{\partial Y}\right)_{Y=0} = -\frac{1}{\delta^2}\frac{\partial^2}{\partial X^2}\int_0^1 \theta dY + \frac{M^2}{\delta^2}\int_0^1 \theta dY - \frac{N}{\delta^2} \tag{5.11}$$

Combining Eqs. (5.7), (5.10) and (5.11) gives

$$\frac{\partial^2 \bar{\theta}(X)}{\partial X^2} - g^2 \bar{\theta}(X) + N = 0 \tag{5.12}$$

$$\text{where } g^2 = \left(M^2 + \frac{4\delta^2 Bi}{4 + Bi}\right) \tag{5.12a}$$

It is noteworthy that Eq. (5.12) serves as the differential equation that governs for the modified one-dimensional model and is of an identical kind to that of the classical one-dimensional model [52], with the exception of the value of $g$ .Equation (5.12) is solved with the boundary condition obtained from Eqs.(5.2a) and (5.2b) as

$$\bar{\theta}(X) = C_1 \cosh(gX) + C_2 \sinh(gX) + \frac{N}{g^2} \tag{5.13}$$

$$\text{at } X = 0,\ \frac{\partial \bar{\theta}(X)}{\partial X} = 0 \Rightarrow \left[C_1 \sinh(gX) + C_2 \cosh(gX)\right] g = 0 \Rightarrow C_2 = 0 \tag{5.14}$$

$$\text{at } X = 1, \frac{\partial \bar{\theta}(X)}{\partial X} = -A \Rightarrow C_1 \sinh(m) m = -A \Rightarrow \boxed{C_1 = \frac{-A}{m \sinh(m)}} \tag{5.14b}$$

Hence the modified temperature distribution can be given as

$$\bar{\theta}(X) = \frac{N}{g^2} - \frac{A}{m \sinh(g)} \cosh(gX) \tag{5.15}$$

### 5.2.3 Classical 1-D model

Neglecting the temperature gradient in the transverse direction $(Y)$, the differential equation obtained from the energy balance for the absorber plate becomes

$$\frac{d^2\theta}{dX^2} - M^2\theta + N = 0 \tag{5.16}$$

Equation (5.16) along with the boundary conditions from Eqs. (5.2a) and (5.2b) can be solved analytically as

$$\theta(X) = \frac{N}{M^2} - \frac{A\cosh(MX)}{M\sinh M} \tag{5.17}$$

## 5.3 Results and Discussion

For the validation purpose, there are insufficient results available in the literature. Therefore, the temperature distribution over the absorber plate for various design parameters were obtained for the proposed modified 1-D model and the classical 1-D model analytically, and they have been compared with the 2-D heat transfer model numerically. Fig. 5.2 depicts the temperature distribution predicted by three different models for a set of design parameters and different biot number. It is observed that there is an excellent match between the 2-D numerical and 1-D modified models.

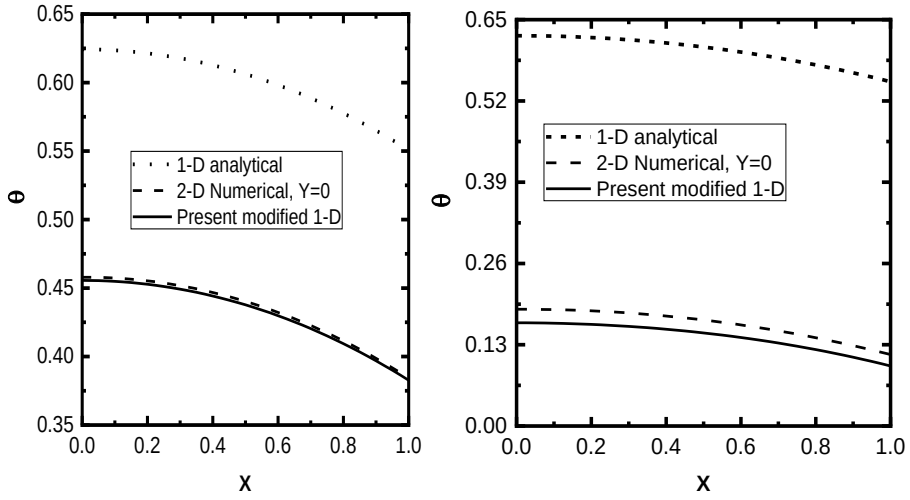


(a) Bi=0.1 (b) Bi=1.0

**Fig. 5.2** Effects of $Bi$ on temperature distribution in an absorber plate predicted by different methods at $N = 0.3$, $M = 0.5$, $\delta = 1.0$, and $A = 0.15$

The temperature variation for 1-D classical model over predicts with respect to the values obtained from the other two models. In Fig. 5.2a temperature distribution is drawn for $Bi = 0.1$ and Fig. 5.2b is plotted for $Bi = 1.0$. As Biot number increases the conductive resistance increases and a result, it decreases the heat transfer rate. This effect can be visualized graphically from these two figures. In both the cases, the temperature range for 2-D model and 1-D modified model matches closely.

Fig. 5.3 depicts the temperature distribution determined by three different methods with the variation of solar flux. For each case, there is a good agreement between 2-D and 1-D modified model. For the lower value of solar insolation, the absorber plate temperature is low. As the insolation increases the temperature of the absorber plate increases. This situation can be clearly justified from Figs. 5.3a and 5.3b. In both the cases the result of 2-D and modified 1-D models matches closely

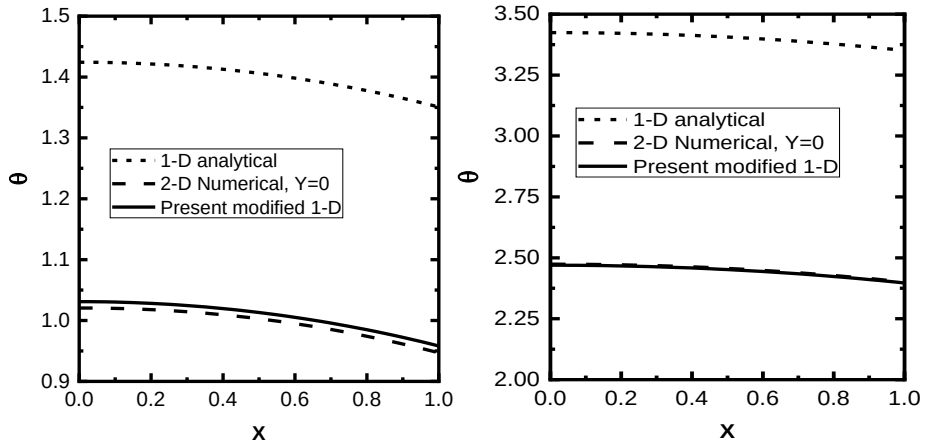


(a) N=0.5 (b) N=1.0

**Fig. 5.3** Influences of design variable $N$ on temperature distribution in absorber plates for $Bi = 1.0$, $M = 0.5$, $\delta = 1.0$, and $A = 0.15$

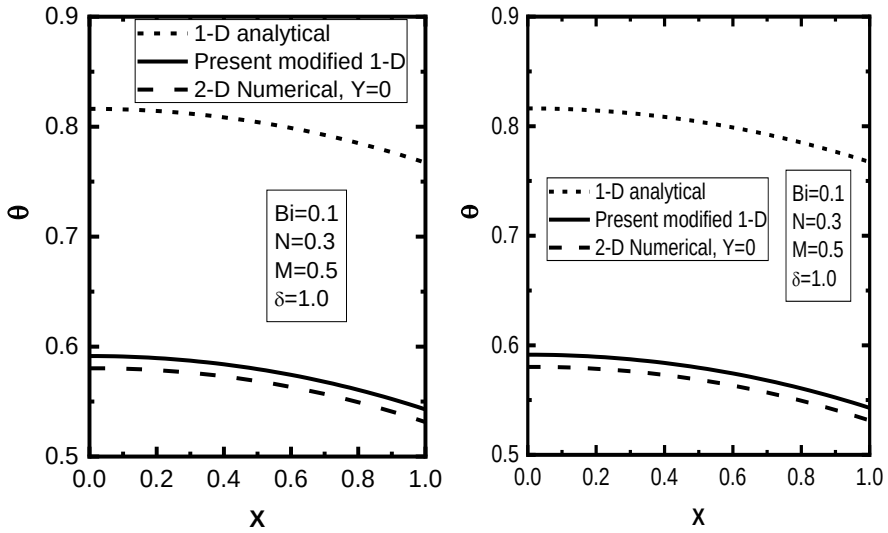


(a) M=0.5 (b) M=1.0

**Fig. 5.4** Temperature distribution in absorber plates in x-direction for $Bi = 0.1$, $N = 0.3$, $\delta = 1.0$, and $A = 0.1$

Figs. 5.4a and 5.4b predict the temperature distribution for different values of thermo-geometric parameter $M$. Since the thermo-geometric factor is directly related to the overall heat loss, an increasing $M$ means there is an upsurge in overall heat loss coefficient and hence temperature field decreases due to more heat transfer rate among the absorber plate and surrounding. This effect can be verified from these two figures. It can also be observed that there is a good arrangement between the results of 2-D and 1-D modified model and they are very closer to each other

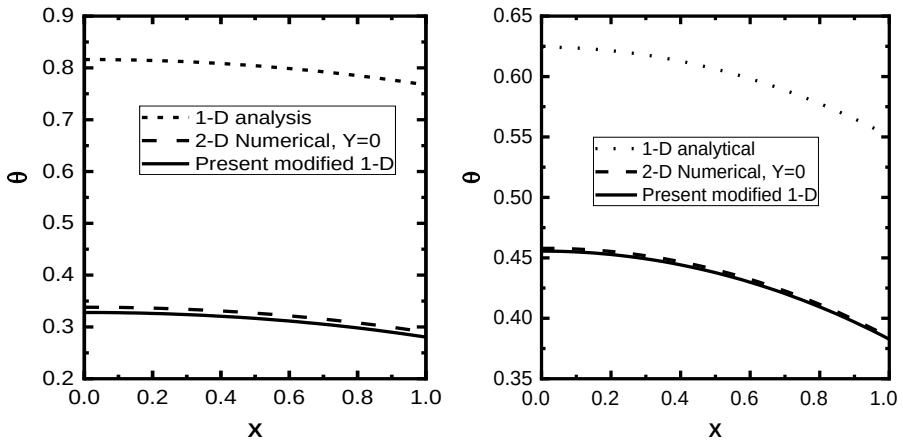


(a) $\delta = 1.0$ (b) $\delta = 2.0$

**Fig. 5.5** Different methods used to determine temperature distribution in absorber plates in x-direction for $Bi = 0.1$, $N = 0.3$, $M = 0.5$, $\delta = 2.0$, and $A = 0.15$

The impact of $\delta$, i.e. width to length ratio, on the distribution of temperature is also predicted and it can be done by comparing Figs. 5.5(a) and 5.5(b). An upsurge in $\delta$ diminishes the absorber plate temperature owing to an surge in thermal resistance for the heat flow

## 5.4 Summary

In the present study, an investigation is done by developed 2-D and modified 1-D models to predict the temperature profile in an absorber plate for a flat-plate solar collector. The determination of the performance of absorber plates based on 1-D heat conduction may not be an correct methodology in any design context [13-15]. Therefore, 2-D models can be used for the thermal investigation of an absorber plate accurately. But in many situations the 2-D analysis has increased the complexity to establish an analytical solution. From the result and discussion section, it was noted that the results show a high degree of consistency of 2-D model determined by the finite difference method and the modified 1-D model. In every case study, The construction of the current study (2-D and modified 1-D models) has been executed meticulously to facilitate comprehension of the offered results. Alternatively, the proposed modified 1-D model is continuously superior to the classical 1-D model for the analysis of an absorber plate in flat plate solar collector.

# Chapter 6

## Heat transfer dynamics in absorber plates of a flat-plate solar collector: Fourier and revised non-Fourier analyses

### 6.1 Introduction

There has been a rising attention in employing non-Fourier heat conduction model to simulate microscale and ultrafast transient non-equilibrium responses in heat and mass transfer, characterized by non-classical phenomena and thermal delays. This chapter analytically inspects the impact of FHC and NFHC in the absorber plate of a FPSC. Literature studies indicate that only a limited number of research have examined using Fourier and non-Fourier in the absorber plate of a FPSC, wherein a simplified version of the governing differential relations for the absorber plate has been considered by neglecting the time relaxation term related to the loss coefficient. This study used the S-P-L model, which includes a temporal relaxation term with the loss coefficient, in the energy equation to investigate the NFHC behaviour. A repetitive symmetrical heat transfer module of the collector plate is analysed, and the relevant parabolic and hyperbolic heat conduction equations are derived utilizing the separation of variables technique. The analytical conclusions are validated by numerical simulations using the finite difference approach. The impact of critical factors, such as the Vernotte number, dimensionless time, and thermo-geometric parameter, on the temperature response of the absorber plate is examined. The proposed model is further authenticated by comparison with the published results of Kundu and Lee, which did not account for the phase lag associated

with the loss coefficient. A significant difference in temperature distribution is observed, highlighting the importance of phase lag effects in accurately predicting the transient thermal response of the absorber plate.

## 6.2 Mathematical formulation

Figure 6.1 illustrates a schematic representation of the absorber plate of a flat-plate collector with uniform thickness. For thermal analysis a symmetrical area situated among the two fluid-carrying tubes is considered. The following assumptions were considered for the heat transfer analysis on the absorber plate of the flat-plate solar collector:

- The plate's internal heat conduction is one-dimensional.
- Throughout the whole plate surface, the total loss coefficient remains constant.
- The temperature of the surrounding is constant.
- The plate material's thermal characteristics remain unchanged.
- The absorber plate’s width is fixed and regarded as unity.

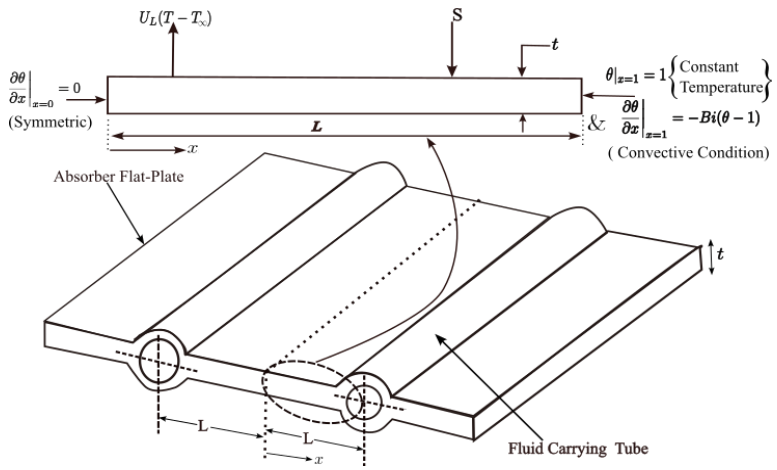


**Fig. 6.1**Schematic of the Heat Transfer Model for an Absorber Plate

Generally, in transient heat conduction considering the FHC model, the heat propagation takes place with an infinite rate which might not at all times be satisfied as shown by Peshkov [75] by his experimental method. Rather than the infinite speed of heat propagation, he suggested a finite one which is extensively reported as a NFHC phenomenon. The model incorporates the effect of finite wave speed via the relaxation time ($\tau$), which signifies the time delay or accumulation period before heat movement commences following the establishment of a temperature differential in the medium. This signifies that heat transfer does not begin instantly but evolves gradually throughout the relaxation period subsequent to the imposition of a temperature gradient. Similarly, when the temperature gradient is eliminated, heat transfer does not stop instantaneously but rather decreases progressively over time. When the relaxation time $\tau \to 0$, heat diffusion occurs instantaneously with an infinite propagation velocity, aligning with the classical Fourier heat conduction concept. However, for relatively large values of $\tau$, thermal disturbances propagate as waves at finite speeds, deviating from the conventional diffusion model.

Thus, in the S-P-L model [84], the heat flux vector $q$ and the temperature $T$ at time $\iota$ and spatial location $x$ are described by Eq. (6.1) as follows:

$$q(x,\iota) + \tau \frac{\partial q(x,\iota)}{\partial \iota} = -k\nabla T \tag{6.1}$$

The energy equation for an absorber plate in a flat-plate collector, taking into account one-dimensional heat conduction, may be expressed as follows using Eq. (6.2):

$$-\nabla q + \frac{S}{t} - \frac{U_L(T-T_\infty)}{t} = \rho c_p \frac{\partial T}{\partial \iota} \tag{6.2}$$

Combining equations (6.1) & (6.2) the mathematical model of the absorber plate governed by NFHC can be expressed in Eq. (6.3) as follows:

$$k\frac{\partial^2 T}{\partial x^2} - \frac{\tau U_L}{t}\frac{\partial\left(T-T_\infty\right)}{\partial \iota} + \frac{S}{t} - \frac{U_L(T-T_\infty)}{t} = \rho c_p\left(\frac{\partial T}{\partial \iota} + \tau\frac{\partial^2 T}{\partial \iota^2}\right) \tag{6.3}$$

The corresponding dimensionless variables are introduced to formulate the non-dimensional equations.

$$\theta = \frac{T-T_\infty}{T_{in}-T_\infty},\ X = \frac{x}{L}, Fo = \frac{\kappa \iota}{L^2},\ \kappa = \frac{k}{\rho c_p},$$

$$C^2 = \frac{\kappa}{\tau},\ V_e = \sqrt{\frac{\tau_q \kappa}{L^2}} or = \frac{\tau C}{L} \tag{6.4}$$

By utilizing dimensionless parameters the Eq. (6.3) can be inscribed in non-dimensional form as follows

$$\frac{\partial^2 \theta}{\partial X^2} - M^2\theta + N = P\frac{\partial \theta}{\partial Fo} + Ve^2\frac{\partial^2 \theta}{\partial Fo^2} \tag{6.5}$$

Where

$$M^2 = \frac{U_L L^2}{kt},\ N = \frac{SL^2}{kt(T_{in}-T_\infty)},\ P = \left(1+Ve^2M^2\right) \tag{6.6}$$

in Eq. (6.4) the thermal wave speed or the propagation speed $C$ is defined based on $\tau$. The distinction between FHC and NFHC models depends on the magnitude of the dimensionless Vernotte number $(Ve)$. When $Ve = 0$, the propagation speed approaches infinity, corresponding to the instantaneous heat transfer anticipated by the FHC model. However, for

every nonzero value of $Ve$, the propagation speed remains limited, so validating the NFHC model. The subsequent beginning and boundary conditions in non-dimensional form are employed for NFHC to investigate the thermal wave characteristics of the absorber plate.

$$\text{at } Fo = 0,\ \theta(X,0) = 0 \tag{6.7}$$

$$\frac{\partial\theta(X,0)}{\partial Fo} = 0 \tag{6.8}$$

$$\text{at } Fo > 0,\ X = 0,\ \frac{\partial\theta}{\partial X} = 0 \tag{6.9}$$

$$X = 1,\ \theta(1,Fo) = 1 \tag{6.10a}$$

The boundary condition in Eq. (6.10a) is applied to maintain a particular plate temperature at the plate-tube junction $(X = 1)$ that facilitates fluid flow for energy extraction. However, ensuring a constant plate temperature at the plate-tube junction may not be practical, especially during the initial phase of unsteady conditions. In reality, the solar energy absorbed by the plate is transported to the fluid flowing, converting it into useful energy [16]. Taking this into account, a convected boundary condition at $X = 1$ in non-dimensional form can be directly expressed as

$$\frac{\partial\theta(1,Fo)}{\partial X} = -Bi(\theta - 1) \tag{6.10b}$$

The temperature discrepancy in the plate can be calculated analytically using all these initial and boundary conditions Eq. (6.7)–(6.10). For both FHC and NFHC analysis, two set of conditions; constant temperature

condition with Eq. (6.10a) and convected heat transfer condition with Eq. (10b), has been considered.

### *6.2.1 Analysis for non-Fourier model*

The separation of variables technique can be utilized to solve Eq. (6.5) [158]. The following variables were chosen for the approach of the solution:

$$\theta\left(X, Fo\right) = \psi(X) + \phi(X, Fo) \tag{6.11}$$

By applying Eq. (6.11) in Eq. (6.5), the following expression are obtained:

$$\frac{d^2\psi}{dX^2} - M^2\psi + N = 0 \tag{6.12}$$

and

$$\frac{\partial^2\phi}{\partial X^2} - M^2\phi = P\frac{\partial\phi}{\partial Fo} + Ve^2\frac{\partial^2\phi}{\partial Fo^2} \tag{6.13}$$

The boundary conditions derived from Eqs. (6.7)–(6.10) for Eq. (6.12) areas follows

at $X = 0$, $\frac{\partial\psi}{\partial X} = 0$ (6.14)

$X = 1$, $\psi\left(1, F_0\right) = 1$ (6.15a)

& $\frac{d\psi\left(1\right)}{dX} + Bi\psi\left(1\right) = Bi$ (6.15b)

The boundary conditions for Eq. (6.13) are derived from Eqs. (6.7)–(6.10) as follows.

at $Fo = 0$, $\phi\left(X, 0\right) = -\psi(X)$ (6.16)

$$\frac{\partial\phi\left(X, 0\right)}{\partial Fo} = 0 \tag{6.17}$$

$$Fo > 0.\ X = 0,\ \frac{\partial \phi(0, Fo)}{\partial X} = 0 \tag{6.18}$$

$$X = 1,\ \phi(1, Fo) = 0 \tag{6.19a}$$

$$and \quad \frac{\partial \phi(1, Fo)}{\partial X} + Bi\phi(1, Fo) = 0 \tag{6.19b}$$

The solution of Eq. (6.12) along with the boundary conditions (6.14), (6.15a) and (6.15b) yields

$$\psi(X) = \frac{N}{M^2} + \left(1 - \frac{N}{M^2}\right)\frac{\cosh(MX)}{\cosh(M)} \tag{6.20a}$$

and

$$\psi(X) = \frac{N}{M^2} + \frac{Bi\left(1 - N/M^2\right)\cosh(MX)}{M\sinh(M) + Bi\cosh(M)} \tag{6.20b}$$

For the solution of Eq. (6.13) the variable $\phi(X, Fo)$ is separated by using the product rule as follows

$$\phi(X, Fo) = U(X)V(Fo) \tag{6.21}$$

Combining Eqs. (6.13) and (6.21), the obtained expressions with an Eigen constant are as follows

$$\frac{d^2U}{dX^2} + \lambda^2 U = 0 \tag{6.22}$$

and

$$Ve^2\frac{d^2V}{dFo^2} + P\frac{dV}{dFo} + \left(M^2 + \lambda^2\right)V = 0 \tag{6.23}$$

The modified boundary conditions are obtained by imposing Eq.(6.21) into Eqs. (6.16) – (6.19) and can be written as

$$U(X)V(0) = -\psi(X) \tag{6.24}$$

$$\frac{dV(0)}{dF_0} = 0 \tag{6.25}$$

$$\frac{dU(0)}{dX} = 0 \tag{6.26}$$

By applying the boundary conditions in Eqs. (6.19a) and (6.19b), the following condition is obtained

$$U(1) = 0 \tag{6.27a}$$

$$\text{and } \frac{dU(1)}{dX} + BiU(1) = 0 \tag{6.27b}$$

The following equations can be obtained by rewriting Eq. (6.22) using Eq. (6.26) and (6.27a) as well as Eq. (6.26) and (6.27b) respectively.

$$\lambda_m = (2m-1)\pi/2, \quad m = 1, 2, 3..... \tag{6.28a}$$

$$U(X) = \sum_{m=1}^{\infty} C_m \cos(\lambda_m X) \tag{6.28b}$$

and

$$\lambda_n - \tan^{-1}(Bi/\lambda_n) = (n-1)\pi, \; n = 1, 2, 3..... \tag{6.29a}$$

$$U(X) = \sum_{n=1}^{\infty} C_n \cos(\lambda_n X) \tag{6.29b}$$

In Eqs. (6.28b) and (6.29b) $C_m$ and $C_n$ are constants and their value can be found by orthogonality condition.

Using differential operator, $D$, Eq.(6.23) can be expressed as follows,

$$\left[Ve^2 D^2 + PD + \left(M^2 + \lambda_m^2\right)\right]V = 0 \tag{6.30a}$$

$$\left[Ve^2 D^2 + PD + \left(M^2 + \lambda_n^2\right)\right]V = 0 \tag{6.30b}$$

Where $D$ can be determined from

$$D=\left(D_{1,},D_{2}\right)=\begin{cases}\dfrac{-P\pm\sqrt{P^{2}-4Ve^{2}\left(\lambda_{m}^{2}+M^{2}\right)}}{2Ve^{2}}\\ \dfrac{-P\pm\sqrt{P^{2}-4Ve^{2}\left(\lambda_{n}^{2}+M^{2}\right)}}{2Ve^{2}}\end{cases} \tag{6.31}$$

According to Equation (6.31), the $D$ value have both real& distinct, or a complex conjugate pair, or be zero. Therefore, the solution must take into account the three distinct circumstances must be taken into account. Eqs. (6.20a), (6.24), (6.25), (6.27a), (6.28), and (6.31) are used to get the temperature distribution that follows.

$$\theta\left(X,Fo\right)=\left[\frac{N}{M^{2}}+\left(1-\frac{N}{M^{2}}\right)\frac{\cosh\left(MX\right)}{\cosh\left(M\right)}\right]+2\sum_{m=1}^{\infty}\cos(\lambda_{m}X)$$

$$\times\sin(\lambda_{m})\left[\frac{N}{M^{2}\lambda_{m}}+\frac{\left(1-N/M^{2}\right)\lambda_{m}}{\left(\lambda_{m}^{2}+M^{2}\right)}\right]$$

$$\times\left(\frac{D_{2}\exp\left(D_{1}Fo\right)-D_{1}\exp\left(D_{2}Fo\right)}{D_{1}-D_{2}}\right)\quad\text{for}\left(\lambda_{m}^{2}+M^{2}\right)<\frac{P^{2}}{4Ve^{2}} \tag{6.32}$$

$$\theta\left(X,Fo\right)=\left[\frac{N}{M^{2}}+\left(1-\frac{N}{M^{2}}\right)\frac{\cosh\left(MX\right)}{\cosh\left(M\right)}\right]$$

$$-2\sum_{m=1}^{\infty}\left(1+\frac{PFo}{2Ve^{2}}\right)\exp\left(\frac{-PFo}{2Ve^{2}}\right)\cos(\lambda_{m}X)$$

$$\times\sin(\lambda_{m})\left[\frac{N}{M^{2}\lambda_{m}}+\frac{\left(1-N/M^{2}\right)\lambda_{m}}{\left(\lambda_{m}^{2}+M^{2}\right)}\right]\text{for}\left(\lambda_{m}^{2}+M^{2}\right)=\frac{P^{2}}{4Ve^{2}} \tag{6.33}$$

$$\theta\left(X,Fo\right)=\left[\frac{N}{M^{2}}+\left(1-\frac{N}{M^{2}}\right)\frac{\cosh\left(MX\right)}{\cosh\left(M\right)}\right]$$

$$-2\sum_{m=1}^{\infty}\frac{\cos(\lambda_{m}X)\sin(\lambda_{m})}{D_{0}}\exp\left(\frac{-PFo}{2Ve^{2}}\right)\times\left[\frac{N}{M^{2}\lambda_{m}}+\frac{\left(1-N/M^{2}\right)\lambda_{m}}{\left(\lambda_{m}^{2}+M^{2}\right)}\right]$$

$$\times\left[ D_0 \cos\left(D_0 Fo\right) + \frac{P}{2Ve^2}\sin\left(D_0 Fo\right)\right] \text{for} \left(\lambda_m^2 + M^2\right) > \frac{P^2}{4V_e^2} \tag{6.34}$$

where

$$D_0 = \frac{\sqrt{4Ve^2\left(\lambda_m^2 + M^2\right) - P^2}}{2Ve^2} \tag{6.35}$$

Eqs. (6.32)–(6.34),were derived by ensuring that constant temperature is maintained at plate – tube junction $\left(X = 1\right)$. For a convective boundary condition at $\left(X = 1\right)$ the temperature in the plate can be determined using Eqs. (6.20b), (6.24), (6.25), (6.27b), (6.29), and (6.31) as follows,

$$\theta\left(X, Fo\right) = \left[\frac{N}{M^2} + \frac{Bi\left(1 - N/M^2\right)\cosh\left(MX\right)}{M\sinh\left(M\right) + Bi\cosh\left(M\right)}\right]$$

$$+4\sum_{n=0}^{\infty}\frac{\lambda_n \cos(\lambda_n X)\left[D_2 \exp\left(D_1 Fo\right) - D_1 \exp\left(D_2 Fo\right)\right]}{\left[2\lambda_n + \sin 2(\lambda_n)\right]\left(D_1 - D_2\right)} \times \left[\frac{N\sin(\lambda_n)}{M^2\lambda_n}\right.$$

$$\left. + \frac{Bi\left(1 - N/M^2\right)\left[\lambda_n \cosh\left(M\right)\sin(\lambda_n) + M\sinh(M)\cos(\lambda_n)\right]}{\left[M\sinh\left(M\right) + Bi\cosh\left(M\right)\right]\left(\lambda_n^2 + M^2\right)}\right] \text{for}$$

$$\left(\lambda_n^2 + M^2\right) < \frac{P^2}{4Ve^2} \tag{6.36}$$

$$\theta\left(X, Fo\right) = \left[\frac{N}{M^2} + \frac{Bi\left(1 - N/M^2\right)\cosh\left(MX\right)}{M\sinh\left(M\right) + Bi\cosh\left(M\right)}\right]$$

$$-4\sum_{n=0}^{\infty}\frac{\lambda_n \cos(\lambda_n X)\left(1 + \frac{PFo}{2Ve^2}\right)\exp\left(\frac{-PFo}{2Ve^2}\right)}{\left[2\lambda_n + \sin 2(\lambda_n)\right]}$$

$$\times\left[\frac{N\sin(\lambda_n)}{M^2\lambda_n}+\frac{Bi\left(1-N/M^2\right)\left[\lambda_n\cosh\left(M\right)\sin(\lambda_n)+M\sinh(M)\cos(\lambda_n)\right]}{\left[M\sinh\left(M\right)+Bi\cosh\left(M\right)\right]\left(\lambda_n^2+M^2\right)}\right]$$

$$\text{for}\left(\lambda_n^2+M^2\right)=\frac{P^2}{4Ve^2} \tag{6.37}$$

$$\theta\left(X,Fo\right)=\left[\frac{N}{M^2}+\frac{Bi\left(1-N/M^2\right)\cosh\left(MX\right)}{M\sinh\left(M\right)+Bi\cosh\left(M\right)}\right]$$

$$-4\sum_{n=0}^{\infty}\frac{\exp\left(\frac{-PFo}{2Ve^2}\right)\left[D_0\cos\left(D_0Fo\right)+\frac{P}{2Ve^2}\sin\left(D_0Fo\right)\right]}{D_0\left[2\lambda_n+\sin 2(\lambda_n)\right]\left[\lambda_n\cos(\lambda_nX)\right]^{-1}}$$

$$\times\left[\frac{N\sin(\lambda_n)}{M^2\lambda_n}+\frac{Bi\left(1-N/M^2\right)\left[\lambda_n\cosh\left(M\right)\sin(\lambda_n)+M\sinh(M)\cos(\lambda_n)\right]}{\left[M\sinh\left(M\right)+Bi\cosh\left(M\right)\right]\left(\lambda_n^2+M^2\right)}\right]$$

$$\text{for}\left(\lambda_n^2+M^2\right)>\frac{P^2}{4Ve^2} \tag{6.38}$$

### *6.2.2 Analysis for Fourier model*

Based on Fourier's law of heat conduction, the governing differential equation for the absorber plate temperature is expressed as follows,

$$\frac{\partial^2\theta}{\partial X^2}-M^2\theta+N=\frac{\partial\theta}{\partial Fo} \tag{6.39}$$

For the solution of Eq. (6.39) the initial and boundary conditions are as follows

$$\theta\left(X,0\right)=0\ ,\ \ 0\le X\le 1 \tag{6.40}$$

$$\frac{\partial\theta\left(0,Fo\right)}{\partial X}=0\ ,\ Fo>0 \tag{6.41}$$

The boundary conditions at $X=1$ are as follows

$$\theta(1,Fo)=1,\ Fo>0 \tag{6.42a}$$

$$\frac{\partial\theta(1,Fo)}{\partial X}=-Bi(\theta-1),\ Fo>0 \tag{6.42b}$$

Following the procedures defined in the preceding section, Eq. (6.39) is solved using the separation of variables method, together with the initial and boundary conditions Eqs. (6.40), (6.41) and (6.42a). Thus, the temperature distribution for isothermal condition at $X=1$ can be listed as

$$\theta(X,Fo)=\frac{N}{M^2}+\left(1-\frac{N}{M^2}\right)\frac{\cosh(MX)}{\cosh(M)}$$
$$-2\sum_{n=1}^{\infty}\cos(\lambda_m X)\sin(\lambda_m)\exp\left(-\left(M^2+\lambda_m^2\right)Fo\right)$$
$$\times\left[\frac{N}{M^2\lambda_m}+\frac{\left(1-N/M^2\right)\lambda_m}{\left(\lambda_m^2+M^2\right)}\right] \tag{6.43}$$

and for convective boundary condition at $X=1$ is as

$$\theta(X,Fo)=\left[\frac{N}{M^2}+\frac{Bi\left(1-N/M^2\right)\cosh(MX)}{M\sinh(M)+Bi\cosh(M)}\right]$$
$$-4\sum_{n=1}^{\infty}\frac{\lambda_n\cos(\lambda_n X)\exp\left[-\left(\lambda_n^2+M^2\right)Fo\right]}{\left[2\lambda_n+\sin 2(\lambda_n)\right]}$$
$$\times\left[\frac{N\sin(\lambda_n)}{M^2\lambda_n}+\frac{Bi\left(1-N/M^2\right)}{\left(\lambda_n^2+M^2\right)}\left\{\frac{\lambda_n\cosh(M)\sin(\lambda_n)+M\sinh(M)\cos(\lambda_n)}{M\sinh(M)+Bi\cosh(M)}\right\}\right]$$

(6.44)

## 6.3 Results and discussion

Based on the Cattaneo-Vernotte equation, the current study investigates analytically the thermal behaviour of the absorber plate in a flat plate solar collector while accounting for the time relaxation of the loss coefficient. The results are generated using computer programming utilizing FORTRAN and the variables separation method. The outcomes of both FHC and NFHC models are compared with Kundu and Lee's findings [84] to confirm existing algorithm. By contrasting it with a numerical method, the FHC analysis analytical methodology described above may be verified. Accordingly, Eq. (6.5) is resolved numerically by setting $Ve = 0$ and employing the finite difference method. The difference equation is formulated by discretizing the governing equation using Taylor's theorem. To diminish discretization errors, a forward difference scheme is applied for the time derivative, while a second-order central difference is utilized for the spatial derivative. An explicit method is adopted to resolve these equations. The final solution is obtained by resolving the tri-diagonal matrix system (TDMA) using the Thomas algorithm, ensuring the required accuracy. In this study, a higher-order accuracy of $O\left(10^{-6}\right)$ has been considered to further reduce discretization errors [159].

Figure 6.2 illustrates the temperature variation in the absorber plate for various Fourier numbers, taking into account both FHC and NFHC models with isothermal boundary settings at the plate-tube junction. The analysis was conducted using parameters $M = 0.5$, $N = 1$ $Ve = 0.2$ and $Fo$ 0.01 to 5. Fig.6.2(a). illustrates the temperature field distribution based on FHC model where the analytical results show good agreement with numerical findings. Fig.6.2(b) presents the corresponding

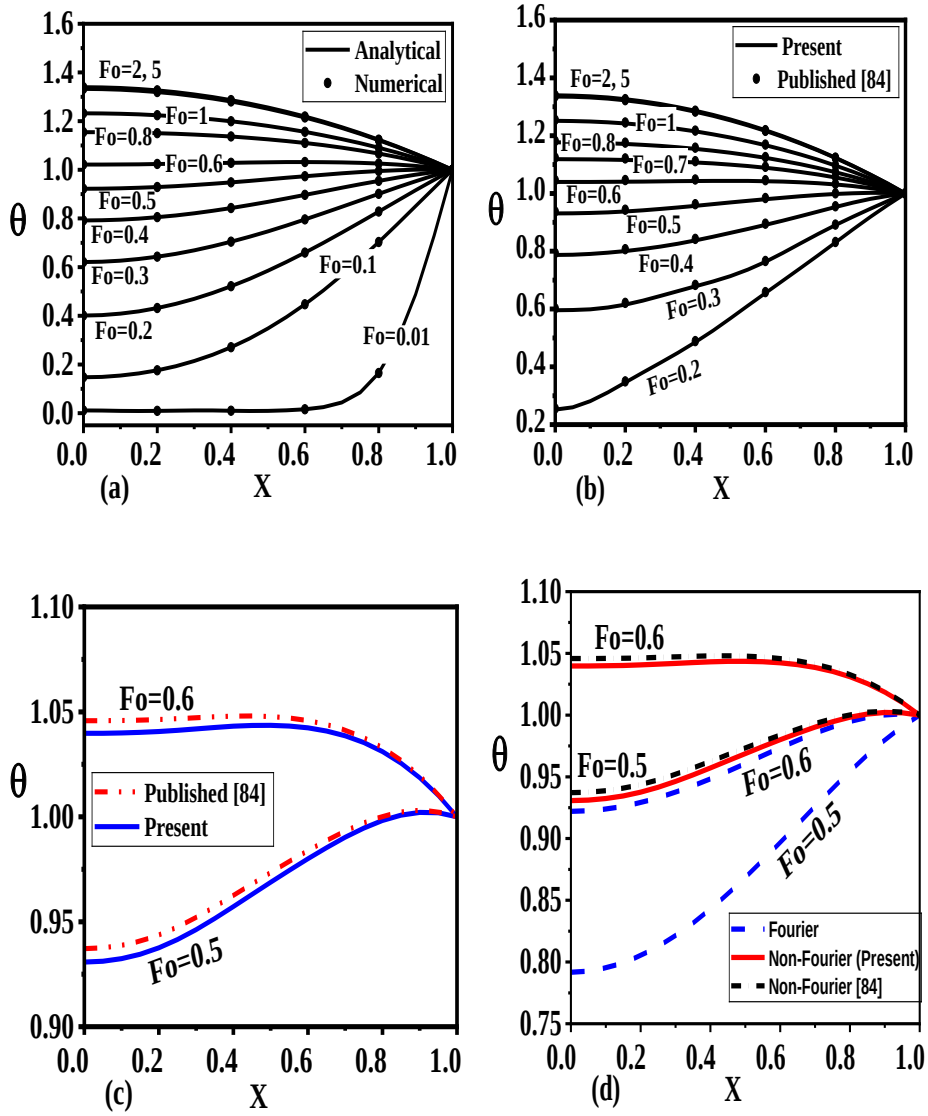


**Fig.6.2** Comparison of temperature distribution over absorber plate obtained in the present work with that of the Kundu and Lee [84] for a constant temperature boundary condition at $X = 1$ for a different Fourier number $Fo$ and $M = 0.5$, $N = 1$ (a) FHC, (b) NFHC, (c) NFHC for $Fo = 0.5 \& 0.6$, and (d) FHC & NFHC for $Fo = 0.5 \& 0.6$.

distribution under the NFHC assumption, demonstrating consistency with previously published work [84] for lower $Fo$ values. However, at higher value like $Fo = 0.5$ and 0.6 a significant deviation is detected between the two models, as shown in Fig. 6.2(c).This suggests that at higher FHC numbers, the temperature distribution decreases when considering the loss relaxation term compared to when it is neglected. For an increased Fourier number, the temperature variation exhibits an opposite trend. Additionally, the NFHC model has a higher temperature distribution than the FHC model, but the overall trend is the same as shown in Fig. 6.2(d).

Solar energy is typically captured by the absorber plate and conducted in the plate to the fluid-carrying tubes. The fluid in the tube absorbs the transferred heat energy thus; useable energy is produced at the outlet of the absorber. As a result, the aforementioned condition can satisfy the convective boundary constraint for the study. The temperature distributions under the convective boundary condition for both FHC and NFHC models for $Bi = 0.5$ are shown in Fig. (6.3). As $Fo$ increases from zero, the plate temperature rises erratically, initially attaining a high value and then gradually decreasing. With a constant $Fo$ the heat conduction for convective boundary condition results in a smaller temperature change within the plate than the isothermal condition Both the FHC and NFHC considerations are suitably matched between the current and published results [84] with the parameters set at the specified values. However, Figure 6.3(c) shows a substantial difference that observed with a higher value of $Fo = 0.6$ and 1.

Figure 6.4 displays the temperature distribution at a specific site for different Vernotte and Fourier numbers under the two boundary conditions used in this investigation. Figure 6.4 (a) illustrates a

comparison of the temperature solutions foreseen by the FHC and NFHC models for the constant temperature boundary condition, while Figure 6.4(b) shows the same for the convective boundary constraint. As the

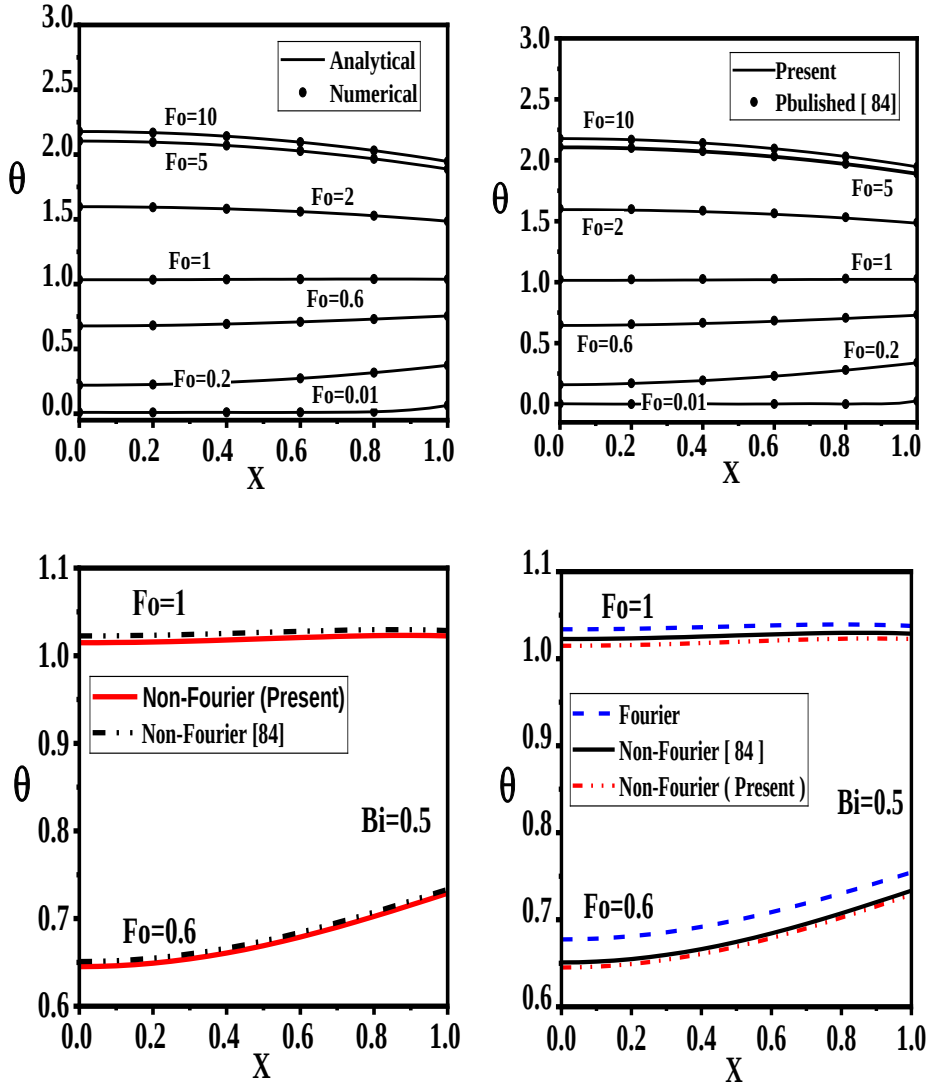


Fig.6.3.The non-dimensional temperature field produced in this study to the results reported by Kundu and Lee for a different $Fo$ and $M = 0.5$, $Bi = 0.5$, and $Ve = 0.2$;(a)FHC, (b)NFHC, (c)NFHC at $Fo = 0.6$, and $Fo = 1$,and (d) FHC & NFHC for higher value of $Fo = 0.6$, and $Fo = 1$.

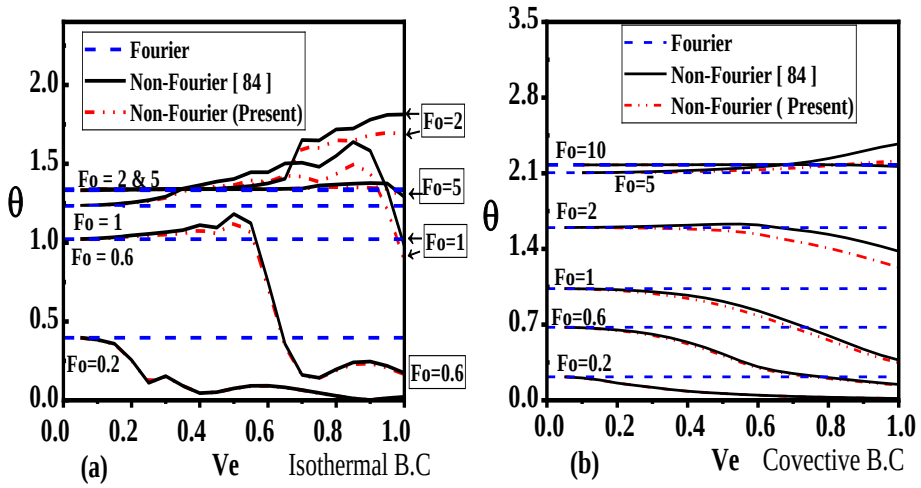


**Fig. 6.4** Temperature comparison along the symmetry line of absorber plates, evaluated using FHC and NFHC models for $M = 0.5$, and $Bi = 0.5$

FHC analysis is independent of $Ve$, the temperature remains unchanged across different $Ve$ values, as indicated by the horizontal dashed lines. Nevertheless, it fluctuates with the Fourier number until attaining a steady temperature. However, in the NFHC model, the extent of the temperature differential is contingent upon both $Ve$ and $Fo$ .As both the $Ve$ and $Fo$ increase, the temperature difference also increases, leading to the formation of a temperature shock in NFHC to keep a constant temperature at the boundary. When the loss relaxation term is considered, the thermal shock is reduced compared to when it is not included. For higher $Fo$, such as $Fo = 1$ and 2, the difference between the two cases is more pronounced. However, this difference decreases and eventually diminishes as $Ve$ decreases. A comparable pattern is noted for the convected boundary condition, as shown in Fig. 6.4(b). Nonetheless, the

range of $Ve$ is somewhat greater for the convected boundary condition to guarantee FHC model without considerable inaccuracy.

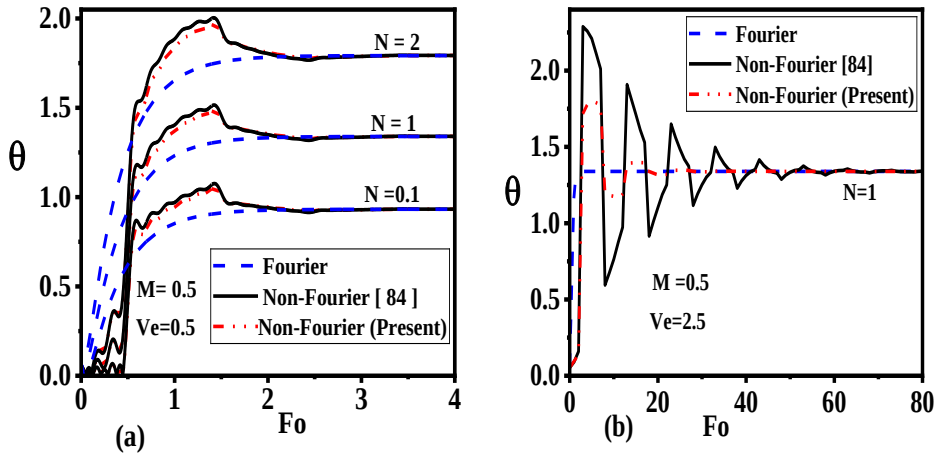


**Fig. 6.5** Influence of $Fo$ on the temperature distribution at the midpoint of the absorber plate between two tubes, considering $M = 0.5$ and a constant plate temperature at the heat transfer boundary.

Fig.6.5 presents the temperature variation at a specific point as a function of $Fo$ under a fixed temperature boundary constraints. This study examines the influence of the Vernotte number on the time-temperature history of the plate between the line of symmetry and the fluid-carrying tube. The analysis was conducted using two Vernotte number values, $Ve = 0.5$ and 2.5. Figure 6.5(a) depicts the temperature response for $Ve = 0.5$ over diverse $Fo$ values for distinct constant N values. In FHC assumptions, the temperature for a certain N grows gradually with $Fo$ and ultimately attains a steady state however, in the NFHC assumptions, the temperature first increases in a fluctuating manner with $Fo$, attains a maximum, then declines abruptly, and then gradually decreases to a stable value, consistent with the FHC model. The NFHC results display a distinct hump in each curve, leading to a notable

deviation from the FHC model. Furthermore, as N increases, the discrepancy between the two models slightly grows. A similar trend is observed when incorporating the phase lag term with the loss coefficient. However, in this case, the temperature rise up to the peak value is lower than when the phase lag term with the loss coefficient is not considered. Fig. 6.5(b) illustrates the evolution of temperature over time as a function of the $Fo$ at a higher Vernotte number. At lower $Fo$ values, temperature oscillations are predominant; however, as $Fo$ increases, these oscillations gradually diminish and converge with the FHC model. Higher $Ve$ values lead to a more pronounced deviation from FHC conduction, indicating that relaxation effects become more significant at elevated $Ve$. This suggests that the temperature response in both FHC and NFHC models may exhibit fluctuations, particularly at lower $Fo$ and higher $Ve$ values. It is observed that incorporating the phase lag term along with the loss coefficient reduces the thermal shock effect. The temperature peak is lower compared to cases where these terms are not considered, indicating that phase lag plays a crucial role in influencing energy dissipation over time.

Fig. 6.6 illustrates the temperature variation at a point as a function of $Fo$ for the convected boundary condition, considering $Ve = 0.5$ and 2.5. For $Ve = 0.5$, no significant difference is observed between the FHC and NFHC models which are depicted in Fig.6.6 (a). However, for $Ve = 2.5$, a substantial deviation occurs, which strongly depends on the dimensionless time, $Fo$ as can be observed in Fig. 6.6(b). The NFHC model exhibits a smooth waviness in temperature change as a function of $Fo$. This fluctuation can be eliminated by using a higher $Fo$ value, causing the results to align with the FHC model. Additionally, the temperature peak is significantly reduced when the phase lag term with

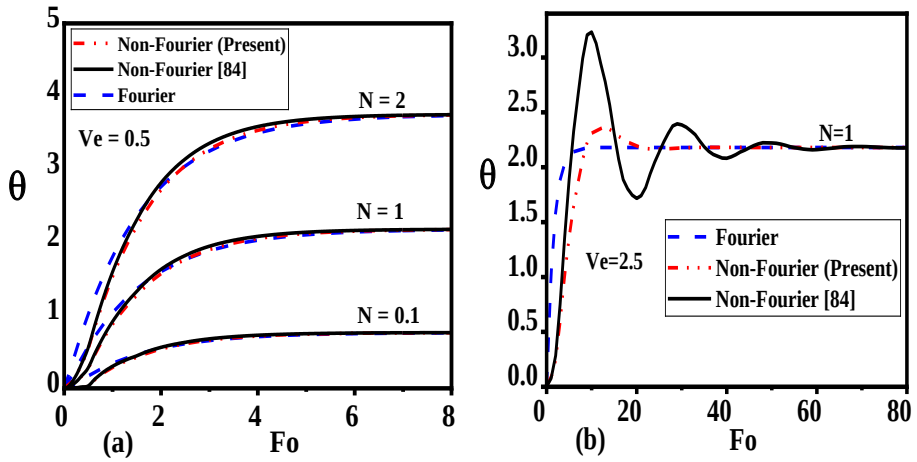


**Fig. 6.6** Impact of $Fo$ on the temperature response at the midpoint of the absorber plate between two tubes, considering $M = 0.5$, $Bi = 0.5$ and a convective heat transfer boundary

the loss coefficient is included compared to cases where it is not considered. Furthermore, when the phase lag term with the loss coefficient is included, the system reaches a steady state more rapidly.

Fig. 6.7 presents the temperature pattern across the plate for both FHC and NFHC conditions after absorbing solar flux, considering a large FHC number $Fo = 5$ and a small Vernotte number $Ve = 2.5$. The results are also compared with published data. Fig. 6.7(a) corresponds to an isothermal temperature condition at the plate-tube junction. In the FHC model, the dimensionless temperature $\theta$, exhibits a smooth, gradually decreasing, and monotonic trend as a function of $X$. In contrast, the NFHC model predicts higher temperatures than the FHC model while following a similar trend, albeit with a wave-like pattern. A significant deviation is observed near the isothermal boundary, where a temperature surge or thermal shock occurs. This jump represents a

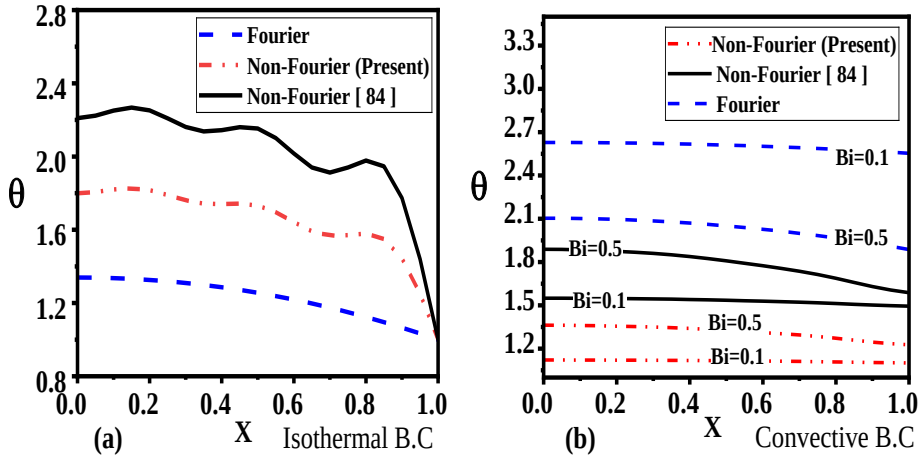


**Fig. 6.7** Comparison of temperature profiles for FHC and NFHC models under $M = 0.5$, $Fo = 5$, and $Ve = 2.5$

point of instantaneous temperature change, appearing adjacent to the thermal boundary. Fig. 6.7(b) depictsthe temperature distribution under the convective boundary condition, considering different convective effects with Biot numbers $Bi = 0.1$and $Bi = 0.5$. As the convective resistance increases, the plate temperature rises in the FHC heat conduction model, which is an expected trend. Conversely, in the NFHC model, the temperature decreases as convective resistance increases at the boundary. In general, the thermal shock effect in NFHC becomes more pronounced at higher Bi, particularly when coupled with a large Vernotte number $Ve$. This phenomenon is likely due to the periodic temperature variations influenced by the Fourier number $Fo$.

The thermo-geometric parameter $M$ significantly affects the thermal behaviour of the absorber plate in FPSC. The impact of $M$ on temperature distribution for NFHC is analyzed under both constant temperature and convective boundary conditions at the plate-tube

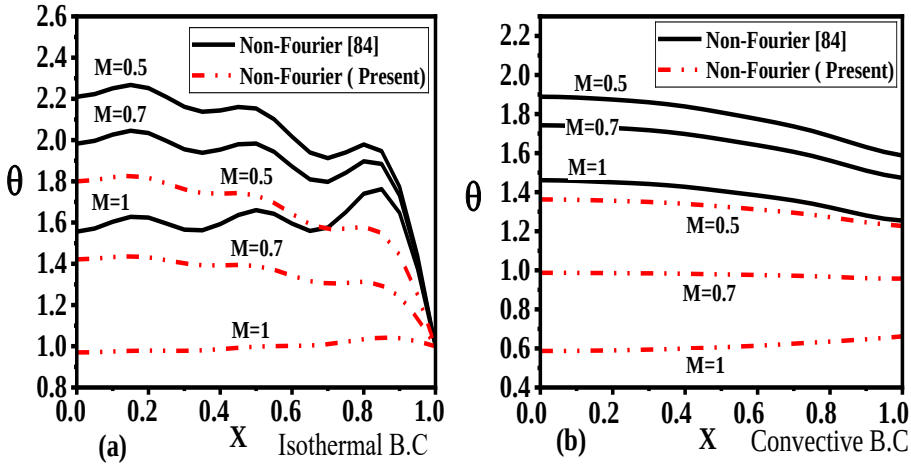


**Fig.6.8** Non-dimensional temperature distribution for various thermo-geometric parameters $M$ under given conditions $Fo = 5$, $N = 1$, $Bi = 0.5$, and $Ve = 2.5$: (a) Isothermal boundary condition and (b) Convective boundary condition.

junction in Fig. 6.8(a) and (b) respectively. Results indicate that as $M$ increases, the temperature field decreases due to its direct dependence on the overall heat loss coefficient $U_L$. This highlights the critical role of $M$ in accurately predicting and optimizing heat transfer performance in solar collectors. Further it can be seen that the NFHC effect is reduced when the phase lag is considered alongside the loss coefficient compared to the case where it is not accounted for.

## 6.4 Summary

This study analytically examines FHC and NFHC in the absorber plate of flat-plate solar collectors, incorporating time relaxation for the loss coefficient under two different boundary conditions at the plate-tube

junction. Using the separation of variables method, the results are compared with those of Kundu and Lee, showing good agreement for lower values of the $Fo$ and $Ve$, though significant deviations arise at higher values. Considering phase lag with the loss coefficient reduces the temperature distribution compared to cases where it is neglected. An in-depth investigation underscores the impact of thermo-geometric factors and boundary conditions. Unlike the FHC model, the NFHC model exhibits a wave-like temperature pattern, demonstrating the finite speed of heat propagation. Finally, it can be demonstrated that

- The FHC model provides a simplified approach but does not capture transient effects like thermal shocks.
- The NFHC model better represents wave-like heat transfer behavior, especially for materials with high relaxation times.
- Higher Ve values and phase lag effects significantly impact heat propagation, leading to deviations from classical FHC model.

# Chapter 7

## Energy and Exergy Assessment of a Flat-Plate Solar Collector Using Single and HybridNanofluid

## 7.1 Introduction

The simultaneous application of the first and second laws of thermodynamics is required for the performance evaluation of any thermal system. The first law determines energy efficiency, while the second law assesses exergy efficiency. According to the first law, energy is conserved in quantity wise, whereas the second law states that energy degrades quality wise with each transfer. Nanofluids are fluids that contains particles less than 100 nm in size and are utilized to improve the rate of heat transfer than conventional fluid. In this chapter, the thermodynamic performance of a flat plate solar collector (FPSC) is analyzed with nanofluid as the working fluid. The impact of different collector fluids—mono, hybrid, and ternary nanofluids (THNF)—on FPSC efficiency is examined based on energy and exergy considerations. The nanofluids used include mono and hybrid combinations of CuO, MgO, and $TiO_2$ with water at volume contentvarying from 0.1% to 0.5%. The study investigates how these nanofluids influence energy and exergy efficiency under varying mass flow rates, volume concentrations, and operating temperatures.

## 7.2 Mathematical Formulation

### 7.2.1. Preparation and characterization of nanofluids:

Nanofluids are specialized fluids that contain nanoparticles, typically in the nanometer range. For optimal performance, these fluids must be free from agglomeration and exhibit long-term stability without sedimentation, making the preparation process crucial. Traditional basic fluids, like water, ethylene glycol, and oil are commonly used, with dispersed nanoscale metal particles to form nanofluids.

There are two primary techniques used for nanofluid synthesis: the single-step and two-step methods. The two-step approach involves producing nanoparticles over various fabrication techniques before dispersing them into the base fluid. In this work, the two-step method was employed for nanofluid preparation. The stability of nanofluids is a crucial factor affecting their thermal performance and practical applications. Maintaining long-term stability requires preventing nanoparticle agglomeration and sedimentation, which can degrade heat transfer efficiency. One key parameter for assessing nanofluid stability is zeta potential**,** which indicates the electrostatic repulsion between particles in suspension. A higher zeta potential (typically above ±30 mV) ensures better dispersion and prevents coagulation. Various stabilization techniques, including surfactant addition, pH adjustment, and ultrasonic agitation, are employed to enhance stability. Additionally, optimizing nanoparticle concentration and selecting suitable base fluids further contribute to maintaining uniform dispersion. To determine the particle size, material identification, and particle morphology, the scanning microscope (SEM) and energy dispersive X-ray (EDX) were conducted.

This study explores the use of mono, hybrid, and ternary nanofluids as working fluids. Their preparation, along with the evaluation of rheological and thermos-physical properties, has been reviewed based on existing literature and tabulated in Table 7.1 however; the thermo-physical characteristics of nanoparticle and base fluid for study are tabulated in Table 7.2.To the writers' utmost knowledge, CuO–MgO–$TiO_2$ is the most reliable synthesis and analysis of DHNFs and THNFs found in the literature, which is why it was chosen for this investigation

For the calculation of specific heat, thermal conductivity following relations are used [107,131,]

For mano nanofluids

$$C_{p,nf} = \frac{\phi\left(\rho C_p\right)_{np} + \left(1-\phi\right)\left(\rho C_p\right)_{bf}}{\phi\rho_{np} + \left(1-\phi\right)\rho_{bf}} \tag{7.1}$$

$$\frac{k_{nf}}{k_{bf}} = \frac{k_{np} + \left(SH-1\right)k_{bf} - \phi\left(SH-1\right)\left(k_{bf} - k_{np}\right)}{k_{np} + \left(SH-1\right)k_{bf} - \phi\left(k_{bf} - k_{np}\right)} \tag{7.2}$$

where $SH$ is the shape factor for and its value for spherical shape nanoparticle is 3.

For binary hybrid nanofluids [131]

$$C_{p,nf} = 4.2049836 + \left(-0.0015513333 \times T\right)$$

$$+\left(2.1030303 \times 10^{-5} \times T^2\right) - \left(8.62 \times \phi\right) \tag{7.3}$$

$$k_{nf} = 0.51116372 + \left(0.020783986 \times T^{0.5}\right)$$

$$+\left(163070.33\times\phi^{2.5}\right)+\left(-1688369.9\times\phi^{3}\right) \quad (7.4)$$

For ternary hybrid nanofluids [132]

$$C_{p,nf}=4.2028064+\left(-0.0015020303\times T\right)$$

$$+\left(2.0272727\times10^{-5}\times T^{2}\right)-\left(17.03\times\phi\right) \quad (7.5)$$

$$k_{nf}=0.72768391+\left(-9.6816854/T\right)+\left(283.69209/T^{2}\right)+\left(4718.8713/T^{3}\right)$$

$$+\left(-175433.68283/T^{5}\right)+\left(274.276\times\phi\right)+\left(-159781.42\times\phi^{2}\right)$$

$$+\left(41691000\times\phi^{3}\right)-\left(3.6405833\times10^{9}\times\phi^{4}\right) \quad (7.6)$$

**Table 7.1** Existing literature for preparation of mano, binary and ternary nanofluids.

| Sl. no | Nanofluid | Shape | Category | Literature |
|---|---|---|---|---|
| 1 | CuO | Spherical | Mano nanofluids | 122, 145 |
| 2 | MgO | Spherical | | 154 |
| 3 | $TiO_2$ | Spherical | | 146 |
| 4 | MgO-$TiO_2$(80wt%MgO–20wt%$TiO_2$) | Spherical | Binary hybrid nanofluid | 131 |
| 5 | CuO-MgO-$TiO_2$ (60 mass % CuO / 30 mass % MgO / 10 mass % $TiO_2$) | Spherical | Ternary hybrid nanofluid | 132 |

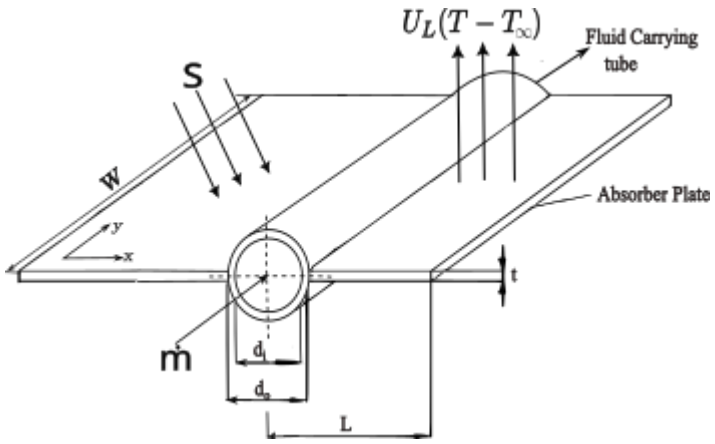


**Fig.7.1** Diagrammatic representation of a sheet& tube FPSC's symmetric module.

**Table7.2** Thermo-physical properties of nanoparticle and base fluid for study [107,143]

| **Nanoparticles** | **Specificheat capacity (J/Kg.K)** | **Density ($kg/m^3$** | **Thermal conductivity (W/m.K)** |
|---|---|---|---|
| Copperoxide(CuO) | 551 | 6000 | 33 |
| Magnesiumoxide(MgO) | 955 | 3560 | 45 |
| Titaniumoxide($TiO_2$) | 692 | 4230 | 8.4 |
| Water($H_2O$),basefluid | 4182 | 997 | 0.6 |
| Binary (MgO-$TiO_2$) | | | |
| Ternary (CuO-MgO-$TiO_2$) | | | |

### 7.2.2 Thermodynamic analysis

Here are the mathematical formulas that were utilized to model the flat plate collector. The process is supposed to operate in steady-state circumstances with a uniform heat flow. The pressure drop within the collector's tube is presumed to be insignificant.

#### *7.2.2.1 Energy Analysis:*

In a stable state, according to the energy balance, the useful energy output of a collector can be given as [15]

$$\dot{Q}_{useful} = A_c\left[S - U_L\left(T_{pm} - T_a\right)\right] \tag{7.7}$$

It is important to note that Eq. (7.7) does not consider the impacts of optical efficiency and the heat transfer coefficient on system performance. Therefore, the following equations are introduced to incorporate these parameters.

$$Q_{useful} = A_c F_R\left[I_T\left(\alpha\zeta\right) - U_L\left(T_{f,in} - T_\infty\right)\right] \tag{7.8}$$

where

$$S = \left(\alpha\zeta\right) I_T \tag{7.9}$$

The coefficient of heat removal, denoted by $F_R$, may be computed as follows [15]

$$F_R = \frac{\dot{m} C_p}{A_c U_L}\left[1 - \exp\left(-\frac{U_L F^1 A_c}{\dot{m} C_p}\right)\right] \tag{7.10}$$

and

The collector efficiency factor is denoted by $F^1$ and can be computed in this way [16]

$$F^1 = \frac{\frac{1}{U_L}}{L\left[\frac{1}{U_L\left[\left(L-d_0\right)F+d_0\right]}+\frac{1}{\pi d_i h_f}\right]} \tag{7.11}$$

Where, $F$ is the standard fin efficiency and can be calculated as

$$F = \frac{\tanh\left(\frac{m\left(L-d_0\right)}{2}\right)}{\frac{m\left(L-d_0\right)}{2}} \tag{7.12}$$

$$m = \sqrt{U_L/kt} \tag{7.13}$$

The collector flow factor is the ratio of $F_R$ to $F^I$, hence can be written as [15]

$$F^{II} = F_R/F^I \tag{7.14}$$

Therefore, the collector heat removal factor can also be given in another way as

$$F_R = F^I F^{II} \tag{7.15}$$

For this study $F^I = 0.841$ is considered [15]

The mean plate temperature for the plate

$$T_{pm} = T_{f,in} + \frac{\dot{Q}_{useful}/A_c}{F_R U_L}\left(1-F_R\right) \tag{7.16}$$

The useful heat gain rate by the fluid from the absorber plate is determined as

$$\dot{Q}_{useful} = \dot{m} c_p \left(T_{f,out} - T_{f,in}\right) \tag{7.17}$$

The collector's thermal efficiency is specified as

$$\eta_{En} = \frac{Q_{useful}}{A_c I_T} = F_R\left[\left(\alpha\zeta\right) - U_L\frac{\left(T_i - T_o\right)}{I_T}\right] \tag{7.18}$$

For the present analysis the normal incidence condition was considered therefore $U_L$ , $F_R$ , $F_R(\alpha\zeta)$ can assumed to be constant.

### *7.2.2.2 Exergy Analysis:*

To accurately assess the system's thermal performance and work potential it is crucial to do an energy analysis using the second law of thermodynamics. The correlations required for the exergy analysis of flat plate solar collectors are shown in this section. Treating the system as a control volume,

The exergy balance calculation is articulated as follows [92, 97-99]

$$\sum \dot{E}_{X,in} - \sum \dot{E}_{X,out} = \sum \dot{E}_{X,dest} \tag{7.19}$$

As can be seen, the collector's exergy input is made up of the exergy of the inlet fluid $\left(\dot{E}_{X,in,f}\right)$ and the exergy of the radiation that the sun absorbs $\left(\dot{E}_{X,sun}\right)$. The collector's exergy output is equal to the exergy of the outlet fluid $\left(\dot{E}_{X,out,f}\right)$. The distinction between these two components indicates the amount of energy lost in the collector.

Assuming the sun to be infinite source, $T_{sun} = 5778K$ , the solar exergy can be determined as

$$\dot{E}_{sun} = (\alpha\zeta) A_c I_T \left(1 - \frac{T_o}{T_{sun}}\right) \tag{7.20}$$

The exergy rate of the working fluid in is calculated using the following equations:

$$\dot{E}_{X,in,f} = \dot{m} c_p \left[ T_{f,in} - T_o - T_o \ln\left( \frac{T_{f,in}}{T} \right) \right] \tag{7.21}$$

By summation of Eqs. (7.20) and (7.21) the inlet exergy rate can be obtained as follows

$$E_{X,in} = \dot{E}_{sun} + \dot{E}_{X,in,f}$$

$$= (\alpha\zeta) A_c I_T \left( 1 - \frac{T_o}{T_{sun}} \right) + \dot{m} c_p \left[ T_{f,in} - T_o - T_o \ln\left( \frac{T_{f,in}}{T} \right) \right] \tag{7.22}$$

The outlet exergy is the exergy rate of the working fluid out and can be calculated as follows

$$\dot{E}_{X,out,f} = -\dot{m} c_p \left[ T_{f,out} - T_o - T_o \ln\left( \frac{T_{f,out}}{T} \right) \right] \tag{7.23}$$

The heat transfer mechanism from the sun to the collector's working fluid has two primary stages: the absorption of solar radiation by the absorber plate and following conduction of the energy from the absorber plate to the working fluid. Consequently, both processes—including the flowing components—involve the loss of energy [97].

The Exergy destruction in the first stage can be evaluated by

$$E_{X,dest,s-p} = A_c I_T \left( 1 - \eta_o + \eta_o \frac{T_o}{T_p} - \frac{T_o}{T_s} \right) \tag{7.24}$$

The Exergy destruction in the second stage can be evaluated by

$$E_{X,dest,p-f} = \dot{m} c_p \left( T_{f,out} - T_{f,in} \right) \left( 1 - \frac{T_o}{T_p} \right) \tag{7.25}$$

The another part of the Exergy destruction is due to collectors heat loss to the surrounding called as Exergy destruction due to leakage is given as

$$\dot{E}_{X,dest,leakage} = U_L A_c \left( T_p - T_o \right) \left( 1 - \frac{T_o}{T_p} \right) \tag{7.26}$$

The exergy destroyed $\dot{E}_{X,dest}$ in the collector as a consequence of irreversibilities inside the system is expressed as

$$\dot{E}_{X,dest} = \dot{E}_{X,dest,s-p} + \dot{E}_{X,dest,p-f} + \dot{E}_{X,dest,leakage} \tag{7.27}$$

The Exergy destruction due to irreversibility can also be found from the following equation $\dot{E}_{X,dest} = T_o \dot{S}_{gen}$ (7.28)

According to Bejan [92], in a non-isothermal solar flat plate collector, the total rate of entropy creation may be expressed as

$$\dot{S}_{gen} = \dot{m} C_p \ln\left(\frac{T_{out}}{T_{in}}\right) - \frac{\dot{Q}_{sun}}{T_{sun}} + \frac{\dot{Q}_{loss}}{T_o} \tag{7.29}$$

$$\dot{Q}_{loss} = \dot{Q}_{sun} - \dot{m} C_p T_o \left(T_{out} - T_{in}\right) \tag{7.30}$$

Exergy efficiency indicates the greatest usable work that may be gained from a system. It is computed as follows.

$$\eta_{Exergy} = \frac{E_u}{E_{sun}} \tag{7.31}$$

where $E_u$ and $E_{sun}$ are the exergy outputs of the collector and the sun, respectively. The exergy efficiency in term of inlet fluid temperature can be written as [99]

$$\eta_{Exergy} = \frac{\dot{m} c_p}{\left[1 - \frac{T_o}{T_{sun}}\right] \dot{Q}_{sun}} \left\{ \left(T_{f,in} - T_o - \frac{S}{U_L}\right)\left[\exp\left(-\frac{U_L A_c F^1}{\dot{m} c_p}\right) - 1\right] - \left[\frac{T_o}{T_{f,in}}\left\{\exp\left(-\frac{U_L A_c F^1}{\dot{m} c_p}\right) - 1\right\}\left(T_{f,in} - T_o - \frac{S}{U_L}\right) + T_o\right] \right\} \tag{7.32}$$

**Table 7.3:** Environmental and analysis conditions for the FPSC [107,143].

| **Parameters** | $W$ | $L$ | $t$ | $d_o$ | $d_i$ | $I_T$ | $T_{fi}$ | $T_o$ | $k$ | $h_f$ | $\eta_o$ | $U_L$ |
|---|---|---|---|---|---|---|---|---|---|---|---|---|
| **Values** | 2 | 0.01 | 0.005 | 0.015 | 0.01 | 757 | 300 | 298 | 385 | 250 | 0.8 | 5 |

## 7.3 Results and discussion

This section evaluates the efficiency of both mono and hybrid nanofluids. This assessment is conducted based on the characteristics of fluid input temperature, mass flow rate inside the collector, and nanoparticle volumetric percent. The working fluid is CuO, MgO and $TiO_2$ with water mano nanofluid, and MgO -$TiO_2$with water for binary hybrid nano fluid and CuO-MgO-$TiO_2$ with water for ternary hybdrid nanofluid. The input data are tabulated in Table 3 based on the previous literatures. A computer code is developed using FORTRAN language and the code is validated with the existing results of the literature [99, 143]. The volume concentration for the study is varied between 0.1% to 0.5%. and all the result were obtained with taking volume concentration, $\phi = 0.1\%$.

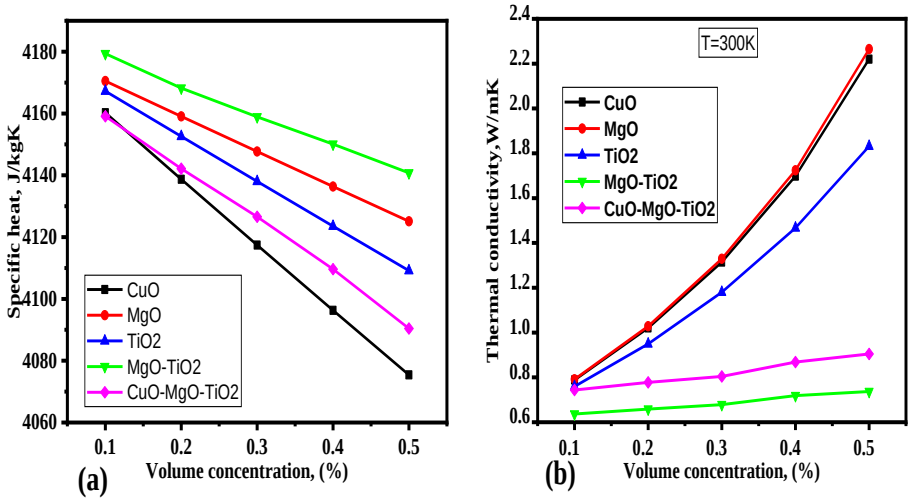


**Fig.7.2** (a) variation of Sp.heat with concentration, (b) variation of thermal conductivity with concentration

Figure 7.2 illustrates the specific heat and thermal conductivity of nanofluids as a proportion of volume fraction. As depicted in Fig. 7.2(a) the specific heat reduces as the volume concentration increases. The binary hybrid nanofluid (MgO-$TiO_2$) has a higher specific heat for a given volume concentration however, the CuO nanofluid has the lower value. The ternary hybrid nanofluid (CuO-MgO-$TiO_2$) has nearly same as that of CuO at lower concentration and as it increases it is just above the CuO mano nanofluid. These results align with those of Mostafizur et al. [122,143]. In Fig.(b), the thermal conductivity upsurges as the volumetric percentage increases. MgO/ water mano nanofluid has a higher value where as MgO-$TiO_2$ binary nanofluid has the lower one for the chosen concentration.

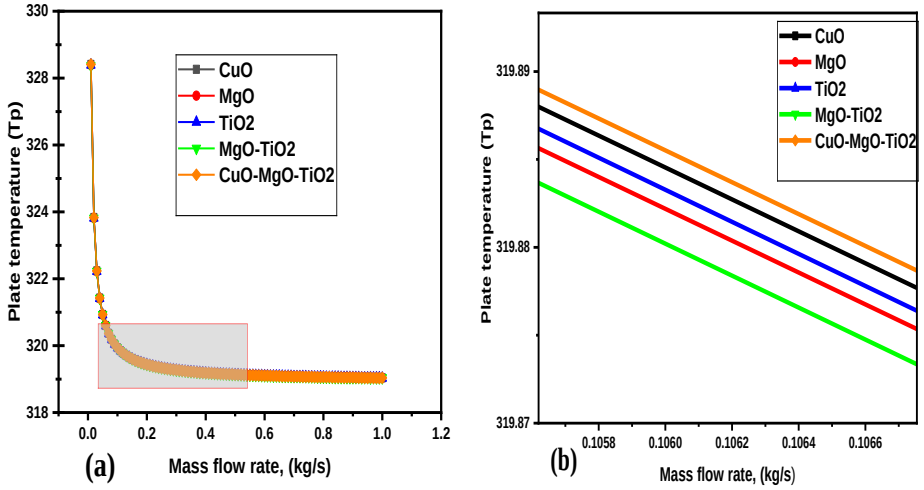


**Fig. 7.3** (a) Variation of plate temperature (b) Enlarged portion with mass flow rate for $\phi = 0.1\%$

Figure 7.3 depicts the variation of absorber plate temperature with inlet mass flow rate. It can be seen from Fig 7.3(a) that with increase in flow rate about 0.01 kg/s tends to a considerable decrease in plate temperature. Fig 7.3(b) is the magnified portion that shows ternary nanofluid has the highest temperature rise and binary has the lower one with the chosen volume concentration. The mano nanofluids have the value lies between the binary and ternary nanofluid. The decreased temperature gradient between plate and environment tends to decline the overall loss coefficient and therefore upsurge in efficiency of the absorber plate as can be seen from Fig.7.5.

The Fig. 7.4(a) represents the energy efficiency as the function of reduced temperature parameter. As the inlet temperature surges the absorber plate temperature upsurges consequently the temperature gradient and also the overall loss coefficient between plate and the environment leds to increase thereby reduction in efficiency. The similar trend is observed from literature [99,128,136]. From it's magnified

Fig.7.4(b) the binary nanofluid has the maximum value for this concentration.

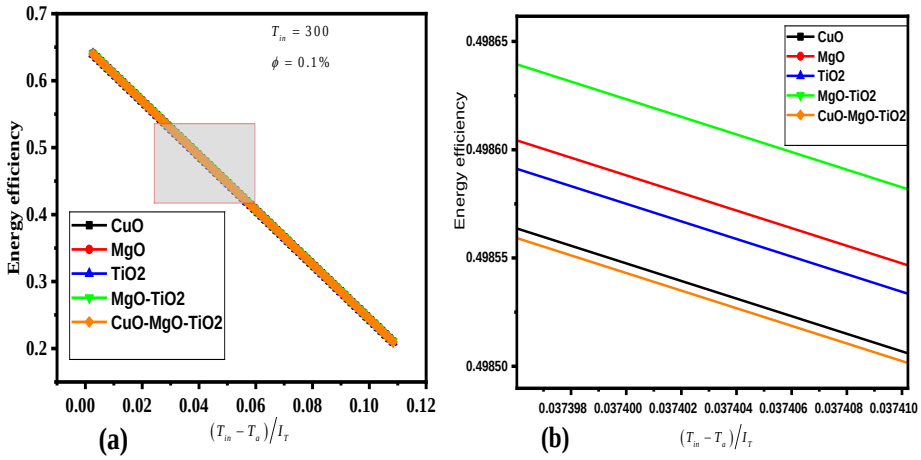


**Fig. 7.4** (a) Variation of plate efficiency (b) Enlarged portion with inlet temperature for $\phi = 0.1\%$

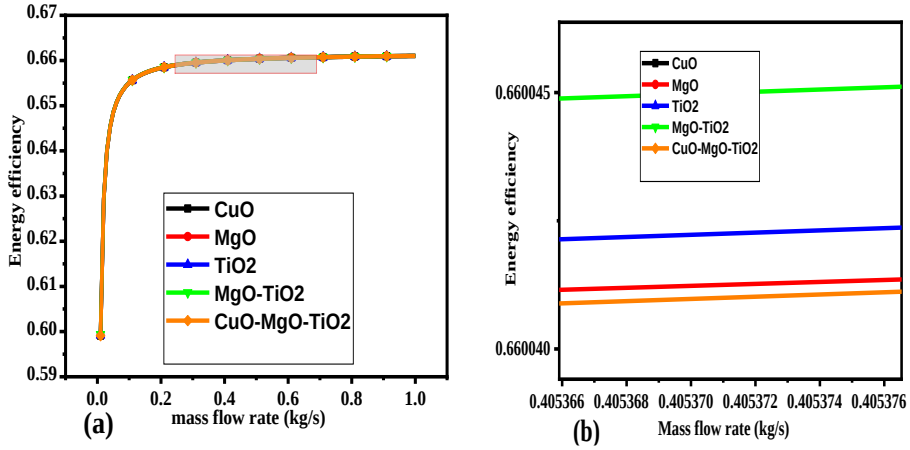


**Fig. 7.5** (a) Variation of plate efficiency (b) Enlarged portion with mass flow rate for $\phi = 0.1\%$

The change of absorber plate efficiency with mass flow rate for $\phi = 0.1\%$ is depicted in Fig. 7.5. Fig (a) shows that for each nanofluid, as inlet mass flow rate increases the efficiency rises. For this flow rate, the binary nanofluid has the maximum rise and CuO mano nanofluid has the lower one.

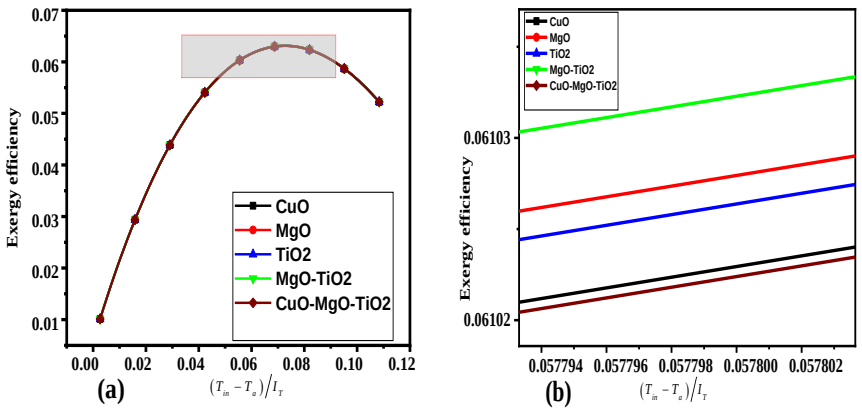


**Fig. 7.6** (a) Variation of exergy efficiency (b) Enlarged portion with inlet temperature for $\phi = 0.1\%$

The exergeti ccharacteristics of the absorber plate as factor of reduced temperature parameter is shown in Fig. 7.6. From Fig (a), it is observed that as temperature at the inlet rises the exergy efficiency of the absorber plate rises. This increase shows the ability of additional heat to be transformed into useable energy by the system. All the working fluid considered for this study shows the similar variation for the considered volume fraction.

The change of exergy efficiency with inlet mass is illustrated in Fig. 7.7. It can be detected in Fig.(a) that an upsurge in mass flow rate exergy efficiency increases and from magnified portion Fig.(b) binary has

the higher value. All the variation may depends on flow property of nanofluid inside the tube.

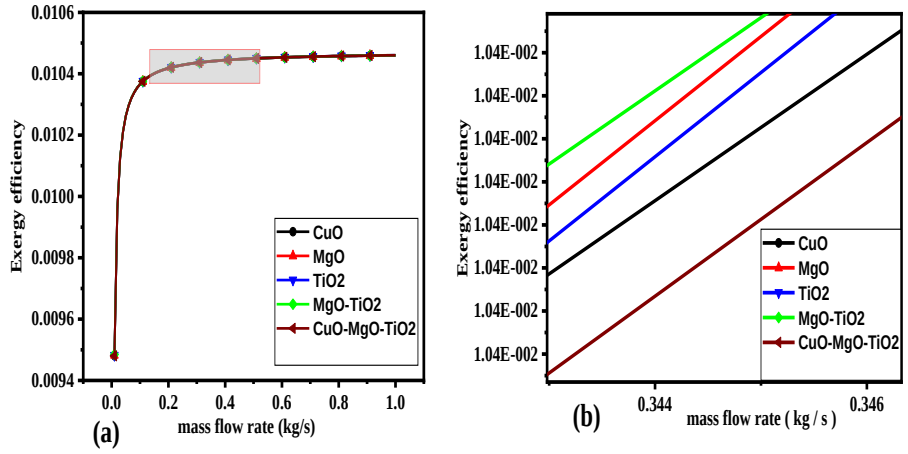


**Fig. 7.7** (a) Variation of exergy efficiency (b) Enlarged portion with inlet mass, for $\phi = 0.1\%$

.

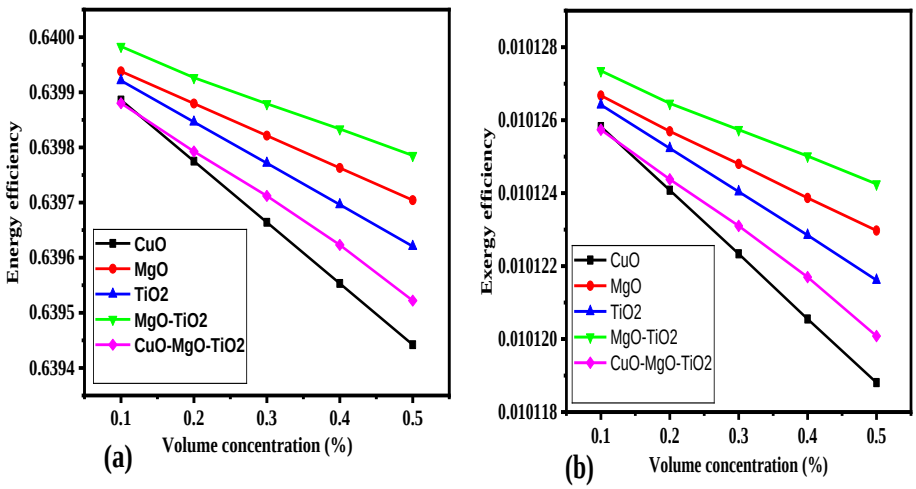


**Fig. 7.8** Variation of Energy and Exergy efficiency with nano particle volume concentration.

Figure 7.8 illustrates the fluctuation of energy and exergy efficiency in relation to nanoparticle concentrations in volumes with a fixed mass flow rate of $\dot{m} = 0.03 kg/s$. From both the Fig.(a) and (b)it is observed that as nanoparticle volume concentration rises the thermal performance of the collector declines. The reason behind this behaviour may be the effect of viscosity of the different nanoparticles.

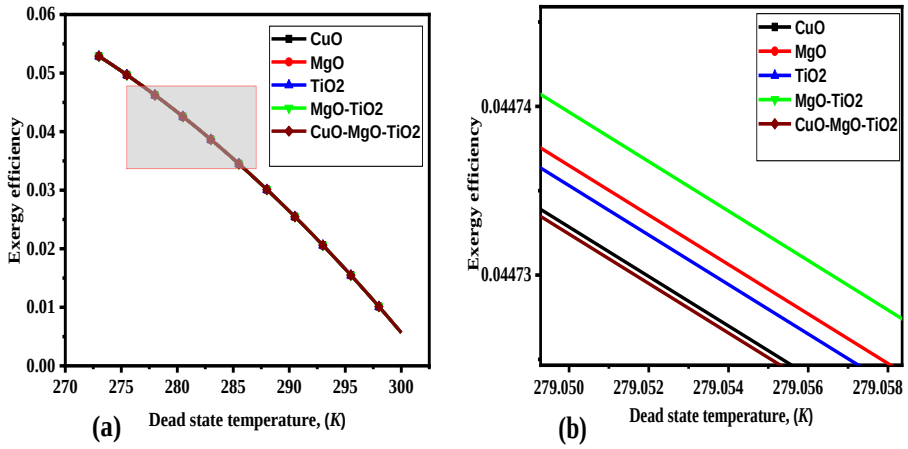


**Fig. 7.9**.Effect of dead state on Exergy efficiency of the plate.

Varying the effect of dead state temperature onthe exergy efficiency is depicted in Fig.7.9. From Fig.(a) it can be predicted that as the temperature of dead state increased from 2°C to 27°C for a fixed mass flow rate and volumetric percentage, the second law efficiency decreased. This trend also verified by [115] and this decreased trend signifies that the environment plays important role for evaluating the exergetic efficiency. As we lower the dead state more will be the exergy value.

## 7.4 Summary

An analytical parametric study was conducted to assess the thermal performance of a flat plate solar collector employing mono and

hybrid nanofluids composed of CuO, MgO, and $TiO_2$ nanoparticles. The investigation considered various operating conditions, including changes in inlet temperature, mass flow rate, and nanoparticle volume concentration, with water serving as the base fluid. The formulation methods and stability characteristics of the selected nanofluids were referenced from established literature sources, as summarized in Table 1. The nanoparticle volume concentrations analyzed in this work range from 0.1% to 0.5%, based on the availability of experimental data from previous studies. At a lower concentration of 0.1% and at a temperature of 300K, although the thermal enhancement is very minimal, the binary mixture of MgO-$TiO_2$ demonstrates superior performance in terms of both energy and exergy efficiencies. In contrast, the ternary nanofluid configuration did not exhibit significant improvements compared to the mono and binary combinations. Additionally, increasing the mass flow rate led to a consistent rise in both energy and exergy efficiencies across all nanofluid formulations considered. The findings suggest that, given the relatively low operating temperature range of flat plate collectors, the application of ternary nanofluids may not be a cost-effective solution for enhancing their performance.

# Chapter 8

# Conclusion

This study presents a comprehensive analytical investigation into the thermal performance of absorber plates in flat-plate solar collectors, focusing on two-dimensional heat conduction, material efficiency, and Fourier and non-Fourier heat transfer models. The proposed analytical models, validated through numerical simulations, demonstrate strong agreement with finite difference method results, with a maximum temperature deviation within 5%, confirming their reliability for steady-state thermal analysis.

Key findings suggest that two-dimensional models offer a more precise representation of heat conduction compared to traditional one-dimensional approaches, despite their increased complexity. Additionally, the study highlights that plate material conductivity has minimal impact on efficiency, supporting the feasibility of using cost-effective alternatives such as aluminum instead of copper. The modified one-dimensional model is shown to be a superior alternative to the classical 1-D approach, balancing computational simplicity and accuracy.

Furthermore, the investigation into Fourier and non-Fourier heat conduction reveals that while the Fourier model provides a simplified approach, it does not account for transient thermal effects. In contrast, the non-Fourier model captures wave-like heat transfer behavior, making it more suitable for materials with high relaxation times. The influence of

phase lag and higher Vernotte numbers (Ve) plays a crucial role in heat propagation, impacting overall thermal performance.

The findings show that, under some circumstances, nanofluids can improve the collector's thermal performance; yet, their actual implementation should take the cost-benefit ratio into account, balancing the performance improvements against the related costs.

Overall, this research provides valuable insights into advanced thermal modeling strategies for absorber plates in flat-plate solar collectors. The proposed methodologies enable accurate, efficient, and cost-effective design optimizations, contributing to the enhancement of solar thermal system performance.

# Future Works

Building upon the findings of this study, several avenues for future research can be explored to further enhance the thermal performance and design optimization of flat-plate solar collectors:

1. **Transient Heat Transfer Analysis** – The current study focuses on steady-state conditions; however, future work should investigate transient thermal behavior under varying environmental and operational conditions. This will provide a more comprehensive understanding of the dynamic performance of absorber plates.
2. **Experimental Validation** – While the proposed analytical models have been validated using numerical simulations, conducting experimental studies would further verify their accuracy and applicability in real-world conditions. Comparative

studies between experimental and analytical results can refine the models for better precision.

3. **Optimization of Geometric Configurations** – Investigating various plate geometries, tube arrangements, and absorber plate thickness variations could lead to design improvements that enhance heat transfer efficiency while minimizing material costs.
4. **Impact of Climate Variability** – Future research could assess the impact of different climatic conditions (e.g., solar radiation levels, ambient temperature variations) on the thermal performance of absorber plates to develop region-specific optimization strategies. By addressing these areas, future research can contribute to the continued development of high-performance, cost-effective, and sustainable flat-plate solar collector systems for renewable energy applications.

# References:


1. Estevão, João, and José Dias Lopes. "SDG7 and renewable energy consumption: The influence of energy sources." Technological Forecasting and Social Change 198 (2024): 123004. https://doi.org/10.1016/j.techfore.2023.123004

2. IEA. (2023). World Energy Outlook 2023. International Energy Agency.

3. Hassan, Qusay, Patrik Viktor, Tariq J. Al-Musawi, Bashar Mahmood Ali, Sameer Algburi, Haitham M. Alzoubi, Ali Khudhair Al-Jiboory, Aws Zuhair Sameen, Hayder M. Salman, and Marek Jaszczur. "The renewable energy role in the global energy Transformations." Renewable Energy Focus 48 (2024): 100545. https://doi.org/10.1016/j.ref.2024.100545

4. REN21. (2022). Renewables 2022 Global Status Report. Renewable Energy Policy Network for the 21st Century.

5. Nahrin, Rifat, MdHasanur Rahman, Shapan Chandra Majumder, and Miguel Angel Esquivias. "Economic growth and pollution nexus in Mexico, Colombia, and Venezuela (G-3 countries): The role of renewable energy in carbon dioxide emissions." Energies 16, no. 3 (2023): 1076. https://doi.org/10.3390/en16031076

**6.** Landqvist, Maria, and Frida Lind. "A start-up embedding in three business network settings–a matter of resource combining." Industrial Marketing Management 80 (2019): 160-171.https://doi.org/10.1016/j.indmarman.2017.12.005

**7.** Hassan, Qusay, Patrik Viktor, Tariq J. Al-Musawi, Bashar Mahmood Ali, Sameer Algburi, Haitham M. Alzoubi, Ali Khudhair Al-Jiboory, Aws Zuhair Sameen, Hayder M. Salman, and Marek Jaszczur. "The renewable energy role in the global energy Transformations." Renewable Energy Focus 48 (2024): 100545. https://doi.org/10.1016/j.ref.2024.100545

**8.** Wisseh, M., &Limin, M. (2024). The Future of Solar Energy in Developing Countries. Asian Journal of Environment & Ecology. https://doi.org/10.9734/ajee/2024/v23i12640.

**9.** Cui, Dingyue, Asim A. Ditta, and Shi-Jie Cao. "Energy justice and sustainable urban renewal: A systematic review of low-income old town communities." Journal of Cleaner Production (2024): 143470.https://doi.org/10.1016/j.jclepro.2024.143470.

**10.** Bhattacharyya, Subhes C. "Energy access and development." The Handbook of Global Energy Policy (2013): 227-243..

**11.** Kumar, L., Hasanuzzaman, M. and Rahim, N.A., 2019. Global advancement of solar thermal energy technologies for industrial process heat and its future prospects: A review. Energy conversion and management, 195, pp.885-908.https://doi.org/10.1016/j.enconman.2019.05.081

**12.** El-Sebaey, Mahmoud S., Seyed MT Mousavi, RavishankarSathyamurthy, Hitesh Panchal, and Fadl A. Essa. "A detailed review of various design and operating parameters affecting the thermal performance augmentation of flat-plate solar collectors." International Journal of Ambient Energy 45, no. 1 (2024): 2351100.https://doi.org/10.1080/01430750.2024.2351100

**13.** Kalogirou, S. (2009). Solar Energy Engineering: Processes and Systems. Academic Press.

**14.** Soteris, K. (2014). Solar Energy Engineering: Processes and Systems. Elsevier.

**15.** Duffie, J. A., & Beckman, W. A. (2013). *Solar Engineering of Thermal Processes*. John Wiley & Sons

**16.** Sukhatme, S.P. Nayak, J, 2010.Solar Energy Principles of Thermal Collection and Storage Third Edition; McGraw-Hill Education: New York, NY, USA.

**17.** Hottel, Hoyt Clarke, and B. B. Woertz. "The performance of flat-plate solar-heat collectors." Transactions of the American Society of Mechanical Engineers 64, no. 2 (1942): 91-103.https://doi.org/10.1115/1.4018980

**18.** Hottel HC, Whillier A Evaluation of flat-plate collector performance. In: Transactions of the conference on the use of solar energy, vol 2, (1955) Pt. 1. University of Arizona Press, Tuscan, Arizona, p 74

**19.** Bliss Jr, Raymond W. "The derivations of several "plate-efficiency factors" useful in the design of flat-plate solar heat collectors." Solar energy 3, no. 4 (1959): 55-64.https://doi.org/10.1016/0038-092X(59)90006-4

**20.** Phillips, Warren F. "The effects of axial conduction on collector heat removal factor." Solar Energy 23, no. 3 (1979): 187-191.https://doi.org/10.1016/0038-092X(79)90156-7

**21.** Cooper, P. I., and R. V. Dunkle. "A non-linear flat-plate collector model." Solar Energy 26, no. 2 (1981): 133-140.https://doi.org/10.1016/0038-092X(81)90076-1

**22.** Chiou, J. P. "The effect of nonuniform fluid flow distribution on the thermal performance of solar collector." Solar Energy 29, no. 6 (1982): 487-502. https://doi.org/10.1016/0038-092X(82)90057-3

**23.** Francken, J. C. "On the effectiveness of a flat plate collector." Solar energy 33, no. 3-4 (1984): 363-366. 10.1016/0038-092X(84)90166-X

**24.** O'Brien-Bernini, Frank C., and Jon G. McGowan. "Performance modeling of non-metallic flat plate solar collectors." Solar Energy 33, no. 3-4 (1984): 305-319.https://doi.org/10.1016/0038-092X(84)90161-0

**25.** Samdarshi, S. K., and S. C. Mullick. "Analysis of the top heat loss factor of flat plate solar collectors with single and double glazing." International Journal of Energy Research 14, no. 9 (1990): 975-990.https://doi.org/10.1002/er.4440140908

**26.** Hollands, K. G. T., and B. A. Stedman. "Optimization of an absorber plate fin having a step-change in local thickness." Solar Energy 49, no. 6 (1992): 493-495.https://doi.org/10.1016/0038-092X(92)90157-6

**27.** Matrawy, K. K., and I. Farkas. "Comparison study for three types of solar collectors for water heating." Energy conversion and management 38, no. 9 (1997): 861-869.https://doi.org/10.1016/S0196-8904(96)00089-1

**28.** Kundu, Balaram. "Performance analysis and optimization of absorber plates of different geometry for a flat-plate solar

collector: a comparative study." Applied thermal engineering 22, no. 9 (2002): 999-1012. https://doi.org/10.1016/S1359-4311(01)00127-2

**29.** Kaushika, N. D., and K. Sumathy. "Solar transparent insulation materials: a review." Renewable and sustainable energy reviews 7, no. 4 (2003): 317-351.https://doi.org/10.1016/S1364-0321(03)00067-4

**30.** Kalogirou, Soteris A. "Solar thermal collectors and applications." Progress in energy and combustion science 30, no. 3 (2004): 231-295.https://doi.org/10.1016/j.pecs.2004.02.001

**31.** Kundu, Balaram. "The influence of collector fluid inlet temperature on the performance of a solar-assisted absorption system using step-finned flat-plate collector." Heat transfer engineering 28, no. 5 (2007): 496-505. https://doi.org/10.1080/01457630601166150

**32.** Kundu, B. "Performance and optimum design analysis of an absorber plate fin using recto-trapezoidal profile." Solar Energy 82, no. 1 (2008): 22-32.https://doi.org/10.1016/j.solener.2007.05.002

**33.** Badran, Ali A., Mohammed F. Mustafa, Walid K. Dawood, and Zaid K. Ghazzawi. "On the measurement of bond conductance in

solar collector absorber plate." Energy conversion and management 49, no. 11 (2008): 3305-3310.

**34.** Villar, N. Molero, JM Cejudo Lopez, F. Domínguez Muñoz, E. Rodríguez García, and A. Carrillo Andrés. "Numerical 3-D heat flux simulations on flat plate solar collectors." Solar energy 83, no. 7 (2009): 1086-1092.https://doi.org/10.1016/j.solener.2009.01.014

**35.** Kundu, B. "Analytic method for thermal performance and optimization of an absorber plate fin having variable thermal conductivity and overall loss coefficient." Applied Energy 87, no. 7 (2010): 2243-2255.https://doi.org/10.1016/j.apenergy.2010.01.008

**36.** Kundu, B., P. K. Mondal, S. P. Datta, and S. Wongwises. "Operating design conditions of a solar-powered vapor absorption cooling system with an absorber plate having different profiles: An analytical study." International communications in heat and mass transfer 37, no. 9 (2010): 1238-1245.https://doi.org/10.1016/j.icheatmasstransfer.2010.08.012

**37.** Alvarez, A., O. Cabeza, M. C. Muñiz, and L. M. Varela. "Experimental and numerical investigation of a flat-plate solar

collector." Energy 35, no. 9 (2010): 3707-3716.https://doi.org/10.1016/j.energy.2010.05.016

**38.** Roberts, D. E., and A. Forbes. "An analytical expression for the instantaneous efficiency of a flat plate solar water heater and the influence of absorber plate absorptance and emittance." Solar energy 86, no. 5 (2012): 1416-1427.https://doi.org/10.1016/j.solener.2012.01.032

**39.** Subiantoro, Alison, and Kim TiowOoi. "Analytical models for the computation and optimization of single and double glazing flat plate solar collectors with normal and small air gap spacing." Applied energy 104 (2013): 392-399.https://doi.org/10.1016/j.apenergy.2012.11.009

**40.** Eismann, Ralph, and Horst-Michael Prasser. "Correction for the absorber edge effect in analytical models of flat plate solar collectors." Solar Energy 95 (2013): 181-191.https://doi.org/10.1016/j.solener.2013.06.009

**41.** Bhowmik, Himangshu, and Ruhul Amin. "Efficiency improvement of flat plate solar collector using reflector." Energy Reports 3 (2017): 119-123. https://doi.org/10.1016/j.egyr.2017.08.002

**42.** Grossman, Gershon, Avraham Shitzer, and YoramZvirin. "Heat transfer analysis of a flat-plate solar energy collector." Solar Energy 19, no. 5 (1977): 493-502. https://doi.org/10.1016/0038-092X(77)90104-9

**43.** Rao, Prabhakar P., John E. Francis, and Tom J. Love Jr. "Two-dimensional analysis of a flat-plate solar collector." Journal of Energy 1, no. 5 (1977): 324-328. https://doi.org/10.2514/3.62342

**44.** Rahman, Faizur, A. S. Al-Zakri, and M. A. A. Rahman. "Two-dimensional mathematical model of evacuated tubular solar collector." (1984): 341-346.https://doi.org/10.1115/1.3267605

**45.** Lund, Kurt O'Ferrall. "General thermal analysis of parallel-flow flat-plate solar collector absorbers." Solar Energy 36, no. 5 (1986): 443-450. https://doi.org/10.1016/0038-092X(86)90092-7

**46.** Wijeysundera, N. E., and V. Thevendran. "A two-dimensional heat transfer analysis of the thermal-trap collector." Solar energy 40, no. 2 (1988): 127-133.https://doi.org/10.1016/0038-092X(88)90080-1

**47.** Hobson, P. A., and B. Norton. "Verified accurate performance simulation model of direct thermosyphon solar energy water heaters." (1988): 282-292. https://doi.org/10.1115/1.3268269

**48.** Kazeminejad, H. "Numerical analysis of two-dimensional parallel flow flat-plate solar collector." Renewable energy 26, no. 2 (2002): 309-323. https://doi.org/10.1016/S0960-1481(01)00121-5

**49.** Varol, Yasin, and Hakan F. Oztop. "A comparative numerical study on natural convection in inclined wavy and flat-plate solar collectors." Building and environment 43, no. 9 (2008): 1535-1544. https://doi.org/10.1016/j.buildenv.2007.09.002

**50.** Li, QinYi, and Qun Chen. "Application of entransy theory in the heat transfer optimization of flat-plate solar collectors." Chinese science bulletin 57 (2012): 299-306.

**51.** Mortazavinejad, Seyyed Mohsen, and MiladMozafarifard. "Numerical investigation of two-dimensional heat transfer of an absorbing plate of a flat-plate solar collector using dual-reciprocity method based on boundary element." Solar Energy 191 (2019): 332-340.https://doi.org/10.1016/j.solener.2019.08.075

**52.** Kundu, Balaram, and Kwan-Soo Lee. "An appropriate analysis for optimum design of wet fins based on modified 1-D and 2-D approaches." Energy Conversion and Management 103 (2015): 814-826.https://doi.org/10.1016/j.enconman.2015.07.024

**53.** Kundu, Balaram, Pratul Biswas, and Kwan-Soo Lee. "Establishment of modified-one-dimensional and two-dimensional models for two-directional heat conduction in a wet fin assembly." Heat Transfer Engineering 38, no. 2 (2017): 190-205.https://doi.org/10.1080/01457632.2016.1177402

**54.** Onyegegbu, S. O., and J. Morhenne. "Transient multidimensional second law analysis of solar collectors subjected to time-varying insolation with diffuse components." Solar Energy 50, no. 1 (1993): 85-95. https://doi.org/10.1016/0038-092X(93)90010-L

**55.** Al-Tabbakh, Aouf Abdulrahman. "Numerical transient modeling of a flat plate solar collector." Results in Engineering 15 (2022): 100580. https://doi.org/10.1016/j.rineng.2022.100580

**56.** Klein, S. A., J. A. Duffie, and W. A. Beckman. "Transient considerations of flat-plate solar collectors." (1974): 109-113. https://doi.org/10.1115/1.3445757

**57.** Grossman, Gershon, Avraham Shitzer, and YoramZvirin. "Heat transfer analysis of a flat-plate solar energy collector." Solar Energy 19, no. 5 (1977): 493-502. https://doi.org/10.1016/0038-092X(77)90104-9

**58.** De Ron, A. J. "Dynamic modelling and verification of a flat-plate solar collector." Solar Energy 24, no. 2 (1980): 117-128. https://doi.org/10.1016/0038-092X(80)90386-2

**59.** Mather Jr, G. R. "Transient response of solar collectors." (1982): 165-172. https://doi.org/10.1115/1.3266298

**60.** Tiwari, G. N., and Alok Srivastava. "Simple transient analysis of plate temperature in flat-plate solar collectors." Applied Energy 12, no. 3 (1982): 177-183. https://doi.org/10.1016/0306-2619(82)90037-X

**61.** Saito, Akio, Yoshio Utaka, TakehisaTsuchio, and Kozo Katayama. "Transient response of flat plate solar collector for periodic solar intensity variation." Solar energy 32, no. 1 (1984): 17-23. https://doi.org/10.1016/0038-092X(84)90044-6

**62.** Kamminga, W. "Experiences of a Solar Collector Test Method Using Fourier Transfer Functions." International Journal of Heat and Mass Transfer 28, no. 7 (1985): 1393-1404. https://doi.org/10.1016/0017-9310(85)90170-X.

**63.** Yadav, Y. P., G. N. Tiwari, and D. K. Dutt. "Transient analysis of parallel flat-plate water collector." Energy conversion and management 26, no. 3-4 (1986): 369-373. https://doi.org/10.1016/0196-8904(86)90019-1

**64.** Zhao, Qiqiu, G. W. Sadler, and J. J. Leonard. "Transient simulation of flat-plate solar collectors." Solar energy 40, no. 2 (1988): 167-174. https://doi.org/10.1016/0038-092X(88)90086-2

**65.** Zeroual, A., E. L. Agouriane, M. Ankrim, and A. J. Wilkinson. "A new method for testing the performance of flat-plate solar collectors." Renewable energy 4, no. 7 (1994): 825-832.https://doi.org/10.1016/0960-1481(94)90234-8

**66.** Amer, E. H., P. Jadeja, J. K. Nayak, and G. K. Sharma. "Comparison of two dynamic test methods for solar flat-plate collectors." Energy conversion and management 39, no. 3-4 (1996): 285-293. https://doi.org/10.1016/S0196-8904(96)00199-9

**67.** Amer, E. H., J. K. Nayak, and G. K. Sharma. "Transient method for testing flat-plate solar collectors." Energy Conversion and Management 39, no. 7 (1998): 549-558. https://doi.org/10.1016/S0196-8904(97)10014-0

**68.** El-Adawi, M. K. "New approach to modelling a flat plate collector: the Fourier transform technique." Renewable energy 26, no. 3 (2002): 489-506. https://doi.org/10.1016/S0960-1481(01)00135-5

**69.** Dhariwal, S. R., and U. S. Mirdha. "Analytical expressions for the response of flat-plate collector to various transient

conditions." Energy Conversion and Management 46, no. 11-12 (2005): 1809-1836 https://doi.org/10.1016/j.enconman.2004.08.008

**70.** Cadafalch, J. "A detailed numerical model for flat-plate solar thermal devices." Solar Energy 83, no. 12 (2009): 2157-2164. https://doi.org/10.1016/j.solener.2009.08.013

**71.** Alvarez, A., O. Cabeza, M. C. Muñiz, and L. M. Varela. "Experimental and numerical investigation of a flat-plate solar collector." Energy 35, no. 9 (2010): 3707-3716. https://doi.org/10.1016/j.energy.2010.05.016

**72.** Zima, Wiesław, and Piotr Dziewa. "Mathematical modelling of heat transfer in liquid flat-plate solar collector tubes." Archives of Thermodynamics 31, no. 2 (2010): 45-62. https://doi.org/10.1177/09576509JPE1044

**73.** Zima, W., and P. Dziewa. "Modelling of liquid flat-plate solar collector operation in transient states." Proceedings of the Institution of Mechanical Engineers, Part A: Journal of Power and Energy 225, no. 1 (2011): 53-62.

**74.** Rodríguez-Hidalgo, M. C., P. A. Rodríguez-Aumente, A. Lecuona, G. L. Gutiérrez-Urueta, and R. Ventas. "Flat plate thermal solar collector efficiency: Transient behavior under

working conditions. Part I: Model description and experimental validation." Applied thermal engineering 31, no. 14-15 (2011): 2394-2404 https://doi.org/10.1016/j.applthermaleng.2011.04.003

**75.** Peshkov, V., 1944. Second sound in helium II. Journal of Physics (Moscow) 8, 381–382

**76.** Cattaneo, Carlo. "Sur uneforme de l'equation de la chaleureliminant la paradoxed'une propagation instantantee." Compt. Rendu 247 (1958): 431-433.

**77.** Vernotte, Pierre. "Les paradoxes de la theorie continue de l'equation de la chaleur." Comptesrendus 246 (1958): 3154.

**78.** Tzou, Da Yu. "Experimental support for the lagging behavior in heat propagation." Journal of thermophysics and heat transfer 9, no. 4 (1995): 686-693 https://doi.org/10.2514/3.725

**79.** Tzou, Da Yu. "A unified field approach for heat conduction from macro-to micro-scales." (1995): 8-16.https://doi.org/10.1115/1.2822329

**80.** Antaki, Paul. "Key features of analytical solutions for hyperbolic heat conduction." In 30th Thermophysics Conference, p. 2044. 1995 https://doi.org/10.2514/6.1995-2044

**81.** Lin, Jae-Yuh. "The non-Fourier effect on the fin performance under periodic thermal conditions." Applied Mathematical

Modelling 22, no. 8 (1998): 629-640.https://doi.org/10.1016/S0307-904X(98)10061-6

**82.** Moosaie, Amin. "Non-Fourier heat conduction in a finite medium subjected to arbitrary non-periodic surface disturbance." International communications in heat and mass transfer 35, no. 3 (2008): 376-383 https://doi.org/10.1016/j.icheatmasstransfer.2007.08.007

**83.** Ahmadikia, Hossein, and MiladRismanian. "Analytical solution of non-Fourier heat conduction problem on a fin under periodic boundary conditions." Journal of mechanical science and technology 25 (2011): 2919-2926. DOI:10.1007/s12206-011-0720-5

**84.** Kundu, Balaram, and Kwan-Soo Lee. "Fourier and non-Fourier heat conduction analysis in the absorber plates of a flat-plate solar collector." Solar Energy 86, no. 10 (2012): 3030-3039.https://doi.org/10.1016/j.solener.2012.07.011

**85.** Castro, M. A., Francisco Rodríguez, J. Escolano, and J. A. Martín. "Exact and Analytic-Numerical Solutions of Lagging Models of Heat Transfer in a Semi-Infinite Medium." In Abstract and Applied Analysis, vol. 2013, no. 1, p. 397053. Hindawi

Publishing Corporation, 2013. https://doi.org/10.1155/2013/397053

**86.** Kundu, Balaram, and Kwan-Soo Lee. "A non-Fourier analysis for transmitting heat in fins with internal heat generation." International Journal of Heat and Mass Transfer 64 (2013): 1153-1162.https://doi.org/10.1016/j.ijheatmasstransfer.2013.05.057

**87.** Bhowmik, Arka, Rohit K. Singla, Ranjan Das, A. Mallick, and R. Repaka. "Inverse modeling of a solar collector involving Fourier and non-Fourier heat conduction." Applied Mathematical Modelling 38, no. 21-22 (2014): 5126-5148 https://doi.org/10.1016/j.apm.2014.04.001.

**88.** Panda, Srikumar, Rohit K. Singla, Ranjan Das, and Subash C. Martha. "Identification of design parameters in a solar collector using inverse heat transfer analysis." Energy conversion and management 88 (2014): 27-39.https://doi.org/10.1016/j.enconman.2014.08.013

**89.** Wankhade, Pramod A., BalaramKundu, and Ranjan Das. "Establishment of non-Fourier heat conduction model for an accurate transient thermal response in wet fins." International

Journal of Heat and Mass Transfer 126 (2018): 911-923. https://doi.org/10.1016/j.ijheatmasstransfer.2018.05.094

**90.** Mozafarifard, Milad, Aziz Azimi, HossienSobhani, Ghassan Fadhil Smaisim, DavoodToghraie, and MaedehRahmani. "Numerical study of anomalous heat conduction in absorber plate of a solar collector using time-fractional single-phase-lag model." Case Studies in Thermal Engineering 34 (2022): 102071.https://doi.org/10.1016/j.csite.2022.102071

**91.** Gamaoun, Fehmi, Amal Abdulrahman, G. Sowmya, Raman Kumar, Umair Khan, Abeer M. Alotaibi, Sayed M. Eldin, and RS Varun Kumar. "Non-Fourier heat transfer in a moving longitudinal radiative-convective dovetail fin." Case Studies in Thermal Engineering 41 (2023): 102623.https://doi.org/10.1016/j.csite.2022.102623

**92.** Bejan, A. "Extraction of exergy from solar collectors under time-varying conditions." International Journal of Heat and Fluid Flow 3, no. 2 (1982): 67-72. https://doi.org/10.1016/0142-727X(82)90002-9

**93.** Fujiwara, M. (1983). "Exergy analysis for the performance of solar collectors." ASME Journal of Solar Energy Engineering, 105(2), 163-167. https://doi.org/10.1115/1.3266360

**94.** Gribik, J. A., and J. F. Osterle. "The second law efficiency of solar energy conversion." (1984): 16-21. https://doi.org/10.1115/1.3267555

**95.** Chelghoum, DjamelEddine, and A. Bejan. "Second-law analysis of solar collectors with energy storage capability." (1985): 244-251. https://doi.org/10.1115/1.3267686

**96.** Suzuki, Akio, H. Okamura, and I. Oshida. "Application of exergy concept to the analysis of optimum operating conditions of solar heat collectors." (1987): 337-342. https://doi.org/10.1115/1.3268226

**97.** Suzuki, Akio. "A fundamental equation for exergy balance on solar collectors." (1988): 102-106. https://doi.org/10.1115/1.3268238

**98.** Farahat, S., F. Sarhaddi, and H. Ajam. "Exergetic optimization of flat plate solar collectors." Renewable energy 34, no. 4 (2009): 1169-1174.https://doi.org/10.1016/j.renene.2008.06.014

**99.** Jafarkazemi, Farzad, and Emad Ahmadifard. "Energetic and exergetic evaluation of flat plate solar collectors." Renewable energy 56 (2013): 55-63.https://doi.org/10.1016/j.renene.2012.10.031

**100.** Ge, Zhong, Huitao Wang, Hua Wang, Songyuan Zhang, and Xin Guan. "Exergy analysis of flat plate solar collectors." Entropy 16, no. 5 (2014): 2549-2567. https://doi.org/10.3390/e16052549

**101.** Wang, Xinwei, Xianfan Xu, and Stephen US Choi. "Thermal conductivity of nanoparticle-fluid mixture." Journal of Thermophysics and Heat Transfer 13, no. 4 (1999): 474-480. https://doi.org/10.2514/2.6486

**102.** Said, Zafar, and Rahman Saidur. "Thermophysical properties of metal oxides nanofluids." Nanofluid Heat and Mass Transfer in Engineering Problems (2017): 39. http://dx.doi.org/10.5772/62719

**103.** Duangthongsuk, Weerapun, and SomchaiWongwises. "Measurement of temperature-dependent thermal conductivity and viscosity of TiO2-water nanofluids." Experimental Thermal and Fluid Science 33, no. 4 (2009): 706-714. https://doi.org/10.1016/j.expthermflusci.2009.01.005

**104.** Yousefi, Tooraj, FarzadVeysi, Ehsan Shojaeizadeh, and SirusZinadini. "An experimental investigation on the effect of $Al_2O_3$-$H_2O$ nanofluid on the efficiency of flat-plate solar collectors." Renewable Energy 39, no. 1 (2012): 293-298. https://doi.org/10.1016/j.renene.2011.08.056

**105.** Rahman, M. M., and A. Aziz. "Heat transfer in water based nanofluids (TiO2-H2O, $Al_2O_3$-$H_2O$ and Cu-$H_2O$) over a stretching cylinder." International Journal of Heat and Technology 30, no. 02 (2012): 31-42.

**106.** Faizal, M., Rahman Saidur, SaadMekhilef, and Mohammad A. Alim. "Energy, economic and environmental analysis of metal oxides nanofluid for flat-plate solar collector." Energy Conversion and Management 76 (2013): 162-168. https://doi.org/10.1016/j.enconman.2013.07.038

**107.** Alim, M. A., Z. Abdin, R. Saidur, A. Hepbasli, M. A. Khairul, and N. A. Rahim. "Analyses of entropy generation and pressure drop for a conventional flat plate solar collector using different types of metal oxide nanofluids." Energy and Buildings 66 (2013): 289-296. https://doi.org/10.1016/j.enbuild.2013.07.027

**108.** Said, Zid, Mohammad H. Sajid, Mohammad A. Alim, Rahman Saidur, and Nasrudin A. Rahim. "Experimental investigation of the thermophysical properties of AL2O3-nanofluid and its effect on a flat plate solar collector." International Communications in Heat and Mass Transfer 48 (2013): 99-107. https://doi.org/10.1016/j.icheatmasstransfer.2013.09.005

**109.** Mahian, Omid, Ali Kianifar, Ahmet Z. Sahin, and SomchaiWongwises. "Performance analysis of a minichannel-based solar collector using different nanofluids." Energy Conversion and Management 88 (2014): 129-138. https://doi.org/10.1016/j.enconman.2014.08.021

**110.** Madhesh, Devasenan, RajagopalanParameshwaran, and Siva Kalaiselvam. "Experimental investigation on convective heat transfer and rheological characteristics of Cu-$TiO_2$ hybrid nanofluids." Experimental Thermal and Fluid Science 52 (2014): 104-115. https://doi.org/10.1016/j.expthermflusci.2013.08.026

**111.** Verma, Sujit Kumar, and Arun Kumar Tiwari. "Progress of nanofluid application in solar collectors: a review." Energy Conversion and Management 100 (2015): 324-346. https://doi.org/10.1016/j.enconman.2015.04.071

**112.** Gupta, Munish, Vinay Singh, Rajesh Kumar, and Zafar Said. "A review on thermophysical properties of nanofluids and heat transfer applications." Renewable and Sustainable Energy Reviews 74 (2017): 638–670. https://doi.org/10.1016/j.rser.2017.02.073

**113.** Shojaeizadeh, Ehsan, FarzadVeysi, and Ahmad Kamandi. "Exergy efficiency investigation and optimization of an $Al_2O_3$-

water nanofluid based Flat-plate solar collector." Energy and Buildings 101 (2015): 12-23. https://doi.org/10.1016/j.enbuild.2015.04.048

**114.** Faizal, M. S. R. M. S., Rahman Saidur, SaadMekhilef, A. Hepbasli, and I. M. Mahbubul. "Energy, economic, and environmental analysis of a flat-plate solar collector operated with $SiO_2$ nanofluid." Clean Technologies and Environmental Policy 17 (2015): 1457-1473.

**115.** Said, Zid, Mohammad A. Alim, and IsamJanajreh. "Exergy efficiency analysis of a flat plate solar collector using graphene based nanofluid." In IOP Conference Series: Materials Science and Engineering, vol. 92, no. 1, p. 012015. IOP Publishing, 2015. https://ioppublishing.org/contacts/

**116.** Esfe, MohammdHemmat, SomchaiWongwises, Ali Naderi, Amin Asadi, Mohammad Reza Safaei, HadiRostamian, Mahidzal Dahari, and ArashKarimipour. "Thermal conductivity of Cu/$TiO_2$-water/EG hybrid nanofluid: Experimental data and modeling using artificial neural network and correlation." International Communications in Heat and Mass Transfer 66 (2015): 100-104. https://doi.org/10.1016/j.icheatmasstransfer.2015.05.014

**117.** Esfe, Mohammad Hemmat, Ali Akbar AbbasianArani, Mohammad Rezaie, Wei-Mon Yan, and ArashKarimipour. "Experimental determination of thermal conductivity and dynamic viscosity of Ag-MgO/water hybrid nanofluid." International Communications in Heat and Mass Transfer 66 (2015): 189-195. https://doi.org/10.1016/j.icheatmasstransfer.2015.06.003

**118.** Verma, Sujit Kumar, Arun Kumar Tiwari, and Durg Singh Chauhan. "Performance augmentation in flat plate solar collector using MgO/water nanofluid." Energy Conversion and Management 124 (2016): 607-617. https://doi.org/10.1016/j.enconman.2016.07.007

**119.** Said, Zafar, Rahman Saidur, and N. A. Rahim. "Energy and exergy analysis of a flat plate solar collector using different sizes of aluminium oxide based nanofluid." Journal of Cleaner Production 133 (2016): 518-530. https://doi.org/10.1016/j.jclepro.2016.05.178

**120.** Nemade, Kailash, and Sandeep Waghuley. "A novel approach for enhancement of thermal conductivity of $CuO/H_2O$ based nanofluids." Applied Thermal Engineering 95 (2016): 271-274. https://doi.org/10.1016/j.applthermaleng.2015.11.053

**121.** Agarwal, Ravi, KamaleshVerma, Narendra Kumar Agrawal, Rajendra Kumar Duchaniya, and Ramvir Singh. "Synthesis, characterization, thermal conductivity and sensitivity of CuOnanofluids." Applied Thermal Engineering 102 (2016): 1024-1036. https://doi.org/10.1016/j.applthermaleng.2016.04.051

**122.** Verma, Sujit Kumar, Arun Kumar Tiwari, and Durg Singh Chauhan. "Experimental evaluation of flat plate solar collector using nanofluids." Energy Conversion and Management 134 (2017): 103–115. https://doi.org/10.1016/j.enconman.2016.12.037

**123.** Dasaien, AninVincely, and Natarajan Elumalai. "Performance enhancement studies in a thermosyphon flat plate solar water heater with CuOnanofluid." Thermal Science 21, no. 6 Part B (2017): 2757–2768. https://doi.org/10.2298/TSCI151005012D

**124.** Sint, Nang Khin Chaw, I. A. Choudhury, H. H. Masjuki, and Hideki Aoyama. "Theoretical analysis to determine the efficiency of a CuO-water nanofluid based-flat plate solar collector for domestic solar water heating system in Myanmar." Solar energy 155 (2017): 608-619. https://doi.org/10.1016/j.solener.2017.06.055

**125.** Tong, Yijie, Hoseong Lee, Woobin Kang, and Honghyun Cho. "Energy and exergy comparison of a flat-plate solar collector

using water, $Al_2O_3$ nanofluid, and CuOnanofluid." Applied Thermal Engineering 159 (2019): 113959. https://doi.org/10.1016/j.applthermaleng.2019.113959

**126.** Kiliç, Faruk, Tayfun Menlik, and Adnan Sözen. "Effect of titanium dioxide/water nanofluid use on thermal performance of the flat plate solar collector." Solar Energy 164 (2018): 101–108. https://doi.org/10.1016/j.solener.2018.02.002

**127.** Ziyadanogullari, N. Budak, H. L. Yucel, and C. J. T. S. Yildiz. "Thermal performance enhancement of flat-plate solar collectors by means of three different nanofluids." Thermal Science and Engineering Progress 8 (2018): 55–65. https://doi.org/10.1016/j.tsep.2018.07.005

**128.** Verma, Sujit Kumar, Arun Kumar Tiwari, Sandeep Tiwari, and Durg Singh Chauhan. "Performance analysis of hybrid nanofluids in flat plate solar collector as an advanced working fluid." Solar Energy 167 (2018): 231–241. https://doi.org/10.1016/j.solener.2018.04.017

**129.** Farajzadeh, Ehsan, SaeidMovahed, and Reza Hosseini. "Experimental and numerical investigations on the effect of $Al_2O_3/TiO_2H_2O$ nanofluids on thermal efficiency of the flat plate

solar collector." Renewable Energy 118 (2018): 122–130. https://doi.org/10.1016/j.renene.2017.10.102

**130.** Dehaj, Mohammad Shafiey, and Mostafa ZamaniMohiabadi. "Experimental investigation of heat pipe solar collector using MgOnanofluids." Solar Energy Materials and Solar Cells 191 (2019): 91–99. https://doi.org/10.1016/j.solmat.2018.10.025

**131.** Mousavi, S. M., F. Esmaeilzadeh, and X. P. Wang. "A detailed investigation on the thermo-physical and rheological behavior of MgO/TiO2 aqueous dual hybrid nanofluid." Journal of Molecular Liquids 282 (2019): 323–339. https://doi.org/10.1016/j.molliq.2019.02.100

**132.** Mousavi, S. M., F. Esmaeilzadeh, and X. P. Wang. "Effects of temperature and particles volume concentration on the thermophysical properties and the rheological behavior of CuO/MgO/$TiO_2$ aqueous ternary hybrid nanofluid: Experimental investigation." Journal of Thermal Analysis and Calorimetry 137 (2019): 879–901. https://doi.org/10.1007/s10973-018-7981-5

**133.** Okonkwo, Eric C., Ifeoluwa Wole-Osho, DogaKavaz, and Muhammad Abid. "Comparison of experimental and theoretical methods of obtaining the thermal properties of alumina/iron mono

and hybrid nanofluids." Journal of Molecular Liquids 292 (2019): 111377. https://doi.org/10.1016/j.molliq.2019.111377

**134.** Tong, Yijie, Hoseong Lee, Woobin Kang, and Honghyun Cho. "Energy and exergy comparison of a flat-plate solar collector using water, $Al_2O_3$ nanofluid, and CuOnanofluid." Applied Thermal Engineering 159 (2019): 113959. https://doi.org/10.1016/j.applthermaleng.2019.113959

**135.** Choudhary, Suraj, Anish Sachdeva, and Pramod Kumar. "Investigation of the stability of MgOnanofluid and its effect on the thermal performance of flat plate solar collector." Renewable Energy 147 (2020): 1801–1814. https://doi.org/10.1016/j.renene.2019.09.126

**136.** Okonkwo, Eric C., IfeoluwaWole-Osho, DogaKavaz, Muhammad Abid, and Tareq Al-Ansari. "Thermodynamic evaluation and optimization of a flat plate collector operating with alumina and iron mono and hybrid nanofluids." Sustainable Energy Technologies and Assessments 37 (2020): 100636. https://doi.org/10.1016/j.seta.2020.100636

**137.** Tong, Yijie, Xiaoni Chi, Woobin Kang, and Honghyun Cho. "Comparative investigation of efficiency sensitivity in a flat plate solar collector according to nanofluids." Applied Thermal

Engineering 174 (2020): 115346. https://doi.org/10.1016/j.applthermaleng.2020.115346

**138.** Sundar, L. Syam, E. VenkataRamana, Zafar Said, V. Punnaiah, Kotturu VV Chandra Mouli, and Antonio CM Sousa. "Properties, heat transfer, energy efficiency and environmental emissions analysis of flat plate solar collector using nanodiamondnanofluids." Diamond and Related Materials 110 (2020): 108115. https://doi.org/10.1016/j.diamond.2020.108115

**139.** Liu, Suhong, HaithamAbdulmohsinAfan, Mohammed SulemanAldlemy, Nadhir Al-Ansari, and ZaherMundherYaseen. "Energy analysis using carbon and metallic oxides-based nanomaterials inside a solar collector." Energy Reports 6 (2020): 1373–1381. https://doi.org/10.1016/j.egyr.2020.05.015

**140.** Sarsam, Wail Sami, Salim NewazKazi, and Ahmad Badarudin. "Thermal performance of a flat-plate solar collector using aqueous colloidal dispersions of graphene nanoplatelets with different specific surface areas." Applied Thermal Engineering 172 (2020): 115142. https://doi.org/10.1016/j.applthermaleng.2020.115142

**141.** Eltaweel, Mahmoud, Ahmed A. Abdel-Rehim, and Ahmed AA Attia. "A comparison between flat-plate and evacuated tube solar collectors in terms of energy and exergy analysis by using

nanofluid." Applied Thermal Engineering 186 (2021): 116516. https://doi.org/10.1016/j.applthermaleng.2020.116516

**142.** Akram, Naveed, ElhamMontazer, S. N. Kazi, ManzooreElahi M. Soudagar, Waqar Ahmed, MohdNashrulMohdZubir, Asif Afzal et al. "Experimental investigations of the performance of a flat-plate solar collector using carbon and metal oxides based nanofluids." Energy 227 (2021): 120452. https://doi.org/10.1016/j.energy.2021.120452

**143.** Mostafizur, R. M., M. G. Rasul, and MdNurunNabi. "Energy and exergy analyses of a flat plate solar collector using various nanofluids: An analytical approach." Energies 14, no. 14 (2021): 4305. https://doi.org/10.3390/en14144305

**144.** Adun, Humphrey, Michael Adedeji, Victor Adebayo, Ali Shefik, OlusolaBamisile, DogaKavaz, and Mustafa Dagbasi. "Multi-objective optimization and energy/exergy analysis of a ternary nanofluid based parabolic trough solar collector integrated with kalina cycle." Solar Energy Materials and Solar Cells 231 (2021): 111322. https://doi.org/10.1016/j.solmat.2021.111322

**145.** Nfawa, Sadeq R., AdiAzriffBasri, and SitiUjilaMasuri. "Novel use of MgO nanoparticle additive for enhancing the thermal conductivity of CuO/water nanofluid." Case Studies in Thermal

Engineering 27 (2021): 101279. https://doi.org/10.1016/j.csite.2021.101279

**146.** Asadi, Amin, Ibrahim M. Alarifi, and LokeKokFoong. "An experimental study on characterization, stability and dynamic viscosity of CuO-$TiO_2$/water hybrid nanofluid." Journal of Molecular Liquids 307 (2020): 112987. https://doi.org/10.1016/j.molliq.2020.112987

**147.** Said, Zafar, Ahmed Amine Hachicha, SadeghAberoumand, Bashria AA Yousef, EnasTaha Sayed, and EvangelosBellos. "Recent advances on nanofluids for low to medium temperature solar collectors: energy, exergy, economic analysis and environmental impact." Progress in Energy and Combustion Science 84 (2021): 100898. https://doi.org/10.1016/j.pecs.2020.100898

**148.** Kumar, L. Harish, S. N. Kazi, H. H. Masjuki, M. N. M. Zubir, Afrin Jahan, and C. J. A. T. E. Bhinitha. "Energy, exergy and economic analysis of liquid flat-plate solar collector using green covalent functionalized graphene nanoplatelets." Applied Thermal Engineering 192 (2021): 116916. https://doi.org/10.1016/j.applthermaleng.2021.116916

**149.** Choudhary, Suraj, Anish Sachdeva, and Pramod Kumar. "Time-based assessment of thermal performance of flat plate solar collector using magnesium oxide nanofluid." International Journal of Sustainable Energy 40, no. 5 (2021): 460–476. https://doi.org/10.1080/14786451.2020.1814288

**150.** Esfe, Mohammad Hemmat, ErfanMohammadnejadArdeshiri, and DavoodToghraie. "Experimental study and sensitivity analysis of a new generation of special ternary hybrid nanofluids (THNFs) and investigation of factors affecting its thermal conductivity." Case Studies in Thermal Engineering 34 (2022): 101940. https://doi.org/10.1016/j.csite.2022.101940

**151.** Khan, Sohail A., T. Hayat, and A. Alsaedi. "Thermal conductivity performance for ternary hybrid nanomaterial subject to entropy generation." Energy Reports 8 (2022): 9997–10005. https://doi.org/10.1016/j.egyr.2022.07.149

**152.** Ajeena, Ahmed M., PiroskaVíg, and IstvanFarkas. "A comprehensive analysis of nanofluids and their practical applications for flat plate solar collectors: Fundamentals, thermophysical properties, stability, and difficulties." Energy Reports 8 (2022): 4461–4490. https://doi.org/10.1016/j.egyr.2022.03.088

**153.** Desisa, TikoRago. "Experimental and numerical investigation of heat transfer characteristics in solar flat plate collector using nanofluids." International Journal of Thermofluids 18 (2023): 100325. https://doi.org/10.1016/j.ijft.2023.100325

**154.** Kumar, J. Sathish, G. Senthilkumar, and S. Ramachandran. "Novel strategy of mixing MgO in CuO/water nanofluid for thermal conductivity improvement: Experimental study." Case Studies in Thermal Engineering 52 (2023): 103723. https://doi.org/10.1016/j.csite.2023.103723

**155.** Ajeena, Ahmed M., IstvanFarkas, and PiroskaVíg. "Energy and exergy assessment of a flat plate solar thermal collector by examine silicon carbide nanofluid: An experimental study for sustainable energy." Applied Thermal Engineering 236 (2024): 121844. https://doi.org/10.1016/j.applthermaleng.2023.121844

**156.** Senthilkumar, G. "Novel Approach to Augment Thermal Conductivity of Dihybrid Nanofluids." Journal of Thermophysics and Heat Transfer 38, no. 4 (2024): 468–477. https://doi.org/10.2514/1.T6932

**157.** Khan, Shan Ali, Muhammad Imran, Hassan Waqas, Taseer Muhammad, Sumeira Yasmin, and Abdullah Alhushaybari. "Numerical analysis of multiple slip effects on CuO/MgO/$TiO_2$-

water ternary hybrid nanofluid with thermal and exponential space-based heat source." Tribology International 197 (2024): 109778. https://doi.org/10.1016/j.triboint.2024.109778

**158.** Arpaci, V.S. and Arpaci, V.S., 1966. *Conduction heat transfer* (Vol. 237). Reading, MA: Addison-Wesley.

**159.** Mazumder, S., 2015. *Numerical methods for partial differential equations: finite difference and finite volume methods*. Academic Press.

**160.** Patankar, S.V.: Numerical Heat Transfer and Fluid Flow. New York: Hemisphere Publishing, Taylor and Francis Group (1980).

Jayanarayan Mahanad
31.12.2025

31-12-2025

Professor
Dept. of Mechanical Engineering
Jadavpur University, Kolkata-32

*energies*

MDPI

*Article*

# Two-Dimensional Analysis of Absorber Plates in Solar Collectors with a Nonlinear Plate Temperature at the Tube Section

**Jayanarayan Mahakud [1,2] and Balaram Kundu [1,*]**

[1] Mechanical Engineering Department, Jadavpur University, Jadavpur 700032, Kolkata, India
[2] Mechanical Engineering Department, Parala Maharaja Engineering College, Berhampur 761003, Odisha, India
* Correspondence: bkundu@mech.net.in

**Abstract:** Many investigators have investigated flat-plate solar collector absorber plates based on one-dimensional heat flows. However, the shape of the absorber plate may always create a two-dimensional temperature distribution if it has a thin thickness. Hence, an analysis of the two-dimensional heat flow in absorber plates is always required. The current paper determines a closed-form solution for the energy equation to establish a two-dimensional energy flow for an absorber plate by considering a nonlinear temperature variation at the plate–tube section. The separation of the established variable method solves the energy equation. The same energy equation was also solved numerically using the finite difference method for validation purposes. It emphasizes demonstrating that the analytical and numerical results match closely with each other. Finally, this work concludes by developing an analytical model for the practicable thermal analysis of absorber plates in solar collectors, providing error-free implementation results.

**Keywords:** absorber plate; analytical; solar collector; thermal analysis; 2D heat conduction



**Citation:** Mahakud, J.; Kundu, B. Two-Dimensional Analysis of Absorber Plates in Solar Collectors with a Nonlinear Plate Temperature at the Tube Section. *Energies* **2024**, *17*, 5979. https://doi.org/10.3390/en17235979

Academic Editor: Andrea Frazzica

Received: 24 October 2024
Revised: 18 November 2024
Accepted: 22 November 2024
Published: 28 November 2024



## 1. Introduction

Environmental concerns have limited the use of fossil fuel reserves, and the increases in energy demand and rising costs of conventional energy generation have become major issues in our current climate. To help overcome these problematic aspects, renewable energy has experienced rapid growth in recent years, stepping up to address the looming energy crisis. One such renewable energy source is solar energy, which offers significant advantages due to its eco-friendliness and virtually infinite supply [1]. Solar collectors can obtain thermal energy from solar radiation. Solar flat-plate collectors (SFPCs) convert solar radiation to usable energy through various converting devices. This heating device is more effective than other solar collectors due to its simple structure and low running costs [2,3]. SFPCs are primarily employed in low- and medium-temperature systems, from household hot water and space heating to industrial drying, preheating and other engineering applications. They reduce carbon footprints, promote energy independence and mitigate the environmental impacts of conventional energy sources. Low convective heat transfer and thermal efficiency are the major problems with FSPCs [4]. Among their components, the absorber plate plays a pivotal role by absorbing solar energy and transferring it to the fluid in the tubes. This plate can be welded to or integrated with the fluid-carrying tubes, facilitating efficient heat transfer. As a result, the overall performance depends principally on the absorber plate's effectiveness in capturing and transferring solar energy [5]. Hence, researchers focus on improving the collector efficiency. For this, an investigation of two leading research directions, namely heat transfer and optimization of the structure, is required.

In recent years, research has been conducted to analyze FPSCs in order to increase their efficiency and performance. The published work includes several theoretical, analytical, numerical and experimental analyses on finding innovative solutions for collector heat

# Simple Analytical Method for Performance of an Absorber Plate in Flat-Plate Solar Collectors for Two-Dimensional Heat Flow


**Jayanarayan Mahakud and Balaram Kundu**

**Abstract** In this paper, two-dimensional temperature distributions in the absorber plate of a flat-plate solar collector have been determined by an approximate analytical technique. In case of two-dimensional heat flow in the absorber plate under actual boundary conditions, the determination of temperature field using an exact analytical method might not be possible. Alternatively, this temperature field can be evaluated using numerical methods. In the present study, finite difference method has been employed as a numerical tool. However, it is well known that the numerical calculations increase the computational cost. For the ease of calculations, an approximate analytical model has been proposed in the present study and the accuracy of the present analytical method has been checked with the comparison of results obtained between the present analytical and numerical techniques. It can be demonstrated that there is an excellent agreement between two results and the deviation between these two have never exceeded by 5%. Therefore, the present analytical method might have a significant importance for analyzing the performance of an absorber plate in order to avoid difficulties of the numerical solution.

**Keywords** Solar collector · Approximate analytical solution · 2-D heat transfer · Absorber plate

## Nomenclature

| | |
|---|---|
| $A$ | Dimensionless variable defined in Eq. (5b) |
| $D$ | Deviation of temperature, $(\theta_{\text{analytical}} - \theta_{\text{numerical}})/\theta_{\text{analytical}}$ |
| $k$ | Thermal conductivity of an absorber plate material (W m$^{-1}$ K$^{-1}$) |
| $L$ | Half-pitch distance between flow tubes as shown in Fig. 1 (m) |
| $M$ | Dimensionless thermogeometric parameter of absorber plate, see Eq. (3) |
| $N$ | Dimensionless absorbed solar flux, see Eq. (3) |
| $S$ | Absorbed solar flux (W m$^{-2}$) |
| $t$ | Thickness of the absorber plate (m) |

J. Mahakud · B. Kundu (✉)
Department of Mechanical Engineering, Jadavpur University, Kolkata 700032, India
e-mail: bkundu@mech.net.in



P. Saha et al. (eds.), *Advances in Fluid and Thermal Engineering*,
Lecture Notes in Mechanical Engineering,
https://doi.org/10.1007/978-981-13-6416-7_1

# Trapezoidal Approach to Establish One-Dimensional Analysis of an Absorber Plate for Two-Dimensional Heat Flow

**Jayanarayan Mahakud and Balaram Kundu**

**Abstract** The thermal analysis of an absorber plate for flat-plate solar collectors is done by many investigators considering one-dimensional heat conduction. However there always exists a two-dimensional temperature distribution in the absorber plate due to its typical shape. The absorber plate is made of thin thickness and the temperature variation in the thickness direction may not occur. There is always a demand to establish an analytical analysis for two-dimensional heat flow in absorber plates. In this paper, a modified one-dimensional method is proposed to determine a 2-D analysis based on the trapezoidal rule. From the results, it can be emphasized that the modified 1-D model matches closely with the 2-D model. Therefore, the 1-D classical model is unsuitable to predict the performance of an absorber plate. The modified 1-D model is always better than the 1-D classical model. The analysis of the proposed 1-D model is very simple for understanding and calculations.

**Keywords** Absorber plate · 2-D heat conduction model · Modified 1-D model · Trapezoidal approach

## Nomenclature

| | |
|---|---|
| $A$ | Dimensionless constant, see Eq. (5e) |
| $Bi$ | Biot number, defined in Eq. (5e) |
| $k$ | Thermal conductivity (W $m^{-1}$ $K^{-1}$) |
| $L$ | Half-pitch distance between flow tubes (m) |
| $M$ | Dimensionless thermo-geometric parameter of the absorber plate, see Eq. (3) |
| $m$ | Modified dimensionless thermo-geometric parameter, defined in Eq. (14) |
| $N$ | Dimensionless absorbed solar flux, see Eq. (3) |
| $S$ | Absorbed solar flux (W $m^{-2}$) |
| $T$ | Local absorber plate temperature (°C) |
| $T_\infty$ | Ambient temperature (°C) |

J. Mahakud · B. Kundu (✉)
Department of Mechanical Engineering, Jadavpur University, Kolkata 700032, India
e-mail: mahakud.kundu@springernature.com



B. B. Biswal et al. (eds.), *Advances in Mechanical Engineering*, Lecture Notes in Mechanical Engineering, https://doi.org/10.1007/978-981-15-0124-1_120